University of Adelaide

Doctoral Dissertation

Dense Nuclear Matter and Astrophysical Probes of Nuclear Physics

---

Author:
Theo F. Motta

Supervisor:
Prof. Anthony W. Thomas

Co-Supervisor:
Prof. Derek B. Leinweber

A thesis submitted in fulfillment of the requirements
for the degree of Doctor of Philosophy

in the

School of Physical Sciences
Faculty of Sciences

THE UNIVERSITY
of ADELAIDE

July 28, 2021

To Basil

Abstract of thesis entitled

Dense Nuclear Matter and Astrophysical Probes of Nuclear Physics

Submitted by

Theo F. Motta

for the degree of Doctor of Philosophy

at the University of Adelaide

in September, 2021

The physics of nuclear interactions at the density frontier and its interplay with neutron star astrophysics is studied within the framework of the quark-meson coupling model. Specifically, the isovector-scalar meson channel is included self-consistently in the model and its consequences for neutron star physics are investigated. Works on the crust effects on the tidal deformability of neutron stars and other quantities, a possible neutron to dark matter decay and its consequences to neutron star physics and the issue of Δ isobars in dense nuclear matter are also discussed.

Dense Nuclear Matter and Astrophysical Probes of Nuclear Physics

by

Theo F. Motta
B.S. University of São Paulo
M.S. University of São Paulo

A Thesis Submitted in Partial Fulfilment
of the Requirements for the Degree of
Doctor of Philosophy

at

University of Adelaide
September, 2021

Declaration

I certify that this work contains no material which has been accepted for the award of any other degree or diploma in my name, in any university or other tertiary institution and, to the best of my knowledge and belief, contains no material previously published or written by another person, except where due reference has been made in the text. In addition, I certify that no part of this work will, in the future, be used in a submission in my name, for any other degree or diploma in any university or other tertiary institution without the prior approval of the University of Adelaide and where applicable, any partner institution responsible for the joint-award of this degree. I give permission for the digital version of my thesis to be made available on the web, via the University's digital research repository, the Library Search and also through web search engines, unless permission has been granted by the University to restrict access for a period of time. I acknowledge the support I have received for my research through the provision of an Australian Government Research Training Program Scholarship.

Signed: _____

Date: July 28, 2021

Acknowledgements

I would like to, first and foremost, thank my supervisor Tony Thomas for the immense support he provided me during my PhD and for the opportunities he has given me to help initiate my career. I would also like to thank my collaborators, Sofija Antić, Anthony Kalaitzis, Jirina Stone and Pierre Guichon, all of whom contributed to the work presented here, and for that I am very thankful.

On a personal level I would like to extend my infinite gratitude to the students of rooms 119, 123 and 128a. The impact that each has had on me cannot be overstated. I will only give special mention to a few cases: Joe Hall, for the pandemic-proof friendship. Rob Perry, Andre Scaffidi and Abhishek Sharma for the kindness and camaraderie. Bertie, for being such a kindred spirit. And to Anna Mullin, for reigniting my passion for science when I most needed, for providing a model of what good principled science is and for reminding me of the importance of simplicity as a virtue.

Finally, I would like to thank my mother and father for the unfaltering love, support, and patience.

Theo F. Motta
University of Adelaide
September 14, 2021

Was sich überhaupt sagen lässt, lässt sich klar sagen; und wovon man nicht reden kann, darüber muss man schweigen

– Wittgenstein, L.

Contents

List of Figures

Chapter 1

Theory of Nuclear Interactions

This chapter will review some aspects of basic nuclear theory. The intention is both to give a phenomenological introduction to nuclear physics and to motivate the next chapters ahead. We discuss some of the properties of the nuclear strong force and introduce some aspects of relativistic Quantum Hadrodynamics (QHD) before moving on to the next chapter which is focused on the quark-meson coupling model (QMC) of nuclear interactions and how the nuclear medium affects the properties of the hadron and, consequentially, the nucleus. Some of the most comprehensible books on the subject are the small lecture series by L. D. Landau [44], which I highly recommend, and J. D. Walecka's [85] of which Part II is specially excellent.

Nuclear Physics Phenomenology

1.1 The Nuclear Force

Of the four fundamental forces known to this day to exist, the strong force is perhaps one of the most puzzling. From the discovery of the atomic nucleus with Rutherford's group's historical experiment of scattering α particles through a gold foil, to eventually the discovery of the neutron by James Chadwick almost three decades later, it became clear that a new force must exist in order to tightly bind together these nuclear constituents, namely, the proton and the neutron.

The fact that the proton is positively charged and the neutron is neutral immediately pointed to the fact that the force should be stronger than the electric repulsion amongst the protons. With more and more research, new indications of the nature of such a force came to light. From scattering experiments to observations of few-body bound states such as the deuteron, tritium and other light nuclei as well as many body states, physicists gathered together a list of properties that this force should abide by. Let's go through a few of the most important ones

1.1.1 Properties of the Nuclear Force

From the most basic observations it was easy to see that the nuclear potential had to both attractive and, differently from the electromagnetic potential, of finite range.

- Attractive
- Short-ranged.

It must be attractive, to counteract the electromagnetic repulsion amongst the protons and also to bind the neutrons to the nucleus and short ranged given evidence from high energy[1] scattering experiments that are able to get nucleons very close together, when only then the nuclear force comes into play. Note how, on Fig. 1.1 the lowest energy scattering presents a flat differential crossection. That implies that the nuclear force does not

[1] High energy relative to nuclear parameters such as, say, the mass of the pion.

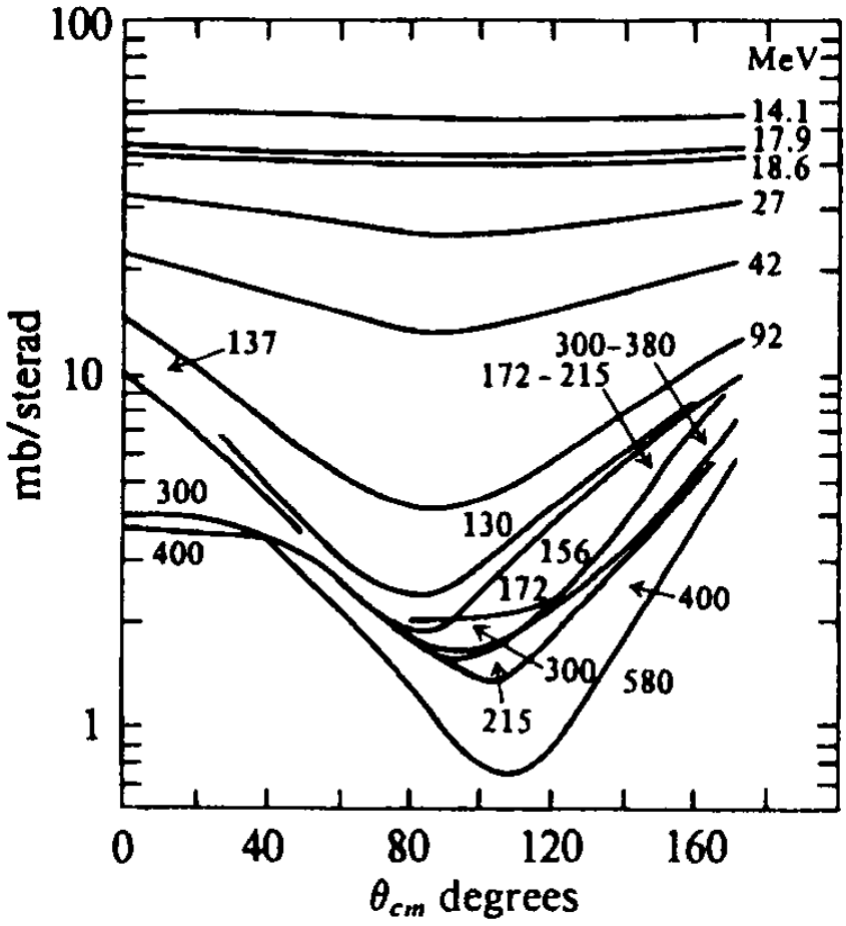

Figure 1.1: Neutron-Proton scattering cross-sections from ref. [65]

kick in until the bodies are very close together. All the evidence points to it having a range of only a few Fermi or "femtometers" (fm= 10^{-15}m).

Scattering experiments also tell us, however, that the force must be repulsive at even shorter distances.

- Repulsive

So at very close proximity, much less than the broader nuclear range of a few Fermi, the potential has been determined to be highly repulsive. As an example we can look at the central part of the Reid Potential (see ref. [66]) shown on Fig. 1.2 which was designed to reproduce nucleon-nucleon

scattering data

$$V_{\text{Reid}}(r) = -10.463\frac{e^{-\mu r}}{\mu r} - 1650.6\frac{e^{-4\mu r}}{\mu r} + 6484.2\frac{e^{-7\mu r}}{\mu r}$$

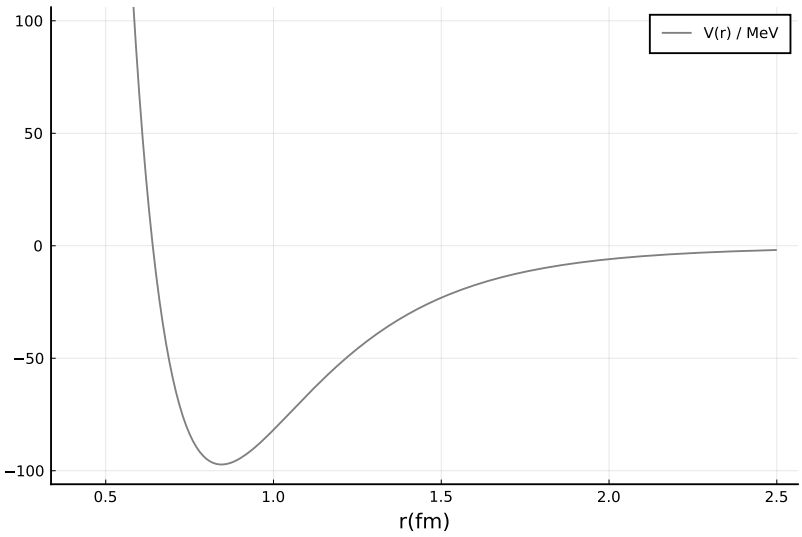

Figure 1.2: Reid Potential for $\mu = 0.7\text{fm}^{-1}$.

Many important properties come from this form. One of which we will revisit shortly, but it is worth mentioning now. If the force is attractive at a certain distance and repulsive at a shorter distance (which can be seen on the Reid potential by the slope being positive to the right of the minimum and negative to the left of it), it is clear that there will be a point in which the force is zero (the minimum of the potential). Therefore, the nuclear strong force, which is orders of magnitude stronger than the electromagnetic, is also zero at a specific distance. That, alongside some other properties of the interaction and a fundamentally relativistic effect, will give rise to the property of saturation of nuclear matter, which we will discuss in a later section.

Facts about the simplest few-body bound state, the deuteron, also reveal two important properties of such a force. For instance, the deuteron ground state is a superposition of two states with different orbital angular

momenta, ${}^3S_1 + {}^3D_1$. It has total angular momentum 1 and it has a non-zero quadrupole moment. That indicates that the force cannot simply be spherically symmetric and that is likely spin dependent.

- Spin Dependent
- Anisotropic

Of course it is needless to say that the anisotropy and spin dependence of the nuclear force can also be seen in scattering experiments as well as most other properties.

1.1.2 Spin and Isospin

Following a similar argument to Landau's in [44], we can use the following evidence to write general a spin-dependent, anisotropic potential. First of all, although the potential itself is not spherically symmetric, nothing prohibits that one of its components could in fact be simply a function of $r = |\vec{r}|$. Therefore, the general form should include a $V_1(r)$ central potential. Spin dependence may come in many ways, since the potential has to be scalar, the combination $\vec{s}_1 \cdot \vec{s}_2$ is one possibility. However, two spin vectors can make up two different linearly independent scalar combinations, another possibility would be $(\vec{s}_1 \cdot \vec{n})(\vec{s}_2 \cdot \vec{n})$ where $\vec{n} = \vec{r}/r$ and that also takes care of our anisotropy. The potential so far looks like

$$\hat{V}(r) = \hat{V}_1(r) + \hat{V}_2(r)(\vec{s}_1 \cdot \vec{s}_2) + \hat{V}_3(r)(\vec{s}_1 \cdot \vec{n})(\vec{s}_2 \cdot \vec{n}) + \cdots \tag{1.1}$$

There is, however, something else. We have mentioned that the interaction is spin dependent, however, isospin dependence we have not yet discussed. Isospin is a quantum number that obeys an algebra mathematically identical to spin, hence the name isospin. Like spin, isospin is a vector, the quantum number characterising its magnitude is "1/2" and we tend to write our states as eigenstates of both the magnitude and the z projection. The nucleon is a particle with isospin 1/2 and, when the isospin is up the nucleon manifests itself as a proton, when it is down it is a neutron.

The question now is, could the nuclear interaction be isospin dependent? The evidence for that is rather latent compared with the previous

properties we discussed. However it has been found that the interaction is indeed isospin dependent but to a very good approximation rotationally invariant in isospace (see for instance [12]). Therefore isospin dependent terms such as $(\vec{\tau}_1 \cdot \vec{\tau}_2)$ and $(\vec{\tau}_1 \cdot \vec{n})\,(\vec{\tau}_2 \cdot \vec{n})$ and other combinations with both spin and isospin dependence, e.g. $(\vec{\tau}_1 \cdot \vec{\tau}_2)\,(\vec{s}_1 \cdot \vec{s}_2)$ and so on are allowed. These terms can be added to 1.1 as well as others (such as spin-orbit terms) to describe different observed phenomena about nuclear interactions. The point here is that the nuclear force is a combination of these linearly independent potentials, each with a different nature.

Finally, this discussion is exclusive to two bodies. In general, there could be many-body forces at play which severely complicates our modelling. Let us then skip some historically important steps in the investigations of the nuclear force and talk about the so called meson theory of nuclear interactions.

1.2 Mesons

The example potential in Fig. 1.2 is a sum of three terms with similar functional form. The Yukawa potential

$$V_{\text{Yukawa}}(r) = g^2 \frac{e^{-\mu r}}{r}. \tag{1.2}$$

Hideki Yukawa proposed in 1935 [93] that the nuclear force would be shaped as such. This accounts for the short-range nature of the interaction (the exponential) and can be attractive or repulsive by a change of sign. Reid [66] used this as a template to create his model.

In a quantum field theory language, forces are mediated by bosons. Yukawa proposed that the nuclear forces are mediated by mesons which give rise to a potential like 1.2. Since most field theory is done in momentum space, the Fourier transform of this potential is more enlightening

$$\mathcal{F}[V_{\text{Yukawa}}] \propto \frac{g^2}{\vec{k}^2 + m^2}, \tag{1.3}$$

and as the field theory initiate has probably already spotted, something very similar to that[2] is present in the propagator of every massive boson, be it a Lorentz scalar or vector, isospin carrying or not. Mesons that propagate like 1.3 mediate the nuclear force and all of them will give rise (in configuration space) to a potential that carries a term like 1.2. It is also known that an interaction such as the electromagnetic force which is mediated by a vector boson gives rise to spin-orbit terms and other spin dependent properties. The pieces for putting together the potential in 1.1 are coming together. Different mesons take care of different properties that we enumerated above. For instance, the first term $V_1(r)$ comes from a spin zero massive boson, the second and third could be associated with a massive vector boson, and the isospin dependent terms to mesons for which the coupling to the nucleon is isospin dependent.

1.2.1 Sigma

As mentioned above, the V_1 part of 1.1 is due to a Lorentz scalar massive boson that couples to the nucleon indifferently of its isospin, which is equivalent to say that it is an isoscalar meson. The σ meson is the elected representative of the scalar-isoscalar sector. It is a massive, spin zero, isospin zero boson that couples to the nucleon with a minimal Yukawa coupling $\mathcal{L}_I = g_\sigma \bar{\Psi}\sigma\Psi$. That is, its equation of motion will be

$$(\partial_\mu \partial^\mu - m_\sigma^2)\sigma = g_\sigma \bar{\Psi}\Psi \tag{1.4}$$

One important point to mention is that what is comonly referred to as the σ meson is the entire scalar-isoscalar sector which is more than one particle. The $f_0(500)$ meson is a real particle and it is sometimes referred to as σ. However, in a more general sense the sigma meson represents all exchanges which yield a scalar nuclear interaction. For instance, two pion exchanges such as

[2] Or exactly like that if we consider the so called static field approximation for the meson propagators.

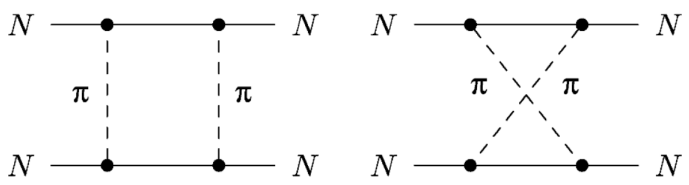

have a strong scalar component [41]. That, added to other scalar contributions from other interactions and added to $f_0(500)$ exchange compose what is most commonly referred to as the σ. Therefore, its mass is commonly used as a parameter to be fitted by data generally and not simply set as 500MeV which is the mass of the $f_0(500)$.

1.2.2 Omega

The ω meson is a vector-isoscalar meson, ω^μ, satisfying the wave equation

$$(\partial_\mu F_\omega^{\mu\nu} - m_\sigma^2)\omega^\nu = g_\sigma \bar{\Psi}\gamma^\nu\Psi \tag{1.5}$$

where $F_\omega^{\mu\nu} = \partial^\mu\omega^\nu - \partial^\nu\omega^\mu$. Its mass is measured to be ~ 782MeV and its lifetime $(7.75 \pm 0.07) \times 10^{-23}$ seconds.

1.2.3 Rho

The ρ meson is a vector-isovector meson. That is, it is similar to the ω as it is a Lorentz vector but it does carry isospin and it also carries electric charge. It satisfies the wave equation

$$(\partial_\mu F_\rho^{\mu\nu} - m_\rho^2)\boldsymbol{\rho}^\nu = g_\rho \bar{\Psi}\boldsymbol{t}\gamma^\nu\Psi \tag{1.6}$$

where $F_\rho^{\mu\nu} = \partial^\mu\rho^\nu - \partial^\nu\rho^\mu$. Its mass is measured to be ~ 775MeV and its lifetime $(4.41 \pm 0.02) \times 10^{-24}$ seconds. Here, for a nucleon, $\boldsymbol{t} = \boldsymbol{\tau}/2$, where $\boldsymbol{\tau}$ represents the Pauli matrices of isospin algebra. As indicated by the bold symbol, the ρ is a vector in isospin space and the three components of this vector can be put on a basis of raising and lowering operators in isospin space plus the isospin z component, i.e. $\boldsymbol{t} = (t^+, t^-, t^z)$ where $\pm$ represent raising and lowering of isospin. In fact $\boldsymbol{\rho} = (\rho^+, \rho^-, \rho^0)$. Respectively, they also carry electric charge +1,-1 and 0.

1.2.4 Delta

In the scalar sector we also have, the δ meson, which is a scalar-isovector meson. The $a_0(980)$ meson is its most prominent contribution. Its equation of motion is

$$(\partial_\mu \partial^\mu - m_\delta^2)\boldsymbol{\delta} = g_\rho \bar{\Psi} \boldsymbol{t} \Psi. \tag{1.7}$$

The delta is not electrically charged. Much like the ρ it is a vector in isospin space $\boldsymbol{\delta} = (\delta^+, \delta^-, \delta^0)$.

1.2.5 Pion

The pion is a very important meson. It is the lightest and therefore represents the longest range part of the nuclear force. The pion is a pseudoscalar-isovector meson

$$(\partial_\mu \partial^\mu - m_\pi^2)\boldsymbol{\pi} = g_\pi \partial^\mu \left(\bar{\Psi} \gamma_\mu \gamma_5 \boldsymbol{\tau} \Psi\right). \tag{1.8}$$

However, one other thing that sets it apart from the others is the fact that it does not have a mean field $\langle \pi \rangle = 0$, because $\left\langle \bar{\Psi} \gamma_\mu \gamma_5 \boldsymbol{\tau} \Psi \right\rangle = 0$, unless parity is violated. This makes it so that its contribution in nuclear matter is significantly smaller than the other mesons. Moreover, as discussed above, two pion exchanges are already taken care of by the scalar sector.

1.3 Nuclear Matter

As mentioned above, two important ways to probe the nuclear force are the study of scattering experiments of nucleons and light nuclei and the structure of simple few-body bound states such as the deuteron. There is, however, much more to nuclear physics than just these systems. In fact, some of the most interesting systems are what is usually called many body systems such as heavier nuclei.

Consider a system of many nucleons in which the separation between the protons and neutrons is on average much smaller than the system itself such as a large nucleus. It is a characteristic of these many body systems

that the density of nucleons inside the system quickly reaches a plateau and becomes constant. Figure 1.3 shows an example of that. This is because

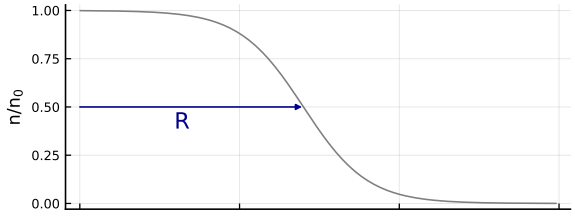

Figure 1.3: Sketch of density profile of large nuclei

of the property alluded to a few pages earlier, the so called saturation of nuclear matter. By looking at 1.2 we observe that the potential has a minimum and thus there is a separation at which the potential energy is minimised (aside from a constant). That is the origin of the behaviour in Fig. 1.3. The nucleons tend to stay at such a distance from one another that will minimise the interaction energy and consequentially the energy density. Therefore, if one would add another neutron to the nucleus depicted in Fig. 1.3, making it into a heavier isotope, the nucleus finds it energetically favourable to increase its radius and rearrange its constituents in order to maintain the central density constant. That density is what we call saturation density n_0 and it is roughly $n_0 = 0.16 \pm 0.1\text{fm}^{-3}$.

As mentioned in the previous paragraph the saturation of nuclear matter is a phenomenon that does not differentiate between systems, its density will be more or less the same for the centre of every single nucleus from Oxygen to Calcium to Uranium. Therefore, most properties of nuclei will depend gravely on the properties of nuclear matter. Let us look at a few of those properties.

1.3.1 Binding Energy

Saturation of nuclear matter does not mean that the nucleons are not interacting, they are just arranged in such a way that minimises the interaction energy. However, the nucleons are interacting, and via this interaction are bound to the system. The binding energy is defined as the difference between the energy of the unbound state with the energy of the bound state.

That is, the binding energy of a system of N particles would be just

$$\epsilon = E_{\text{Bound}} - E_{\text{Unbound}} \tag{1.9}$$

If the bound state is a stable bound state, we obviously expect that

$$E_{\text{Bound}} < E_{\text{Unbound}}$$

given that the stable configuration is, by definition, the one that minimises the energy (in static systems). Therefore the binding energy is negative.

Specifically for the saturated state of nuclear matter, the binding energy per nucleon is[3]

$$\mathcal{E} = \frac{\epsilon}{n} = -15.8\text{MeV} \tag{1.10}$$

1.3.2 Symmetry Energy, Slope and Incompressibility

Another known property which we can take from looking at light nuclei with less than ~ 40 nucleons is that these systems tend to prefer roughly equal numbers of protons and neutrons, even though the Coulomb force opposes this tendency. Therefore, there must be some energy dialogue associated with this. Deviations from the symmetric case cause an increase in energy. That is, the preferred case is the symmetric one. This does not mean that, for every nucleus, $Z = A/2$. Obviously that is not the case. However, this is roughly the case for light to mid-range nuclei.

One way of defining the symmetry energy as a function of the baryon number density is by taking the difference of the binding energy in pure neutron matter (nuclear matter composed of neutrons only) with symmetric nuclear matter (number density of protons identical to number density of neutrons) $S(n_B) = \mathcal{E}(n_p = 0, n_N = n_B) - \mathcal{E}(n_p = n_B/2, n_N = n_B/2)$

[3] The uncertainty on this quantity is largely debated, usual values range from -17MeV to -15MeV, however in Ref.[7] it has been claimed it could be as high as -13MeV.

At saturation density the symmetry energy is measured to be

$$S(n_0) = 30 \pm 2\text{MeV}. \tag{1.11}$$

Derivatives of the symmetry energy with respect to number density are also measurable and are also some of the most important bulk properties of nuclear matter. Finding out and measuring the exact value of these derivative quantities is of extreme value to nuclear physics. From nuclei to neutron stars, a lot can be said about the properties of nuclear systems by these numbers alone. Measurements of the so called slope $L(n_B) = 3n_B\left(\frac{\partial \mathcal{S}}{\partial n_B}\right), L_0 \equiv L(n_0)$ and incompressibility $K_{\text{sym}} = 9n_0^2\left(\frac{\partial^2 \mathcal{S}}{\partial n_B^2}\right)_{n_B=n_0}$ have been attempted many times, however the results tend to have large errors and are a little bit all over the place. Compilations of different measurements and predictions can be found in [77] and [48], however for the intents and purposes of this thesis we can say that, roughly

$$L_0 = 60 \pm 20\text{MeV}, \quad K_{\text{sym}} = 240 \pm 20\text{MeV} \tag{1.12}$$

1.4 Quarks, Gluons and Confinement

In the course of the many puzzling discoveries made by nuclear physicists, many other manifestations of this nuclear strong force appeared, the number of known mesons multiplied, the concept of strangeness came to be, and heavier versions of the nucleon – the so called Δ baryons – with different spin and isospin started to show up. In the midst of this confusion, Gell-Mann [23] devised what at first seemed to be a bookkeeping device to make sense of this: the quark. A new quantum number was introduced and mesons and baryons became part of a much more organised scheme. Of course quarks are now considered more than bookkeeping devices and a whole theory of how they interact (Quantum Chromodynamics or QCD) was developed. For the purpose of this chapter, little or nothing is needed on the details of QCD. We will revisit this topic in a future chapter. Readers interested in a more ample and comprehensive historical and phenomenological account of this topic can also refer to Ref. [29] as an excellent introduction.

1.4.1 Baryons and Mesons as Bags

According to the quark model, mesons are composed of one quark and one anti-quark. baryons are composed of three quarks, and anti-baryons are composed of three anti-quarks. The new quantum number that Greenberg (in 1964) and Nambu (in 1966) introduced was the "colour" of the quarks. Each quark carries a colour charge of r, g, or b (in reference to the colours red, green and blue) and anti-quarks carry $\bar{r}, \bar{g}, \bar{b}$ anti colours. The way quarks interact with each other is via the exchange of gluons, which are also colour charged, obeying the theory of QCD. One of the most impactful properties of this theory is that quarks are permanently confined to the hadrons, meaning that hadrons are not simply bound states of quarks. Unlike atoms which are bound states of electrons where one could ionise an atom by knocking an electron out, quarks are permanently confined in the sense that they can never be unbound.

One attempt to model such a system was the so called MIT bag model [16]. In its simplest form it describes three fermions (the quarks) in a infinite spherical well potential (namely, the bag). The quarks bounce off the walls of the bag elastically and do not interact with each other. The idea is that the the potential, or, the bag, models the true interaction of the three quarks in a way that confines them permanently to the system, as an infinite well does. The model was rather successful, specially considering its simplicity and it is still used till this day in many types of calculations. The true physics of a hadron is vastly more complicated than that. However, for our intents and purposes, the bag model is quite adequate. In fact, full QCD calculations done on the lattice actually support these assumptions of the bag model. On 1.4 we can see some visualisations of these lattice calculations done in [9]. The quarks are overlaid to a surface plot which shows the value of the action density. We can see that, while the quarks remain closer to the centre, the system is perfectly spherically symmetric and the action density outside the system is flat and stable. When the quarks are distanced from each other we have the formation of the flux tubes which draw the quarks back to the stable spherically symmetric position. In some sense, that is the bag, only in the bag model what brings the quarks back is a hard wall. We will see shortly an example of a calculation using

the bag model.

1.5 Studying the Nuclear Force

What we have discussed so far about the strong nuclear force is all based on observations. Fundamentally, all we can do is design experiments that will enlighten us to how quantum systems bound by this potential work. Traditionally, we have a few ways of probing such systems and they all fall neatly into three categories. We can observe properties of bound systems such as the deuteron, triton, and other nuclei; design scattering experiments either to see how these bound systems break up and gather data to help infer the individual nucleon-nucleon potential; or we can do our best to study unbound systems in the laboratory. The latter usually entails designing an experiment involving a many body state, a system large enough, dense enough or hot enough such that the forces between the particles will be averaged.

Let us look at these three approaches for the more familiar case of electromagnetism. In studying bound states we can solve the Schrödinger equation for, say, a hydrogen atom, and design experiments to test the properties of the hydrogen atom, such as its light emission and absorption spectrum. We can design scattering experiments, such as Rutherford's in which he determined the charge of the nucleus, or experiments designed to ionise atoms by bombarding them with electrons or photons. Or alternatively we can study electron gasses or super hot plasmas, systems in which the particles are unbound, and measure their properties, thermodynamical behaviours, etc.

The same can be done for nuclear physics. Bound states being nuclei and scattering experiments being done in an immense variety of ways at facilities such as Jefferson Lab, Argonne National Lab, the Large Hadron Collider, and many others. The case of unbound nucleons, however, is rather complicated. The strong force is strong enough to be utterly indifferent to temperatures below 10^{10}K and, as we have seen, the property of saturation of nuclear matter also puts the scale of density at a rather large

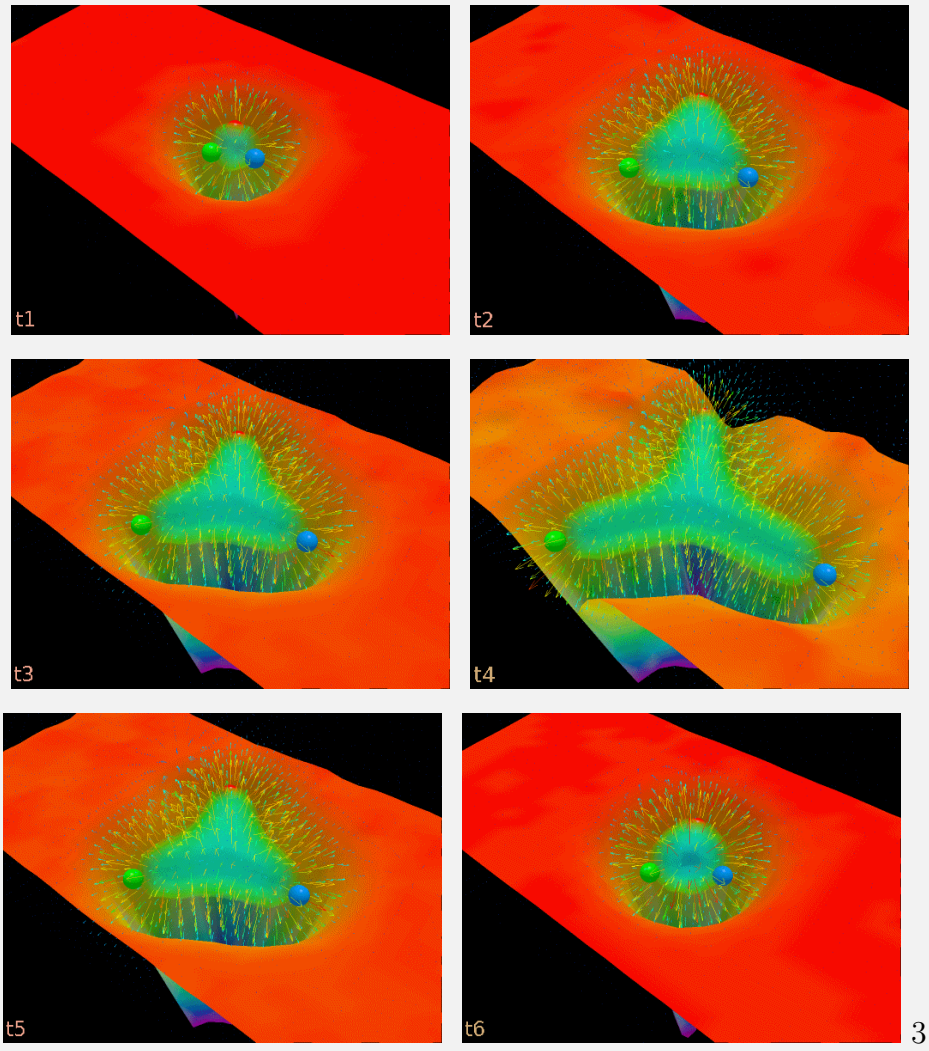

Figure 1.4: Lattice calculations of baryon structure. Ref. [9]. Time indicated in the lower left corner. One can clearly see that it deviates and then returns to a mostly spherical bag-like structure.

value given that the saturation mass density is $2.04 \cdot 10^{17} \mathrm{kg/m^3}$. Fortunately, there is a naturally occurring phenomenon that gives us exactly what we need, a system with densities well above nuclear saturation and, at times, temperatures well above 10^{10}K, namely, neutron stars.

The density in the core of a neutron star can go above five times nuclear matter density. We will not deal with temperature effects in this thesis, however, at times, neutron stars can be far hotter than the minimum necessary to affect the nuclear force. These systems are extremely important as they give us invaluable information that is otherwise impossible to attain. The next chapter is devoted entirely to neutron star phenomenology, however, in order to study such systems we must have a model for nuclear interactions. The next part of this chapter exposes one such model.

Chapter 2

The Quark-Meson Coupling Model

This chapter provides a detailed review of the Quark-Meson Coupling (QMC) model and a calculation of the energy density of infinite nuclear matter in the Hartree-Fock approximation.

2.1 A Model for Nuclear Interactions

In this section we will go much more in depth on the modelling of the physics of nuclear interactions. We will look into the Quark-Meson Coupling (QMC) model which considers the underlying quark structure of the baryons and how the dense medium affects their properties. At first, We will lay the foundations of the theory for a simpler version of the model, only one scalar meson and only one vector meson, to avoid unnecessary complications on the first exposure. Later we will introduce the isovector mesons and complete the model. Then, we will move on to calculating and discussing the effects of this model and its approach. We will go through the calculation of the energy density of nuclear matter and its properties, which we will use in a later chapter to model neutron star cores.

2.1.1 A Simpler Case

In order to avoid creating extra complications, let's derive the foundations of the QMC model in a simpler version. The so called $\sigma - \omega$ models of nuclear matter contain only the scalar-isoscalar and vector-isoscalar sectors. Let us derive the QMC model as such.

When studying a nucleon embedded in nuclear matter, there are two relevant reference frames we should consider. The Nuclear Matter Rest Frame (NMRF), is the reference frame relative to which the nucleus is at rest. The Instantaneous Rest Frame (IRF) is the frame relative to which the nucleon is at rest, see Figure 2.1. Considering that, in general, the nucleon is moving relative to the NMRF, the following Lorentz transformation relates the coordinates of the two frames.

$$\begin{aligned} r_L &= r'_L \cosh\xi + t' \sinh\xi \\ \vec{r}_\perp &= \vec{r'}_\perp \\ t &= t' \cosh\xi + r'_L \sinh\xi. \end{aligned} \tag{2.1}$$

Where the subscript L denotes the longitudinal direction, the primed coordinates $(t', \vec{r'})$ are the IRF coordinates and the non primed $(t, \vec{r})$ denote the NMRF. Naturally ξ denotes the rapidity and, identically, the relativistic hyperbolical rotation angle of the Lorentz transformation. Also let $\vec{R}(t)$ be

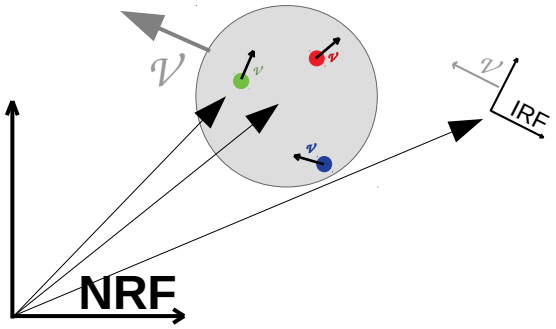

Figure 2.1: Differences between the two types of reference frame. They have a relative velocity and a relative inclination. Note that the spatial dilation occurs only in the direction of movement.

the trajectory of the nucleon in the NMRF and, naturally, $\vec{v} = d\vec{R}/dt$.

We start by describing the internal structure of the nucleon with the MIT bag model, i.e.,

$$\mathcal{L}_0 = \bar{\psi}'_q(i\partial\!\!\!/ - m_q)\psi'_q - \mathcal{B} \quad \text{for } |\vec{u}'| \leq R_B \tag{2.2}$$

Where the primes again denote the IRF. The quark wave functions are evaluated on the variable $\vec{u'}$ which is the quark's relative position to the centre of the bag, in the IRF, i.e. $\vec{u'} = \vec{r'} - \vec{R}'$. Respecting the boundary condition

$$(1 + i\vec{\gamma} \cdot \hat{u}')\psi'_q(\vec{u'}) = 0 \quad \text{at } |\vec{u'}| = R_B \tag{2.3}$$

Then we incorporate scalar meson $\hat{\sigma}(\vec{r})$ and vector meson $\hat{\omega}_\mu(\vec{r})$ field operators. Considering that the entire system is crowded with nucleons all around and every nucleon is a source of meson fields, with that many sources we can assume that at least in a first approximation the meson fields are homogeneous and isotropic. That motivates treating them as mean classical fields $\bar{\sigma}(\vec{r})$ and $\bar{\omega}_\mu(\vec{r}) = (\bar{\omega}(\vec{r}), \vec{0})$. In the IRF they are Lorentz transformed

to

$$\begin{aligned}\bar{\sigma}_{IRF}(u') &= \bar{\sigma}(\vec{r}) \\ \bar{\omega}_{IRF}(u') &= \bar{\omega}\cosh\xi \\ \vec{\bar{\omega}}_{IRF}(u') &= -\bar{\omega}(\vec{r})\hat{v}\sinh\xi.\end{aligned} \tag{2.4}$$

And the interaction Lagrangian in the IRF is

$$\mathcal{L}_I = g^q_\sigma \bar{\sigma}_{IRF}(u')\bar{\psi}'^q(u')\psi'^q(u') - g^q_\omega \bar{\omega}^\mu_{IRF}(u')\bar{\psi}'^q(u')\gamma_\mu\psi'^q(u'), \quad |\vec{u'}| \leq R_B$$

For now on the argument of the quark functions will be omitted. The full Lagrangian is

$$\begin{aligned}\mathcal{L}_0 = \bar{\psi}'_q(i\partial\!\!\!/ - m_q)\psi'_q - \mathcal{B} + g^q_\sigma\bar{\sigma}_I(u')\bar{\psi}'^q\psi'^q - g^q_\omega\bar{\omega}^\mu_I(u')\bar{\psi}'^q\gamma_\mu\psi'^q \\ \forall\ u : |\vec{u'}| \leq R_B\end{aligned} \tag{2.5}$$

Next, since we are mainly concerned with the nucleon physics, we should try and write it all as a function of the nucleon parameters, e.g. the position and momentum of the nucleon, not of the quarks. So say the bag is located at a position, in the IRF, $\vec{R}'$ at time t', in the NMRF they are

$$\begin{aligned}R_L &= R'_L\cosh\xi + t'\sinh\xi \\ \vec{R}_\perp &= \vec{R}'_\perp \\ T &= t'\cosh\xi + R'_L\sinh\xi\end{aligned} \tag{2.6}$$

remembering that the same relation applies for an arbitrary point in the bag

$$\begin{aligned}r_L &= r'_L\cosh\xi + t'\sinh\xi \\ \vec{r}_\perp &= \vec{r'}_\perp \\ t &= t'\cosh\xi + r'_L\sinh\xi\end{aligned} \tag{2.7}$$

and therefore for any point in the bag, that is $\vec{r'} = \vec{u'} + \vec{R'}$, we have

$$\begin{aligned} r_L &= (u'_L + R'_L)\cosh\xi + t'\sinh\xi \\ r_L &= R_L + u'_L\cosh\xi \\ \vec{r}_\perp &= \vec{u'}_\perp + \vec{R'}_\perp. \end{aligned} \tag{2.8}$$

So the meson relations, e.g. $\bar{\sigma}_I(u') = \bar{\sigma}(\vec{r}) = \bar{\sigma}(r_L, \vec{r}_\perp)$, can be written like

$$\bar{\sigma}_I(u') = \bar{\sigma}(r_L, \vec{r}_\perp) = \bar{\sigma}(R_L(T) + u'_L\cosh\xi, \vec{u'}_\perp + \vec{R'}(T)_\perp), \tag{2.9}$$

and similarly for the ω

$$\bar{\omega}^\mu_I(u') = \eta^\mu\bar{\omega}(r_L, \vec{r}_\perp) = \eta^\mu\bar{\omega}(R_L(T) + u'_L\cosh\xi, \vec{u'}_\perp + \vec{R'}(T)_\perp)$$

where $\eta^\mu = (\cosh\xi, -\hat{v}\sinh\xi)$.

For now on we will apply the Born-Oppenheimer approximation and treat the motion of the nucleus and the motion of the nucleons inside the nucleus (i.e. in nuclear matter) as completely independent. That is not exact but it does hold as a good approximation. Also, we are going to neglect contributions of order greater than v in the argument of the meson functions, including $u'_L\cosh\xi \to u'_L$ (for more on this approximation see references [31] and [72]).

So now our Lagrangian density, omitting the meson field energies for simplicity, takes the form

$$\mathcal{L} = \bar{\psi}'_q(i\partial\!\!\!/ - m_q + g^q_\sigma\bar{\sigma}(\vec{R} + \vec{u'}) - g^q_\omega\bar{\omega}(\vec{R} + \vec{u'})\eta^\mu\gamma_\mu)\psi'_q - \mathcal{B}. \tag{2.10}$$

Applying a Legendre transformation we get a Hamiltonian,

$$\begin{gathered} \mathcal{H}(x^\mu;\phi,\pi) = \dot{\phi}\pi - \mathcal{L}(x^\mu;\phi,\partial\phi), \quad \pi = \frac{\partial\mathcal{L}}{\partial_0\phi} \\ \Downarrow \\ \mathcal{H} = \bar{\psi}'_q(-i\vec{\gamma}\cdot\vec{\nabla} + m_q - g^q_\sigma\bar{\sigma}(\vec{R} + \vec{u'}) + g^q_\omega\bar{\omega}(\vec{R} + \vec{u'})\eta^\mu\gamma_\mu)\psi'_q + \mathcal{B}. \end{gathered} \tag{2.11}$$

and a total Hamiltonian which is $H = \int_0^{R_B} d^3u'\ \mathcal{H}$.

Since the meson field variations are expected to be small across the bag, we can separate the Hamiltonian into a leading part and a small perturbation, expanding about the centre value,

$$\bar{\sigma}(\vec{R}+\vec{u'}) = \underbrace{\bar{\sigma}(\vec{R})}_{\text{leading term}} + \underbrace{\bar{\sigma}(\vec{R}+\vec{u'})-\bar{\sigma}(\vec{R})}_{\text{small perturbation}} \tag{2.12}$$

therefore

$$\begin{aligned}
&\mathcal{H} = \mathcal{H}_0 + \mathcal{H}_1 \\
&\mathcal{H}_0 = \bar{\psi}'_q(-i\vec{\gamma}\cdot\vec{\nabla} + m_q - g^q_\sigma\bar{\sigma}(\vec{R}) + g^q_\omega\bar{\omega}(\vec{R})\eta^\mu\gamma_\mu)\psi'_q + \mathcal{B} \\
&\mathcal{H}_1 = \bar{\psi}'_q\left[-g^q_\sigma\left(\bar{\sigma}(\vec{R}+\vec{u'})-\bar{\sigma}(\vec{R})\right) + g^q_\omega\left(\bar{\omega}(\vec{R}+\vec{u'})-\bar{\omega}(\vec{R})\right)\eta^\mu\gamma_\mu\right]\psi'_q + \mathcal{B}.
\end{aligned} \tag{2.13}$$

Now what we want to do is find a useful basis for the quark fields (e.g. $\psi = \sum_a c_a\phi_a$). Particularly we know that it makes sense to expand it in eigenfunctions of the Dirac equation with the appropriate boundary conditions for the bag model, that is, functions ϕ that satisfy

$$\begin{aligned}
&\left(-i\gamma^0\vec{\gamma}\cdot\nabla + \gamma^0 m^*\right)\phi(\vec{u'})^\alpha = \frac{\Omega_\alpha}{R_B}\phi(\vec{u'})^\alpha \\
&(1+i\vec{\gamma}\cdot\hat{u'})\phi'_q(\vec{u'}) = 0, \quad \text{at } |\vec{u'}| = R_B \\
&\int_{V_B} d^3u'\ \phi^i\phi^j = \delta^{ij}
\end{aligned} \tag{2.14}$$

which leads to, for instance for the lowest energy level,

$$\phi^{0m}(t',\vec{u'}) = \frac{\mathcal{N}}{\sqrt{4\pi}}\begin{pmatrix} j_0(xu'/R_B)\chi_m \\ -\beta_q\vec{\sigma}\cdot\hat{u'}j_1(xu'/R_B)\chi_m \end{pmatrix} \tag{2.15}$$

where js represent spherical Bessel functions, m^* is just a parameter at this point (which we will later identify with the effective mass), χ_m is a spin matrix, and the parameters Ω_α, $\mathcal{N}$ and β_q are defined as, say, for the

zero-th energy mode

$$\begin{aligned}
\Omega_0 &= \sqrt{x^2 + (m^* R_B)^2} \\
\beta_q &= \sqrt{\frac{\Omega_0 - m^* R_B}{\Omega_0 + m^* R_B}} \\
\mathcal{N}^{-2} &= 2R_B^3 j_0^2(x) \left[\Omega_0(\Omega_0 - 1) + m^* R_B/2\right] / x^2 \\
x &\leftarrow \text{solve: } j_0(x) = \beta(x) j_1(x)
\end{aligned} \tag{2.16}$$

Using this basis we can construct a function (with a fixed momentum shift $\vec{k}$ to account for the movement of the medium)

$$\psi'_q(t', \vec{u'}) = \sum_\alpha b_\alpha(t') \phi^\alpha(\vec{u'}) e^{-i\vec{k}\cdot\vec{u'}} \tag{2.17}$$

that behaves in such way that the action of the $-i\gamma^0\vec{\gamma}\cdot\vec{\nabla}$ operator results in

$$-i\gamma^0\vec{\gamma}\cdot\vec{\nabla}\psi'_q = \left(-\gamma^0\vec{\gamma}\cdot\vec{k} + \frac{\Omega_\alpha}{R_B} - \gamma^0 m^*\right)\psi'_q. \tag{2.18}$$

Note that there is no sum in the momentum, actually the momentum is a fixed value, there is only a sum in α. Now that we have that we can write the total non-perturbed Hamiltonian (in the IRF) as

$$\begin{aligned}
H_0 = \sum_{\alpha\beta} b_\alpha^\dagger b_\beta \langle\alpha| \Bigg(-\gamma^0\vec{\gamma}\cdot\vec{k} + \frac{\Omega_\alpha}{R_B} - \gamma^0 m^*\Bigg) + \left(m_q - g_\sigma^q \bar{\sigma}(\vec{R})\right)\gamma^0 \\
+ g_\omega^q \bar{\omega}(\vec{R}) \cosh\xi + g_\omega^q \gamma^0\vec{\gamma}\cdot\hat{v}\bar{\omega}(\vec{R}) \sinh\xi |\beta\rangle + \mathcal{B}V_B,
\end{aligned} \tag{2.19}$$

where the average of an operator over these eigenstates of the Dirac operator is simply $\langle i|\hat{A}|j\rangle = \int_{V_B} d^3u' \ \phi_i^\dagger \hat{A} \phi_j$, and therefore if we identify the momentum and the m^* parameter as

$$\vec{k} = g_\omega^q \bar{\omega}(\vec{R})\hat{v}\sinh\xi \quad \text{and} \quad m^* = m_q^* = m_q - g_\sigma^q \bar{\sigma}(\vec{R})$$

it all gets simplified to

$$H_0 = \sum_{\alpha\beta} b_\alpha^\dagger b_\beta \langle\alpha| \left(\frac{\Omega_\alpha}{R_B}\right) + g_\omega^q \bar{\omega}(\vec{R}) \cosh\xi |\beta\rangle + \mathcal{B}V_B, \tag{2.20}$$

which becomes

$$H_0 = \left(\sum_\alpha \frac{\Omega_\alpha}{R_B} b_\alpha^\dagger b_\alpha \right) + \hat{N}_q g_\omega^q \bar{\omega}(\vec{R}) \cosh\xi + \mathcal{B} V_B. \tag{2.21}$$

And the momentum $\vec{P} = \int_{V_B} d^3u' \; \psi_q'^\dagger [-i\vec{\nabla}] \psi_q'$ in the IRF becomes,

$$\vec{P} = \sum_{\alpha\beta} \langle\alpha| -i\vec{\nabla} |\beta\rangle b_\alpha^\dagger b_\beta - \hat{N}_q g_\omega^q \bar{\omega}(\vec{R}) \hat{v} \sinh\xi. \tag{2.22}$$

However, for a nucleon, we are talking of a specific state of 3 quarks in the lowest energy level (we are not considering excited states as of yet). Therefore we can make this even more simplified

$$H_0 = 3\frac{\Omega_0(\vec{R})}{R_B} + 3 g_\omega^q \bar{\omega}(\vec{R}) \cosh\xi + \mathcal{B} V_B \tag{2.23}$$

$$\downarrow$$

$$H_0 = M_N^*(\vec{R}) + 3 g_\omega^q \bar{\omega}(\vec{R}) \cosh\xi \tag{2.24}$$

$$\text{where} \quad M_N^*(\vec{R}) = 3\frac{\Omega_0(\vec{R})}{R_B} + \mathcal{B} V_B \quad \text{and} \quad \vec{P} = -3 g_\omega^q \bar{\omega}(\vec{R}) \hat{v} \sinh\xi.$$

One extra correction is in order here. By looking at 2.14 we see that Ω_0/R_B is the energy eigenvalue of the quarks. Theoretically, there are gluons and other dynamics inside the nucleon as well and we could take them into account by adding another energy parameter z_0/R_B that represents gluon fluctuations and enters $M^\star$ exactly like Ω_0 does.

$$M_N^*(\vec{R}) = 3\frac{\Omega_0(\vec{R}) - z_0}{R_B} + \mathcal{B} V_B \tag{2.25}$$

Now, the results above are valid in the IRF. However, we want to go to the nuclear rest frame, so the Lorentz transformation

$$\begin{aligned} E &= E^{(IRF)} \cosh\xi + P_L^{(IRF)} \sinh\xi \\ P_L &= P_L^{(IRF)} \cosh\xi + E^{(IRF)} \sinh\xi \end{aligned} \tag{2.26}$$

applied to our case is

$$E_0 = (M_N^*(\vec{R}) + 3g_\omega^q \bar{\omega}(\vec{R}) \cosh\xi) \cosh\xi + (-3g_\omega^q \bar{\omega}(\vec{R}) \sinh\xi) \sinh\xi$$
$$P_L = (-3g_\omega^q \bar{\omega}(\vec{R}) \hat{v} \sinh\xi) \cosh\xi + (M_N^*(\vec{R}) + 3g_\omega^q \bar{\omega}(\vec{R}) \cosh\xi) \sinh\xi$$

Since we work only up to leading order in velocity, using the following identities

$$\begin{aligned} \cosh\xi &= \frac{1}{\sqrt{1-\tanh^2\xi}}, \\ \tanh\xi &= |\vec{v}|, \\ \cosh^2\xi - \sinh^2\xi &= 1, \end{aligned} \tag{2.27}$$

we find that

$$\cosh^2\xi = 1, \quad \sinh^2\xi = 0 \tag{2.28}$$

which at last makes

$$\begin{aligned} E_0 &= M_N^*(\vec{R}) \cosh\xi + 3g_\omega^q \bar{\omega}(\vec{R}) \\ P_L &= M_N^*(\vec{R}) \sinh\xi \;\Rightarrow\; \vec{P} = M_N^*(\vec{R}) \hat{v} \sinh\xi \end{aligned} \tag{2.29}$$

and ultimately, with trivial calculations, we get

$$E_0 = \sqrt{M_N^*(\vec{R})^2 + \vec{P}^2} + 3g_\omega^q \bar{\omega}(\vec{R}). \tag{2.30}$$

Finally, for future convenience, it makes sense to eliminate the $\vec{R}$ parameter given the fact that we will soon want to study the bulk properties of nuclear matter and not of individual nucleons. In that case the mean scalar fields $\bar{\sigma}(\vec{R})$ and $\bar{\omega}(\vec{R})$ do not depend on $\vec{R}$, which means that we can eliminate $\vec{R}$ and put everything as a function of the value of the meson fields at that location

$$E_0 = \sqrt{M_N^*(\bar{\sigma})^2 + \vec{P}^2} + 3g_\omega^q \bar{\omega}. \tag{2.31}$$

Unpacking what we have learnt so far

The result derived above is the foundation of the QMC model. Its derivation may lead us to lose sight of what is important. What that result tells us is the energy of a bag of three quarks (an approximate model of the nucleon) embedded in an environment filled with other nucleons surrounding it. These other nucleons all act as sources of meson fields. The meson field created by the surrounding nucleons changes the wave function of the quarks inside the bag and thus changes the bag's properties. This changes the strength of the coupling to the scalar field and consequentially, the mass becomes a self-consistent function of the surrounding scalar meson field $M^\star(\bar{\sigma})$. That is all.

Exactly How does $M^\star(\bar{\sigma})$ depend on $\bar{\sigma}$?

Keeping up the spirit of eliminating $\vec{R}$ for $\bar{\sigma}$, we know that

$$M_N^*(\bar{\sigma}) = 3\frac{\Omega_0(\bar{\sigma}) - z_0}{R_B} + \mathcal{B}V_B \tag{2.32}$$

$$\text{where} \quad \Omega_0(\bar{\sigma}) = \sqrt{x^2 + (m^*(\bar{\sigma})R_B)^2}. \tag{2.33}$$

For simplicity, let us just hide the $\bar{\sigma}$ argument wherever its not imperative. Now, the way that the quark mass depends on the mean scalar field is $m^\star = m - g_\sigma^q \bar{\sigma}$, the volume of the bag is $V_B = \frac{4}{3}\pi R_B^3$, and the x parameter we can get by solving numerically the Dirac equation boundary condition (see 2.16), which means we can get Ω_0.

That is almost all of the ingredients we need to finally see how our effective mass depends on $\bar{\sigma}$. All we need is a value for the radius of the bag R_B, the gluon fluctuations, also known as zero point energy parameter z_0, and a value for the bag constant $\mathcal{B}$. It is common to use the radius of the bag as a parameter input of the model, using what we know from data of scattering experiments which give a charge radius for the proton of around 0.84fm. We can use that value, however, an argument can be made that lattice data indicates that a radius of around $R_B = 1$fm may be more acceptable (for such an argument see ref. [30]). The point here is that the bag model is not reality, it is a model, so setting up a bag radius becomes

a model parameter. In future calculations I will always disclose the value used, however, it is important to notice how, as long as it is within an acceptable range, it can be chosen freely as a model parameter. There is an alternative to this choice and we will touch on that shortly.

For $\mathcal{B}$, assuming R_B has been chosen, we can basically fit it to a value such that 2.32 will reproduce the mass of the nucleon in free space (that is to say when $\bar{\sigma} = 0$). More explicitly, take

$$\frac{3\sqrt{x^2 + (mR_B)^2} - z_0}{R_B} + \mathcal{B}\frac{4}{3}\pi R_B^3 = 940\text{MeV} \tag{2.34}$$

with, say for instance $R_B = 0.8$fm, and solve for $\mathcal{B}$. This defines $\mathcal{B}$, but we still need z_0. Another linearly independent equation could be used to define it and we choose the fact that the mass, i.e. the energy of a stationary bag, is stable. To be very explicit, stable (and stationary) solutions are defined by being minima of the energy. Therefore, to define z_0 we can choose it such that, in free space, it solves

$$\frac{\partial M^\star}{\partial R_B} = 0. \tag{2.35}$$

If we use that equation to define z_0 we will also be guaranteeing that R_B is the value that minimizes the energy of a stationary bag. So we can solve numerically the equation above for z_0 and the equation for $\mathcal{B}$ to determine those parameters and thus, they are no longer free parameters of the model.

Note also that these could be done backwards, we could have used the equation $M^\star(0) = 940$MeV to define z_0 and the vanishing of the derivative of $M^\star$ with R_B to define $\mathcal{B}$. That would not change the result.

We still have one free parameter. That is the coupling constant of the quark-σ interaction, g_σ^q. For purely practical reasons we will need to relate this with the coupling constant of σ with the nucleon as a whole, i.e. the Yukawa coupling we discussed on Part I, which is much more convenient. That is, the strength with which the nucleon interacts with other nucleons by the exchange of mesons. What we need is an equation that ties g_σ^q with g_σ, where g_σ is the σ-baryon coupling strength in free space. This will be done shortly, however, assuming g_σ^q as our free parameter, we can finally

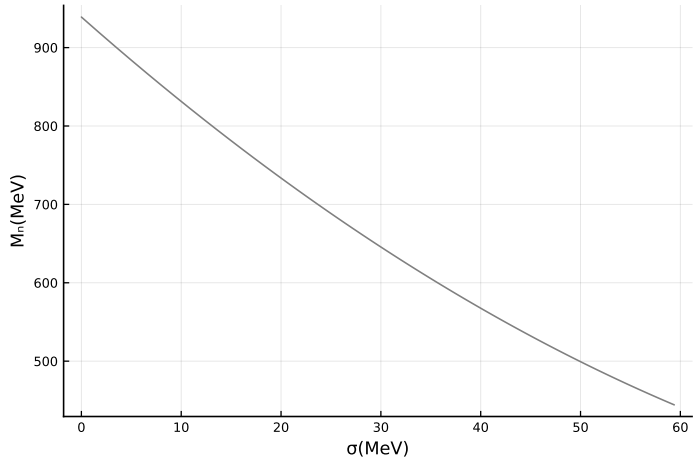

Figure 2.2: Effective mass as a function of the mean σ field for the neutron. The parameters required to reproduce it, including coupling constants and fit parameters for the mass function, will be discussed in the next sections.

see what $M^\star(\bar{\sigma})$ looks like. By setting a value for R_B and g_σ^q we can solve the 2.34 and 2.35 for z_0 and $\mathcal{B}$ and plot the mass as in 2.2. We can fit this to an analytical function and it is well approximated by a parabola. Notably, the term proportional to $\bar{\sigma}$ is going to determine g_σ, the nucleon-σ coupling in free space

$$M^\star(\bar{\sigma}) = M_N - g_\sigma \bar{\sigma} + \frac{d}{2}(g_\sigma \bar{\sigma})^2 \tag{2.36}$$

where $M_N = 940$MeV is the mass of the free nucleon. The d in 2.36 is called the scalar polarizibility and it is a feature of the QMC model. Setting it to zero will recover the so called QHD, or Quantum Hadrodynamics.

As discussed above, having the coupling constant of the quarks with σ a parameter of the model is much less convenient than having as a parameter the nucleon-σ coupling. For that reason, and given that 2.36 is correct for every value of g_σ^q we can choose (it would only change g_σ) it would be nice if we could find an equation that relates one with the other. Looking at 2.36 it is clear that

$$g_\sigma = -\left.\frac{\partial M^\star(\bar{\sigma})}{\partial \bar{\sigma}}\right|_{\bar{\sigma}\to 0} \tag{2.37}$$

unequivocally defines the free σN coupling g_σ. Therefore, we can set g_σ as

a parameter and use this equation together with the equations for z_0 and $\mathcal{B}$ to define g_σ^q (that is, differentiating 2.32 with respect to $\bar{\sigma}$ and solving this equation for g_σ^q having previously set g_σ a priori). This may seem like an unnecessary complication, however, it does pay off in practicality in the future.

2.1.2 Bringing Back the Isovector Sector

As previously discussed, the isovector sector was omitted from the previous calculation and now has to be reintroduced. It isn't hard to see how it would change the calculations, since the δ meson is a Lorentz scalar it will come in much like the σ and the ρ as a Lorentz vector will come in similarly to the ω. The one clarification that has to be done is that the δ as an isovector meson couples differently to the up and the down quark. Therefore, flavour distinction becomes imperative, quark flavour quantum numbers have to be explicit and the calculation just becomes a bit more complicated. The full derivation will be in a subsequent chapter, however, just to highlight some of that effect, the quark masses as a function of the meson fields will be

$$\begin{aligned} m_u^\star &= m_u - g_\sigma^q\bar{\sigma} - \frac{1}{2}g_\delta^q\bar{\delta} \\ m_d^\star &= m_d - g_\sigma^q\bar{\sigma} + \frac{1}{2}g_\delta^q\bar{\delta} \\ \text{or just} \quad m_q^\star &= m_q - g_\sigma^q\bar{\sigma} - I^q g_\delta^q\bar{\delta} \end{aligned} \tag{2.38}$$

where I^q is the quarks isospin $\pm 1/2$.

Since we are already talking about different quark flavours, let's just say that when discussing strange baryons (hyperons) we can use the same approach. For simplicity and motivated by the Zweig rule, we assume that the strange quark does not interact with the σ, the δ, the ρ or the ω. Adding the ϕ meson for instance, which is a vector-isoscalar meson composed of a strange and an anti-strange quarks, could be done. However, adding strange mesons would require adding multiple new free parameters to the model (parameters which would be difficult to fix). Therefore, we choose to leave the strange quark as being completely inert, not interacting with any meson field (that is $m_s^\star(\bar{\sigma}, \bar{\delta}) = m_s$).

Re-deriving the previous results with three different quarks ends up yielding

$$M_N^\star = \frac{\Omega_u N_u + \Omega_d N_d + \Omega_s N_s - z_0}{R_B} + \mathcal{B}V_B, \tag{2.39}$$

where for brevity we are omitting the scalar mean field dependence ($\Omega_q = \Omega_q(\bar{\sigma}, \bar{\delta})$). And we find that the effective mass is well fit by

$$\begin{aligned} M_B^\star(\bar{\sigma}, \bar{\delta}) = M_B - w_{\sigma B} g_\sigma \bar{\sigma} - w_{\delta B} g_\delta \bar{\delta} \times I_B \\ + \frac{d_B}{2}(g_\sigma \bar{\sigma})^2 + d_{2B}(g_\sigma \bar{\sigma})(g_\delta \bar{\delta}) \times I_B \end{aligned} \tag{2.40}$$

where the weights $w_{\sigma,\delta}$ are only not equal to unity for the strange baryons (they are not, however, a linear function of strangeness, given the influence of the hyperfine colour interaction which we will discuss in the next subsection), I_B is the isospin of the baryon (e.g. $I_p = 1/2$, $I_n = -1/2$, $I_{\Sigma^+} = 1$ and so on). For the remaining fit parameters, d_B is commonly referred to as the scalar polarizibility, and d_{2B} is the term that mixes σ and δ. Here the N label was substituted for B, given that this applies to any baryon and not just the nucleon.

With all of that in mind, the energy of the baryon is

$$E_B = \sqrt{M_B^\star(\bar{\sigma}, \bar{\delta})^2 + \vec{P}^2} + 3g_\omega^q \bar{\omega} + g_\rho^q I_B \bar{\rho} \tag{2.41}$$

2.1.3 Extra Corrections to $M^\star(\bar{\sigma})$

Adding extra detail to the description of the baryon is always possible. One thing that so far our model is not able to do is to differentiate, say, the proton from the Δ^+. Given that both are composed of *uud* quarks, 2.39 will give the same mass for both baryons. One thing we can add is single gluon exchanges between the quarks in the bag. This is very important in the QMC model considering the scalar mean-field dependence of the quark effective mass will cause this effect to become mean-field dependent as well. We will not, however, go into much detail about its derivation. References [32] and [68] have detailed descriptions (specially the appendix of reference

[68]). Nevertheless, it can be added, i.e.

$$M_N^\star = \frac{\Omega_u N_u + \Omega_d N_d + \Omega_s N_s - z_0}{R_B} + \mathcal{B} V_B + \Delta E_M \tag{2.42}$$

where ΔE_M symbolises the hyperfine colour interaction.

$$\Delta E_M = 8\alpha_c \sum_{i<j} \left(\frac{\mu_i(R)\mu_j(R)}{R^3} I_{ij} \right) \vec{\sigma}_i \cdot \vec{\sigma}_j \tag{2.43}$$

where [42]

$$\begin{aligned}
\mu_i(R) &= \frac{R}{6} \frac{4\Omega(m_i) + 2Rm_i - 3}{2\Omega(m_i)(\Omega(m_i) - 1) + Rm_i} \\
I_{ij} &= 1 + \frac{-3y_i y_j - 4x_i x_j \sin^2 x_i \sin^2 x_j + x_i x_j K_{ij}}{2\left(x_i \sin^2 x_i - \frac{3}{2} y_i\right)\left(x_j \sin^2 x_j - \frac{3}{2} y_j\right)} \\
K_{ij} &= 2x_i \operatorname{Si}(2x_i) + 2x_j \operatorname{Si}\left(2x_j\right) \\
&\quad - \left(x_i + x_j\right) \operatorname{Si}\left(2x_i + 2x_j\right) - \left(x_i - x_j\right) \operatorname{Si}\left(2x_i - 2x_j\right) \\
y_i &= x_i - \sin x_i \cos x_i, \quad x_i = \sqrt{\Omega(m_i)^2 - (Rm_i)^2}
\end{aligned} \tag{2.44}$$

As a result, by virtue of it depending on the spin of the quarks $\vec{\sigma}_i$, this differentiates excited states of the nucleon and also it gives the model another layer of accuracy. Note that this adds another parameter, the strong coupling α_c. If one desires the different baryons to have different radii we also increase the number of parameters to be determined. However, by extending the model to the full baryon decuplet we now can have several new equations which we can use to determine parameters. Say, for the Λ baryon, which is composed of uds, we can use

$$M_\Lambda^\star(0,0) = 1115.6\text{MeV}$$

to determine the mass of the strange quark m_s, and so on and so forth. The stability condition

$$\frac{\partial M_B^\star}{\partial R_B} = 0$$

can be used to determine each individual baryon radius. The Δ mass $M_{\Delta^0}^\star(0,0) = 1232\text{MeV}$ can be used to eliminate α_c, and thus we end up

with no new parameters but with a much richer model.

The g_ρ^B and g_ω^B couplings

As explained before, having things as a function of the baryonic coupling constants rather then the quark level coupling constants is far more convenient. So as a final point we just need to clarify what will be they be for the vector mesons. For the ω that is simple. We have discussed how the strange quark doesn't couple to anything, but as far as the ω is concerned, the up and the down quarks are identical. Therefore, the baryonic coupling for the omega is simply[1]

$$g_\omega^B = w_B^\omega g_\omega = \left(1 + \frac{s}{3}\right) g_\omega \tag{2.45}$$

where g_ω is the coupling with the nucleon and thus $g_\omega = 3g_\omega^q$.

For the ρ the same ideas apply. However, the fact that its coupling always comes accompanied by the isospin I^B of the baryon basically implies that we can set $g_\rho^q = g_\rho$ where g_ρ is the coupling with the nucleon, and let the isospin factor take care of the rest. This simply follows from the fact that the strange quark doesn't carry isospin and that the isospin of the baryon is simply the sum of the isospins of the non-strange quarks. That is, we could write the baryon flavour independent expression

$$g_\rho^B = g_\rho. \tag{2.46}$$

2.2 Some Remarks on the QMC Family

It is important to say that the QMC model as it was just introduced is not the only version of the model. The confining model, for instance, which here as been taken to be an MIT Bag model infinite square well, can be changed. For instance Refs [Bohr:2015fgc, Panda:2018tax] use the so called Bogoliubov-QMC model where the confining potential is linear. On Ref. [Li:2020dst] the so called Quark-Mean-Field (QMF) model is applied where the quarks are confined by a harmonic potential that mixes the

[1] Obviously this expression only applies to baryons and not anti-baryons.

scalar and vector mean-fields, however the fundamentals of the model are identical to the QMC where the quarks in a baryon interact with quarks on other baryons via the exchange of fundamental meson fields. Another very successful model for low energy QCD is the Nambu–Jona-Lasinio (NJL) model with proper-time regularisation. It has been widely used to simulate confinement and, specifically in Refs [46, 47, 37, 89, 88], it was employed to investigate hadron structure effects in nuclear matter and neutron stars.

2.3 QMC Nuclear Matter

The point of the QMC model, however, is not to study the structure of the hadron. The goal is to study nuclear interactions. For this end we want to write a Lagrangian of fundamental baryons interacting with fundamental baryons via the exchange of mesons. From the point of view of the derivation we just went through, one can think of this step as a "zooming out" and looking at the baryon from farther away, ignoring the quark content of the baryon (the information of which will be contained on the effective mass function).

Fundamentally what we need to do is write a Lagrangian density that yields our previous result for the effective mass of the baryon 2.42 at mean field approximation. So how would that Lagrangian density look? Incidentally one can come up with more than one expression that at mean field approximation will recover the bag energy we had before for a single baryon in medium, meaning, if we wish to go beyond Hartree level there is an arbitrary choice to be made.

Here, we will choose to define the model by making the coupling constants field dependent, i.e.

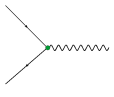

$$= \begin{cases} g_\sigma^B(\sigma,\delta) \text{ for a } \sigma \\ g_\delta^B(\sigma,\delta) \text{ for a } \delta \end{cases} \tag{2.47}$$

where the solid lines are no longer quarks, but rather, baryons. This will become clearer in the next few pages. What we calculated in the section above was an effective mass and not an effective coupling, we will connect the two shortly.

Very importantly, for the vector fields we do not need to do anything special, that dependence on the energy comes from a simple coupling of the nucleon to the meson directly. For the scalar fields we need something that yields an effective mass identical to the one we had before. Take for instance

$$\begin{aligned}\mathcal{L} =&\bar{\Psi}^B\left(i\partial\!\!\!/ - M_B + g^B_\sigma(\sigma,\delta)\sigma + g^B_\delta(\sigma,\delta)\boldsymbol{t}\cdot\boldsymbol{\delta} - g^B_\omega\not{\omega} - g_\rho\boldsymbol{t}\cdot\not{\boldsymbol{\rho}}\right)\Psi^B\\ &+\frac{1}{2}\left(\partial_\mu\sigma\partial^\mu\sigma - m^2_\sigma\sigma^2\right) + \frac{1}{2}\left(\partial_\mu\boldsymbol{\delta}\cdot\partial^\mu\boldsymbol{\delta} - m^2_\delta\boldsymbol{\delta}^2\right)\\ &-\frac{1}{4}\Omega_{\mu\nu}\Omega^{\mu\nu} + \frac{1}{2}m^2_\omega\omega_\mu\omega^\mu - \frac{1}{4}\boldsymbol{R}_{\mu\nu}\cdot\boldsymbol{R}^{\mu\nu} + \frac{1}{2}m^2_\rho\boldsymbol{\rho}_\mu\cdot\boldsymbol{\rho}^\mu.\end{aligned}$$

where the vector meson field tensors are $\Omega_{\mu\nu} = \partial_\mu\omega_\nu - \partial_\nu\omega_\mu$ and $\boldsymbol{R}_{\mu\nu} = \partial_\mu\rho_\nu - \partial_\nu\rho_\mu$ and where $\boldsymbol{t}$ are the isospin matrices for each different baryon, that is, say, for the nucleon (which has total isospin $1/2$) it is $\boldsymbol{t} = \boldsymbol{\tau}/2$ where $\boldsymbol{\tau}$ are the Pauli matrices.

The combination of the mass and the scalar meson terms, the effective mass operator

$$\mathbb{M}^\star_B = M_B - g^B_\sigma(\sigma,\delta)\sigma - g^B_\delta(\sigma,\delta)\boldsymbol{t}\cdot\boldsymbol{\delta}$$

in mean field approximation (where the mean meson fields are denoted by $\bar{\sigma}$ and $\bar{\delta}$ and will be properly defined in the next section) it yields

$$M_B - g^B_\sigma(\bar{\sigma},\bar{\delta})\bar{\sigma} - g^B_\delta(\bar{\sigma},\bar{\delta})I_B\bar{\delta}.$$

Which is what we want (see 2.40) as long as we have

$$\begin{aligned}\mathbb{M}^\star_B =&M_B - g^B_\sigma(\sigma,\delta)\sigma - g^B_\delta(\sigma,\delta)\boldsymbol{t}\cdot\boldsymbol{\delta}\\ =&M_B - \underbrace{\left(g_\sigma + \frac{d}{2}g^2_\sigma\sigma\right)}_{\doteq g_\sigma(\sigma,\delta)}\sigma - \underbrace{\left(+g_\delta - d_2 g_\sigma g_\delta\sigma\right)}_{\doteq g_\delta(\sigma,\delta)}\boldsymbol{t}\cdot\boldsymbol{\delta}\end{aligned} \tag{2.48}$$

This way, as long as we have the coupling functions $g(\sigma,\delta)$ corresponding exactly to 2.40 we have a Lagrangian for baryons in the QMC model. The information of the quark degrees of freedom now is simply contained in the coupling functions.

2.3.1 Meson Equations of Motion

Applying the Euler-Lagrange equations to the Lagrangian above will give us

$$\begin{aligned}
(\partial_\mu \partial^\mu + m_\sigma^2)\sigma &= \sum_B \bar{\Psi}_B \Gamma_\sigma^B(\sigma,\delta)\Psi_B \\
(\partial_\mu \partial^\mu + m_\delta^2)\boldsymbol{\delta} &= \sum_B \bar{\Psi}_B \boldsymbol{\Gamma}_\delta^B(\sigma,\delta)\ \Psi_B \\
(\partial_\mu \Omega^{\mu\nu} + m_\omega^2 \omega^\nu) &= \sum_B g_\omega^B \bar{\Psi}_B \gamma^\nu \Psi_B \\
(\partial_\mu \boldsymbol{R}^{\mu\nu} + m_\rho^2 \boldsymbol{\rho}^\nu) &= \sum_B g_\rho \bar{\Psi}_B \boldsymbol{t} \gamma^\nu \Psi_B,
\end{aligned} \tag{2.49}$$

where

$$\Gamma_\sigma^B(\sigma,\delta) = -\partial_\sigma \mathbb{M}_B^\star \quad \text{and} \quad \boldsymbol{\Gamma}_\delta^B(\sigma,\delta) = -\partial_\delta \mathbb{M}_B^\star. \tag{2.50}$$

It is possible to take the Procca equations (the equations of motion for the ρ and ω mesons) and make them into our typical Klein-Gordon equation by using baryon and isospin current conservations, that is, using

$$\partial_\nu \bar{\Psi}_B \gamma^\nu \Psi_B = 0 \text{ and } \partial_\nu \bar{\Psi}_B \boldsymbol{\tau} \gamma^\nu \Psi_B = 0.$$

on the equations of motion for ρ and ω, after trivial algebra, we obtain

$$\begin{aligned}
(\partial_\mu \partial^\mu + m_\omega^2)\omega^\nu &= \sum_B g_\omega^B \bar{\Psi}_B \gamma^\nu \Psi_B \\
(\partial_\mu \partial^\mu + m_\rho^2)\boldsymbol{\rho}^\nu &= \sum_B g_\rho \bar{\Psi}_B \boldsymbol{t} \gamma^\nu \Psi_B.
\end{aligned} \tag{2.51}$$

In the previous sections we showed how the mass functions (or the coupling constants of the scalar mesons, see 2.48) depend on the meson mean fields. One question that remains to be asked is, how do the meson fields depend on the baryon density? We are now in a position to answer that question. Let us define, without any loss of generality, for any operator, the expansion

$$\hat{\mathcal{O}} = \langle \hat{\mathcal{O}} \rangle + \mathcal{D}\hat{\mathcal{O}} \tag{2.52}$$

where the $\langle \hat{\mathcal{O}} \rangle$ is the mean field value of that operator, also referred to as $\bar{\mathcal{O}}$, and $\mathcal{D}$ represents a functional variation. Simply, $\mathcal{D}\mathcal{O}$ is the operator $\mathcal{O}$

with it's mean removed

$$\mathcal{D}\mathcal{O} = \mathcal{O} - \langle \mathcal{O} \rangle$$

and obviously $\langle \mathcal{D}\mathcal{O} \rangle = 0$. We've just separated one side which contributes to the expectation value and one that doesn't.

Consider for instance the ω meson. Taking its equation of motion

$$(\partial_\mu \partial^\mu + m_\omega^2)\omega^\nu \quad = \sum_B g_\omega^B \bar{\Psi}_B \gamma^\nu \Psi_B \tag{2.53}$$

and separating its mean field component, we obtain an equation for the ω mean field

$$(\partial_\mu \partial^\mu + m_\omega^2) \langle \omega^\nu \rangle \quad = \sum_B g_\omega^B \langle \bar{\Psi}_B \gamma^\nu \Psi_B \rangle . \tag{2.54}$$

The value of $\langle \bar{\Psi}_B \gamma^\nu \Psi_B \rangle$ in nuclear matter at rest is only non zero for $\nu = 0$ and thus, trivially, $\langle \vec{\omega} \rangle = 0$. Calling $\langle \omega^0 \rangle = \bar{\omega}$ we can write

$$m_\omega^2 \bar{\omega} \quad = \sum_B g_\omega^B \left\langle \Psi_B^\dagger \Psi_B \right\rangle . \tag{2.55}$$

Also noting that $\left\langle \Psi_B^\dagger \Psi_B \right\rangle = n_B$ is the number density of the baryon species B and thus we have

$$\bar{\omega} = \sum_B \frac{g_\omega^B}{m_\omega^2} n_B. \tag{2.56}$$

The equation of motion for $\mathcal{D}\omega$ is simply going to be

$$(\partial_\mu \partial^\mu + m_\omega^2)\mathcal{D}\omega^\nu \quad = \sum_B g_\omega^B \mathcal{D} \left[\bar{\Psi}_B \gamma^\nu \Psi_B \right] . \tag{2.57}$$

For the ρ it is trivial to see how the same procedure yields its mean field

$$\bar{\rho} = \sum_B I_B \frac{g_\rho}{m_\rho^2} n_B. \tag{2.58}$$

where again I_B is the isospin of the baryon B.

2.3.2 Self Consistent Scalar Mesons

The scalar mesons are slightly more complicated we can't work them out individually given that their equations of motion are coupled. Take the sigma for instance:

$$(\partial_\mu \partial^\mu + m_\sigma^2)\sigma = \sum_B \bar{\Psi}_B \Gamma_\sigma^B(\sigma, \delta)\Psi_B.$$

Not only the source depends on the σ field itself, it also depends on the δ. Given that the field fluctuations yield small corrections we expand the Γ function around the mean field value for the mesons, that is

$$\Gamma_\sigma^B(\sigma, \delta) = \Gamma_\sigma^B(\bar{\sigma}, \bar{\delta}) + \left(\frac{\partial \Gamma_\sigma^B(\sigma, \delta)}{\partial \sigma}\right)_{\bar{\sigma}} \mathcal{D}\sigma + \cdots \tag{2.59}$$

The term proportional to $\mathcal{D}\sigma$, if maintained, will result on a dynamical correction to the σ mass. That term was maintained in Refs [32, 68, 91] amongst others. We choose to neglect it in here given the fact that if corrections to the meson masses are to be taken into account one would need to also correct the vector meson masses in order for the calculation to be consistent. Furthermore, this correction only fully makes sense if one takes the Fock terms into account in a self-consistent way, which we will not do in this calculation given the fact that it is computationally demanding and that it is numerically minor [91].

The mean field equation for the σ then becomes

$$m_\sigma^2 \bar{\sigma} = \sum_B \Gamma_\sigma^B(\bar{\sigma}, \bar{\delta}) \left\langle \bar{\Psi}_B \Psi_B \right\rangle .$$

The function $\Gamma_\sigma(\bar{\sigma}, \bar{\delta})$ depends on $\bar{\delta}$, therefore, the solution to the mean field σ equation depends on the solution to the δ mean field and vice versa as coupled equations. Note, also, that the $\Gamma_\sigma(\bar{\sigma}, \bar{\delta})$ function could be written as

$$\Gamma_\sigma(\bar{\sigma}, \bar{\delta}) = -\frac{\partial M_B^\star(\bar{\sigma}, \bar{\delta})}{\partial \bar{\sigma}} \tag{2.60}$$

where $M_B^\star$ is simply the mass function of Eq. 2.40.

For the δ it is both similar and different. Neglecting the fluctuation terms on the Γ_δ we have

$$\mathbf{\Gamma}^B_\delta(\sigma,\delta) = \mathbf{\Gamma}^B_\delta(\bar{\sigma},\bar{\delta}) \tag{2.61}$$

where, explicitly, for the δ_0 component we will have

$$\Gamma^B_{\delta_0}(\bar{\sigma},\bar{\delta}) = -\frac{\partial M^\star_B(\bar{\sigma},\bar{\delta})}{\partial\bar{\delta}} \tag{2.62}$$

and for the $\delta_\pm$ component we will have

$$\Gamma^B_{\delta_\pm}(\bar{\sigma},\bar{\delta}) = g^B_\delta(\bar{\sigma},\bar{\delta}). \tag{2.63}$$

all of which follow from trivial algebra that can be derived from the definition of $\mathbf{\Gamma}_\delta$ in Eq. 2.50.

$$\begin{cases} m^2_\sigma\bar{\sigma} = \sum_B \Gamma^B_\sigma(\bar{\sigma},\bar{\delta})\,\langle\bar{\Psi}_B\Psi_B\rangle \\ m^2_\delta\bar{\delta} = \sum_B \left\langle\bar{\Psi}_B\mathbf{\Gamma}^B_\delta(\bar{\sigma},\bar{\delta})\Psi_B\right\rangle \Rightarrow m^2_\delta\bar{\delta} = \sum_B \Gamma^B_{\delta_0}(\bar{\sigma},\bar{\delta})\,\langle\bar{\Psi}_B\Psi_B\rangle\,. \end{cases} \tag{2.64}$$

From now on we will refer to $\Gamma^B_{\delta_0}(\bar{\sigma},\bar{\delta})$ as simply $\Gamma^B_\delta(\bar{\sigma},\bar{\delta})$. As for the ρ meson, in infinite nuclear matter only one component of the delta field has a non-zero expectation value, $\boldsymbol{\delta} = (\delta^+,\delta^-,\delta^0) \to \bar{\boldsymbol{\delta}} = (0,0,\bar{\delta}^0) = \bar{\delta}$. It is quite easy to see this, but just for a matter of completeness, this happens because the $\boldsymbol{\tau}$ matrices act on Ψ_B and, given that $\tau^\pm$ change the isospin of the baryon, the terms involving those matrices will vanish.

So finally, we can write the scalar meson mean fields as

$$\begin{cases} m^2_\sigma\bar{\sigma} = \sum_B \Gamma^B_\sigma(\bar{\sigma},\bar{\delta})\,\langle\bar{\Psi}_B\Psi_B\rangle \\ m^2_\delta\bar{\delta} = \sum_B \Gamma^B_\delta(\bar{\sigma},\bar{\delta})\,\langle\bar{\Psi}_B\Psi_B\rangle \end{cases} \tag{2.65}$$

The average $\langle\bar{\Psi}_B\Psi_B\rangle$ over the Fermi sea is the so called scalar density for a baryon species n^B_s. Calculating the scalar density is simple. Considering

we have only baryons (and no anti-baryons) in our system we can write

$$\Psi(x) = \int \frac{d^3k}{(2\pi)^3} \frac{u(k)a_{ks}}{\sqrt{2E_k}} e^{-i\vec{k}\cdot\vec{x}} \tag{2.66}$$

where $u(k)$ is the Dirac spinor for a fermion of mass $M_B^\star$, and s is the spin. Then it is also trivial to see that

$$\bar{\Psi}(x)\Psi(x) = \int \frac{d^3k}{(2\pi)^3} \frac{\bar{u}(k)u(k)a_{ks}^\dagger a_{ks}}{2E_k} \tag{2.67}$$

remembering that our free Dirac spinors obey the relation $\bar{u}u = 2M$ where M is the mass for the fermion. Then we have

$$\bar{\Psi}(x)\Psi(x) = \int \frac{d^3k}{(2\pi)^3} \frac{M_B^\star}{\sqrt{k^2 + M_B^{\star 2}}} a_{ks}^\dagger a_{ks} \tag{2.68}$$

and the average will yield

$$\langle\bar{\Psi}\Psi\rangle = 2\int \frac{d^3k}{(2\pi)^3} \frac{M_B^\star}{\sqrt{k^2 + M_B^{\star 2}}}. \tag{2.69}$$

One important note is that this makes the meson field equations into non linear self-consistency equations. This is because $M_B^\star(\bar{\sigma}, \bar{\delta})$ and the couplings $g(\bar{\sigma}, \bar{\delta})$ themselves depend on $\bar{\sigma}$ and $\bar{\delta}$ and thus the equations

$$\begin{cases} \bar{\sigma} = \sum_B \dfrac{\Gamma_\sigma^B(\bar{\sigma}, \bar{\delta})}{m_\sigma^2} \dfrac{2}{(2\pi)^3} \displaystyle\int \frac{d^3k}{(2\pi)^3} \frac{M_B^\star}{\sqrt{k^2 + M_B^{\star 2}}} \\ \bar{\delta} = \sum_B \dfrac{\Gamma_\delta^B(\bar{\sigma}, \bar{\delta})}{m_\delta^2} \dfrac{2}{(2\pi)^3} \displaystyle\int \frac{d^3k}{(2\pi)^3} \frac{M_B^\star}{\sqrt{k^2 + M_B^{\star 2}}} \end{cases} \tag{2.70}$$

have to be solved self consistently. This defines the scalar density and we can finally write the meson mean fields explicitly as

Meson Mean Fields

$$\begin{aligned} \bar{\sigma} &= \sum_B \Gamma_\sigma^B(\bar{\sigma},\bar{\delta})\frac{n_s^B}{m_\sigma^2}, \quad \bar{\delta} = \sum_B \Gamma_\delta^B(\bar{\sigma},\bar{\delta})\frac{n_s^B}{m_\delta^2} \\ \bar{\omega} &= \sum_B g_\omega^B \frac{n_B}{m_\omega^2}, \quad \bar{\rho} = \sum_B I_B g_\rho \frac{n_B}{m_\rho^2}. \end{aligned} \tag{2.71}$$

2.3.3 Fluctuation Field Equations

We have solved the equations of motion for the mean fields and managed to express them as a function of the number density of each baryon species and the scalar density which is defined by an integral that is also dependent on the baryon number densities. We now proceed to discuss how to deal with the fluctuation part of the fields and with the full meson fields as well. As we have already discussed the fluctuation equation for the ω field. It reads

$$(\partial_\mu\partial^\mu + m_\omega^2)\mathcal{D}\omega^\nu \;\; = \textstyle\sum_B g_\omega^B \mathcal{D}\left[\bar{\Psi}_B\gamma^\nu\Psi_B\right]. \tag{2.72}$$

Of course, it is trivial to extrapolate that for all other fields and they will read

$$\begin{aligned} (\partial_\mu\partial^\mu + m_\sigma^2)\mathcal{D}\sigma &= \sum_B \Gamma_\sigma^B(\bar{\sigma},\bar{\delta})\mathcal{D}[\bar{\Psi}_B\Psi_B] \\ (\partial_\mu\partial^\mu + m_\delta^2)\mathcal{D}\boldsymbol{\delta} &= \sum_B \mathcal{D}[\bar{\Psi}_B\boldsymbol{\Gamma}_\delta^B(\bar{\sigma},\bar{\delta})\;\Psi_B] \\ (\partial_\mu\partial^\mu + m_\rho^2)\mathcal{D}\boldsymbol{\rho}^\nu &= \sum_B g_\rho\mathcal{D}[\bar{\Psi}_B\boldsymbol{t}\gamma^\nu\Psi_B]. \end{aligned} \tag{2.73}$$

We will need workable expressions for the fluctuation fields and the full meson fields as well. For that reason, let's manipulate one equation as an example and all other equations will follow analogous steps (for more information on dealing with the fluctuations see Ref. [42]). Taking the σ field equation as a template

$$(\partial_\mu\partial^\mu + m_\sigma^2)\sigma = \sum_B \Gamma_\sigma^B(\bar{\sigma},\bar{\delta})\bar{\Psi}_B\Psi_B$$

we can write the solution to the non-homogeneous part of this differential equation by the Green's function method. It states that the non-homogeneous part of the solution to an equation such as

$$Df(x) = g(x),$$

where D is a differential operator and $g(x)$ is the non-homogeneity, can be written as the convolution of its Green function with the non-homogeneity function, i.e.

$$f_{\text{NH}}(x) = \int dx' G(x - x') g(x')$$

where the Green's function for a differential operator is defined as $DG(x - y) = \delta(x - y)$. That is, in our case,

$$\sigma(r) = \sum_B -\Gamma_\sigma^B(\bar{\sigma}, \bar{\delta}) \int d^3r' \int \frac{d^4q}{(2\pi)^4} \frac{e^{-iq\cdot(r-r')}}{q^2 - m_\sigma^2} \bar{\Psi}_B(r') \Psi_B(r')$$

Where the minus sign comes from the derivative of the exponential $i^2 = -1$.

Static Field Approximation

In nuclear physics it is common to take the so called "static field approximation" which basically states that the meson fields do not depend on the time coordinate. In momentum space this means setting q_0 to zero. However, observe that, when a baryon interacts with another exchanging a boson field of momentum q, conservation of momentum tells us that $q = k_1 - k_2$ where $k_{1,2}$ are the momenta of the baryons. This means that the static field approximation basically states that the time component of the baryons four momenta is going to remain unchanged by meson exchange. That is not entirely unreasonable given the fact that its energy $\sqrt{k^2 + M^{\star 2}}$ is overwhelmingly dominated by the mass.

This means that our equations for the meson fields have to be taken at $q^0 = 0$, i.e.

$$\sigma(r) = \sum_B \Gamma_\sigma^B(\bar{\sigma}, \bar{\delta}) \int \frac{d^3q}{(2\pi)^3} \int d^3r' \frac{e^{-iq\cdot(r-r')}}{\vec{q}^2 + m_\sigma^2} \bar{\Psi}_B(r') \Psi_B(r') \qquad (2.74)$$

and an analogous equation is valid for every meson field and their fluctuations. We will use them in determining the energy density of our nuclear matter. For instance, the equation for the fluctuations of the sigma field is

$$\mathcal{D}\sigma(r) = \sum_B \Gamma^B_\sigma(\bar{\sigma},\bar{\delta}) \int \frac{d^3q}{(2\pi)^3} \int d^3r' \frac{e^{-iq\cdot(r-r')}}{\vec{q}^2 + m^2_\sigma} \mathcal{D}[\bar{\Psi}_B(r')\Psi_B(r')] \quad (2.75)$$

and, say, the δ field

$$\delta(r) = \sum_B \int \frac{d^3q}{(2\pi)^3} \int d^3r' \frac{e^{-iq\cdot(r-r')}}{\vec{q}^2 + m^2_\delta} \bar{\Psi}_B(r')\mathbf{\Gamma}^B_\delta(\bar{\sigma},\bar{\delta})\Psi_B(r') \quad (2.76)$$

and its fluctuation term

$$\mathcal{D}\delta(r) = \sum_B \int \frac{d^3q}{(2\pi)^3} \int d^3r' \frac{e^{-iq\cdot(r-r')}}{\vec{q}^2 + m^2_\delta} \mathcal{D}[\bar{\Psi}_B(r')\mathbf{\Gamma}^B_\delta(\bar{\sigma},\bar{\delta})\Psi_B(r')] \quad (2.77)$$

and so on.

2.3.4 Hamiltonian Density

Our goal is to calculate the energy density of nuclear matter, and from it determine other thermodynamical potentials. For that we need to determine the expectation value of the Hamiltonian density, which, by definition, yields the energy density of the system. The energy density is defined as

$$\epsilon = \frac{1}{V} \int d^3r \, \langle \mathcal{H} \rangle \quad (2.78)$$

where V is the volume of the system. In our case, performing the volume integral will simply enforce momentum conservation (via terms like $e^{ir\cdot(k_1+k_2+k_3+\dots)}$ which integrated yield a delta $\delta^4(k_1+k_2+k_3+\dots)$). We can for now on simply enforce momentum conservation whenever we average terms in the Hamiltonian and consider the result integrated in d^4r for convenience.

Without any approximations, the Hamiltonian density is

$$\begin{aligned}\mathcal{H} = \sum_B \bar{\Psi}_B \Big[& -i\vec{\gamma}\cdot\vec{\nabla} + M_B - g_\sigma^B(\sigma,\delta)\sigma - g_\delta^B(\sigma,\delta)\boldsymbol{\delta}\cdot\boldsymbol{t} \\ & + g_{\omega B}\gamma_\mu\omega^\mu + g_{\rho B}\gamma_\mu\boldsymbol{\rho}^\mu\cdot\boldsymbol{t}\Big]\Psi_B \\ & + \frac{1}{2}\dot{\sigma}^2 + \frac{1}{2}\vec{\nabla}\sigma\cdot\vec{\nabla}\sigma + \frac{1}{2}m_\sigma^2\sigma^2 \\ & + \frac{1}{2}\dot{\boldsymbol{\delta}}^2 + \frac{1}{2}\vec{\nabla}\boldsymbol{\delta}\cdot\vec{\nabla}\boldsymbol{\delta} + \frac{1}{2}m_\delta^2\boldsymbol{\delta}^2 \\ & + \Omega_{\mu 0}\dot{\omega}^\mu + \frac{1}{4}\Omega_{\mu\nu}\Omega^{\mu\nu} - \frac{1}{2}m_\omega^2\omega_\mu\omega^\mu \\ & + \boldsymbol{R}_{\mu 0}\cdot\dot{\boldsymbol{\rho}}^\mu + \frac{1}{4}\boldsymbol{R}_{\mu\nu}\cdot\boldsymbol{R}^{\mu\nu} - \frac{1}{2}m_\rho^2\boldsymbol{\rho}_\mu\cdot\boldsymbol{\rho}^\mu\end{aligned} \tag{2.79}$$

We can use the already mentioned relation for the vector meson fields that comes from the conservations of baryonic and isospin current, that is $\partial_\mu\omega^\mu = 0$ and $\partial_\mu\rho^\mu = 0$ and within the static field approximations, the time derivatives will vanish. This simplifies the Hamiltonian significantly.

$$\begin{aligned}\mathcal{H} = \sum_B \bar{\Psi}_B \Big[& -i\vec{\gamma}\cdot\vec{\nabla} + M_B - g_\sigma^B(\sigma,\delta)\sigma - g_\delta^B(\sigma,\delta)\boldsymbol{\delta}\cdot\boldsymbol{t} \\ & + g_{\omega B}\gamma_\mu\omega^\mu + g_{\rho B}\gamma_\mu\boldsymbol{\rho}^\mu\cdot\boldsymbol{t}\Big]\Psi_B \\ & + \frac{1}{2}\left(\vec{\nabla}\sigma\cdot\vec{\nabla}\sigma + m_\sigma^2\sigma^2 + \vec{\nabla}\boldsymbol{\delta}\cdot\vec{\nabla}\boldsymbol{\delta} + m_\delta^2\boldsymbol{\delta}^2\right) \\ & - \frac{1}{2}\left(\vec{\nabla}\omega^\mu\cdot\vec{\nabla}\omega_\mu + m_\omega^2\omega^2 + \vec{\nabla}\boldsymbol{\rho}_\mu\cdot\vec{\nabla}\boldsymbol{\rho}^\mu + m_\delta^2\boldsymbol{\rho}^2\right)\end{aligned} \tag{2.80}$$

In order for us to calculate $\langle\mathcal{H}\rangle$ we need to separate it into convenient bits. First and foremost, we must separate the mean field and the fluctuation terms for the scalar mesons so we can find $M_B^\star$ in the equations. Taking

$$\sigma \to \bar{\sigma} + \mathcal{D}\sigma, \quad \text{and} \quad \boldsymbol{\delta} \to \bar{\delta} + \mathcal{D}\boldsymbol{\delta}$$

taking the first line of 2.80 we can take

$$\sum_B \bar{\Psi}_B \left[-i\vec{\gamma}\cdot\vec{\nabla} + M_B - g_\sigma^B(\sigma,\delta)\sigma - g_\delta^B(\sigma,\delta)\boldsymbol{\delta}\cdot\boldsymbol{t} + g_{\omega B}\gamma_\mu\omega^\mu + g_{\rho B}\gamma_\mu\boldsymbol{\rho}^\mu\cdot\boldsymbol{t} \right] \Psi_B \rightarrow$$
$$\sum_B \bar{\Psi}_B \left[-i\vec{\gamma}\cdot\vec{\nabla} + M_B^\star(\bar{\sigma},\bar{\delta}) \right] \Psi_B$$
$$+ \bar{\Psi}_B \left[g_{\omega B}\gamma_\mu\omega^\mu + g_\rho\gamma_\mu\boldsymbol{\rho}^\mu\cdot\boldsymbol{t} - \Gamma_\sigma^B(\bar{\sigma},\bar{\delta})\mathcal{D}\sigma - \boldsymbol{\Gamma}_\delta^B(\bar{\sigma},\bar{\delta})\cdot\mathcal{D}\boldsymbol{\delta} \right] \Psi_B$$

2.3.5 Remarks on the Baryon Propagator

Our system is basically a fluid of baryons, i.e. fermions, at zero temperature (the strong force is strong enough to be completely indifferent to temperatures below 10^8K). For that reason, it is very useful to calculate the propagator a priori. Take our standard Fermion propagator

$$S(x) = \int \frac{d^4k}{(2\pi)^4}\frac{i}{\not{k} - m}e^{-ik_\mu x^\mu}.$$

It describes both particles and anti particles depending on the how we integrate the k_0 variable. Since in our Fermi sea, we only encounter only fermions and no anti fermions and they are all on shell. Let us specifically extract the relevant part of this propagator there. Using the Feynman presciption, we may write, in momentum space

$$S(k) = \frac{i(\not{k} + m)}{k^2 - m^2 + i\epsilon}. \tag{2.81}$$

This propagator has poles on k_0 space specifically at

$$k_0 = E^\pm = \pm(\sqrt{\vec{k}^2 + m^2} - i\epsilon)$$

where the ϵ has been redefined to absorb some constants. We can then write our propagator as

$$S(x) = \int \frac{d^4k}{(2\pi)^4}\frac{i(\not{k} + m)}{(k_0 - E^+)(k_0 - E^-)}e^{-ik_\mu x^\mu}. \tag{2.82}$$

Since these are first order poles, let's simply integrate out k_0 and we arrive at an on-shell particle (no anti-particles) propagator

$$\begin{aligned} S(x) &= (2\pi i)\int \frac{d^4k}{(2\pi)^4}\frac{i(\not{k}+m)}{2E^+}e^{-ik_\mu x^\mu}\delta(k_0-z^+) \\ &= -\int \frac{d^3k}{(2\pi)^3}\frac{\not{k}+m}{2E^+}e^{-ik_\mu x^\mu}, \end{aligned}$$

where on the last line, it is understood that the remaining factors of k_0 in the numerator and on the exponential argument are all $k_0 = \sqrt{\vec{k}^2+m^2}$ and the integration goes only up to the Fermi momentum for the $k_F(n_B) = \sqrt[3]{3\pi^2 n_B}$. It should be noted that this is not an approximation, this propagator is completely rigorous, it shows how an on shell fermion propagates. I will explicitly state when approximating the expressions.

2.3.6 Part by Part Calculation of $\langle \mathcal{H} \rangle$

Let's start with the easiest, the baryon kinetic part.

$$\mathcal{H}_0 = \sum_B \bar{\Psi}_B \left[-i\vec{\gamma}\cdot\vec{\nabla} + M_B^\star(\bar{\sigma},\bar{\delta})\right]\Psi_B \tag{2.83}$$

We will be averaging these over a Fermi sea filled with baryons that solve the free Dirac equation with an effective mass $M_B^\star(\bar{\sigma},\bar{\delta})$. We need to calculate $\left\langle \bar{\Psi}_B(-i\not{\nabla} + M_B^\star(\bar{\sigma},\bar{\delta}))\Psi_B \right\rangle$. In order to do so, let's simplify this. From the Dirac equation in free space, $(i\not{\partial} - M_B^\star(\bar{\sigma},\bar{\delta}))\Psi_B = 0$ we can see that

$$-i\gamma^0\partial_0\Psi_B = (-i\vec{\gamma}\cdot\vec{\nabla} + M_B^\star(\bar{\sigma},\bar{\delta}))\Psi_B. \tag{2.84}$$

So calculating $\left\langle \bar{\Psi}_B(-i\not{\nabla} + M_B^\star(\bar{\sigma},\bar{\delta}))\Psi_B \right\rangle$ will be identical to calculate

$$-i\left\langle \bar{\Psi}_B\gamma^0\partial_0\Psi_B \right\rangle = -i\left\langle \overbrace{\bar{\Psi}_B\gamma^0\partial_0}\Psi_B \right\rangle.$$

Remembering that $\overbrace{\Psi_B(x_0)\bar{\Psi}_B}(x) = S(x_0 - x)$, since in our case both Ψ_B and $\bar{\Psi}_B$ are evaluated at the same point we need to take the limit as $x_0 \to x$.

This will make

$$-i \lim_{x^\mu \to x_0^+} \mathrm{Tr}\left\{ \int \frac{d^3k}{(2\pi)^3} \frac{(\not{k} + M_{\mathrm{B}}^\star(\bar{\sigma},\bar{\delta}))\gamma^0 \partial_0}{2E^+} e^{-ik_\mu(x_0-x)^\mu} \right\}$$
$$-i \lim_{x^\mu \to x_0^+} \mathrm{Tr}\left\{ \int \frac{d^3k}{(2\pi)^3} \frac{(\not{k} + M_{\mathrm{B}}^\star(\bar{\sigma},\bar{\delta}))\gamma^0 (ik_0)}{2E^+} e^{-ik_\mu(x_0-x)^\mu} \right\}$$
$$\lim_{x^\mu \to x_0^+} \int \frac{d^3k}{(2\pi)^3} \frac{4k_0^2}{2E^+} e^{-ik_\mu(x_0-x)^\mu}.$$

since k_0 is understood (as discussed above) to be $\sqrt{\vec{k}^2 + M_{\mathrm{B}}^\star(\bar{\sigma},\bar{\delta})^2} = E^+$ we have that the result is[2]

$$\langle \mathcal{H}_0 \rangle = \frac{2}{(2\pi)^3} \int d^3k \sqrt{\vec{k}^2 + M_{\mathrm{B}}^\star(\bar{\sigma},\bar{\delta})^2}, \tag{2.85}$$

which is the energy density of the free system of baryons with effective mass $M_{\mathrm{B}}^\star(\bar{\sigma},\bar{\delta})^2$.

Now, let's deal with the meson fields individually. First and foremost, take the ω dependent terms in the Hamiltonian density

$$\mathcal{H}_\omega = \sum_B g_{\omega B} \bar{\Psi}_{\mathrm{B}} \not{\omega} \Psi_{\mathrm{B}} - \frac{1}{2}\left(\vec{\nabla}\omega^\mu \cdot \vec{\nabla}\omega_\mu + m_\omega^2 \omega^2 \right). \tag{2.86}$$

Note that if we integrate by parts the term $\vec{\nabla}\omega^\mu \cdot \vec{\nabla}\omega_\mu$ we obtain, simply

$$\vec{\nabla}\omega^\mu \cdot \vec{\nabla}\omega_\mu \to -\omega^\mu \nabla^2 \omega_\mu \tag{2.87}$$

that is, the second term in 2.86 is

$$-\frac{1}{2}\left(\vec{\nabla}\omega^\mu \cdot \vec{\nabla}\omega_\mu + m_\omega^2 \omega^2 \right) = -\frac{1}{2}\left(-\omega^\mu \nabla^2 \omega_\mu + m_\omega^2 \omega^2 \right). \tag{2.88}$$

If we take the ω field equation of motion (in static field approximation) we have

$$(-\nabla^2 + m_\omega^2)\omega^\mu = g_{\omega \mathrm{B}} \bar{\Psi}_{\mathrm{B}} \gamma^\mu \Psi_{\mathrm{B}} \tag{2.89}$$

[2]Remembering here that the integrals in momentum go up to k_F.

multiply that by ω_μ from the left and we obtain exactly

$$\left(-\omega^\mu \nabla^2 \omega_\mu + m_\omega^2 \omega^2\right) = g_{\omega \mathrm{B}} \bar{\Psi}_{\mathrm{B}} \not{\omega} \Psi_{\mathrm{B}}. \tag{2.90}$$

This way we can conveniently manipulate the Hamiltonian and write

$$\mathcal{H}_\omega = \sum_B \frac{g_{\omega B}}{2} \bar{\Psi}_{\mathrm{B}} \not{\omega} \Psi_{\mathrm{B}} = \sum_B \frac{g_{\omega B}}{2} \omega^\mu \bar{\Psi}_{\mathrm{B}} \gamma_\mu \Psi_{\mathrm{B}}. \tag{2.91}$$

Furthermore, we can use the technique discussed in 2.3.3 to write the meson field as

$$\omega^\mu = \sum_B g_{\omega B}^B \int \frac{d^3q}{(2\pi)^3} \int d^3r' \frac{e^{-iq\cdot(r-r')}}{\vec{q}^2 + m_\omega^2} \bar{\Psi}_B(r') \gamma^\mu \Psi_B(r') \tag{2.92}$$

this way we can further manipulate $\mathcal{H}_\omega$ and write

$$\mathcal{H}_\omega = \sum_{BB'} \frac{g_{\omega B} g_{\omega B'}}{2} \int \frac{d^3q}{(2\pi)^3} \int d^3r' \frac{e^{-iq\cdot(r-r')}}{\vec{q}^2 + m_\omega^2} \bar{\Psi}_B(r') \gamma_\mu \Psi_B(r) \bar{\Psi}_{B'}(r) \gamma^\mu \Psi_{B'}(r').$$

An identical manipulation can be done with the ρ field terms and it trivially yields

$$\mathcal{H}_\rho = \sum_{BB'} \frac{g_\rho^2}{2} \int \frac{d^3q}{(2\pi)^3} \int d^3r' \frac{e^{-iq\cdot(r-r')}}{\vec{q}^2 + m_\rho^2} \bar{\Psi}_B(r') \boldsymbol{t} \gamma_\mu \Psi_B(r) \cdot \bar{\Psi}_{B'}(r) \boldsymbol{t} \gamma^\mu \Psi_{B'}(r').$$

Let us calculate the expectation value of these terms.

Omega

When calculating $\langle \mathcal{H} \rangle$ we have two relevant contractions

$$\begin{aligned} &\left\langle \bar{\Psi}_B(r') \gamma_\mu \Psi_B(r) \bar{\Psi}_{B'}(r) \gamma^\mu \Psi_{B'}(r') \right\rangle \\ &= \left\langle \bar{\Psi}_B \overbrace{(r') \gamma_\mu \Psi_B}(r) \bar{\Psi}_{B'} \overbrace{(r) \gamma^\mu \Psi_{B'}}(r') \right\rangle + \left\langle \bar{\Psi}_B \overbrace{(r') \gamma_\mu \Psi_B(r) \bar{\Psi}_{B'}(r) \gamma^\mu \Psi_{B'}}(r') \right\rangle. \end{aligned}$$

For the first one conservation of momentum will require that $q = k_1 - k_1 = k_2 - k_2 = 0$ and thus we will simply obtain

$$\langle \mathcal{H}_\omega \rangle = \sum_{BB'} \frac{g_{\omega B} g_{\omega B'}}{2} \frac{1}{m_\omega^2} n_B n_{B'} + \cdots \tag{2.93}$$

Note, however, that since $\bar{\omega} = \sum_B g_\omega^B \frac{n_B}{m_\omega^2}$ we can write this more elegantly as

$$\langle \mathcal{H}_\omega \rangle = \frac{m_\omega^2 \bar{\omega}^2}{2} + \cdots \tag{2.94}$$

This is often referred to as the mean field contribution for obvious reasons. The second term, however, is more complicated. It comes from the contraction

$$\begin{aligned} &\left\langle \bar{\Psi}_B(r') \gamma_\mu \Psi_B(r) \bar{\Psi}_{B'}(r) \gamma^\mu \Psi_{B'}(r') \right\rangle = \\ &- \mathrm{Tr}\left\{ \int \frac{d^3k_1}{(2\pi)^3} \frac{d^3k_2}{(2\pi)^3} \gamma_\mu \frac{\not{k}_1 + M_B^\star(\bar{\sigma}, \bar{\delta})}{2E_1} \gamma^\mu \frac{\not{k}_2 + M_B^\star(\bar{\sigma}, \bar{\delta})}{2E_2} \right\} \delta_{BB'} \end{aligned} \tag{2.95}$$

where, as always $E = \sqrt{\vec{k}^2 + M_B^\star(\bar{\sigma}, \bar{\delta})^2}$. The trace in the numerator yields

$$\begin{aligned} &\mathrm{Tr}\{\gamma_\mu(\not{k}_1 + M_B^\star(\bar{\sigma}, \bar{\delta}))\gamma^\mu((\not{k}_2 + M_B^\star(\bar{\sigma}, \bar{\delta}))\} \\ &= \mathrm{Tr}\left\{ \gamma_\mu \not{k}_1 \gamma^\mu \not{k}_2 + 4M_B^\star(\bar{\sigma}, \bar{\delta}))^2 \right\} \\ &= -8k_1 \cdot k_2 + 16M_B^\star(\bar{\sigma}, \bar{\delta}))^2 \end{aligned} \tag{2.96}$$

Therefore, putting it all together, this gives

$$\langle \mathcal{H}_\omega \rangle = \frac{m_\omega^2 \bar{\omega}^2}{2} - \sum_B g_{\omega B}^2 \int \frac{d^3k_1 d^3k_2}{(2\pi)^6} \frac{1}{(\vec{k}_1 - \vec{k}_2)^2 + m_\omega^2} \frac{-k_1 \cdot k_2 + 2M_B^\star(\bar{\sigma}, \bar{\delta}))^2}{E_1 E_2}$$

Where, for clarity, we can expand the term $k_1 \cdot k_2$ in

$$k_1 \cdot k_2 = E_1 E_2 - \vec{k_1} \cdot \vec{k_2} = \sqrt{\vec{k_1}^2 + M_B^{\star 2}} \sqrt{\vec{k_2}^2 + M_B^{\star 2}} - \vec{k_1} \cdot \vec{k_2}$$

Another reasonable approximation that is often used is that the momentum of the baryons is always much smaller than its mass, ergo, $k^2 << M^2$ which

means that

$$\frac{-\sqrt{\vec{k}_1^2+M_B^{\star 2}}\sqrt{\vec{k}_2^2+M_B^{\star 2}}+\vec{k}_1\cdot\vec{k}_2+2M_B^{\star 2}}{\sqrt{\vec{k}_1^2+M_B^{\star 2}}\sqrt{\vec{k}_2^2+M_B^{\star 2}}}\approx\frac{M_B^{\star 2}+\vec{k}_1\cdot\vec{k}_2}{M_B^{\star 2}}\approx 1$$

and that will yield

$$\langle\mathcal{H}_\omega\rangle=\frac{m_\omega^2\bar{\omega}^2}{2}-\sum_B g_{\omega B}^2\int\frac{d^3k_1d^3k_2}{(2\pi)^6}\frac{1}{(\vec{k}_1-\vec{k}_2)^2+m_\omega^2} \quad (2.97)$$

Rho

The ρ is not too dissimilar. In fact, other than the $\boldsymbol{t}$ matrices it is exactly the same.

$$\langle\mathcal{H}_\rho\rangle=\sum_{BB'}\frac{g_\rho^2}{2}\int\frac{d^3q}{(2\pi)^3}\int d^3r'\frac{e^{-iq\cdot(r-r')}}{\vec{q}^2+m_\rho^2}\Big(\Big\langle\bar{\Psi}_B(r')\boldsymbol{t}\gamma_\mu\Psi_B(r)\cdot\bar{\Psi}_{B'}(r)\boldsymbol{t}\gamma^\mu\Psi_{B'}(r')\Big\rangle$$
$$\Big\langle\bar{\Psi}_B(r')\boldsymbol{t}\gamma_\mu\Psi_B(r)\cdot\bar{\Psi}_{B'}(r)\boldsymbol{t}\gamma^\mu\Psi_{B'}(r')\Big\rangle\Big)$$

First and foremost, it is obvious that the first contraction will simply be

$$\left\langle\bar{\Psi}_B(r')\boldsymbol{t}\gamma_\mu\Psi_B(r)\right\rangle\left\langle\bar{\Psi}_{B'}(r')\boldsymbol{t}\gamma_\mu\Psi_{B'}(r)\right\rangle=I_BI_{B'}\left\langle\bar{\Psi}_B(r')\gamma_\mu\Psi_B(r)\right\rangle\left\langle\bar{\Psi}_{B'}(r')\gamma_\mu\Psi_{B'}(r)\right\rangle$$

given the fact that $\boldsymbol{t}=(t^+,t^-,t^0)$ when acting on Ψ will either raise, lower, or in the case of t^0 simply multiply it by I_B given that Ψ is an eigenstate of t^0 with eigenvalue I_B. The terms that were raised/lowered will be zero when contracted with $\bar{\Psi}$ which by definition has a different isospin and thus only the term proportional to I_B will survive. Therefore, the first contraction is trivially

$$\langle\mathcal{H}_\rho\rangle=\sum_{BB'}\frac{g_\rho^2}{2}\frac{1}{m_\rho^2}I_Bn_BI_{B'}n_{B'}+\cdots \quad (2.98)$$

Once more it is not too difficult to see that this can be put as a function of its mean field

$$\left\langle \mathcal{H}_\rho \right\rangle = \frac{m_\rho^2 \bar{\rho}^2}{2} + \cdots \tag{2.99}$$

Now onto the second contraction

$$\sum_{BB'} \frac{g_\rho^2}{2} \int \frac{d^3q}{(2\pi)^3} \int d^3r' \frac{e^{-iq\cdot(r-r')}}{\vec{q}^2 + m_\rho^2} \quad \left(\left\langle \bar{\Psi}_B(r') \boldsymbol{t} \gamma_\mu \Psi_B(r) \cdot \bar{\Psi}_{B'}(r) \boldsymbol{t} \gamma^\mu \Psi_{B'}(r') \right\rangle \right)$$

We can see that the isospin algebra will be more complicated. However, if we explicit the isospin indices we can move the t matrices around. That is

$$\begin{aligned} &\left\langle \bar{\Psi}_B(r')_i \boldsymbol{t}_{ij} \gamma_\mu \Psi_B(r)_j \cdot \bar{\Psi}_{B'}(r)_m \boldsymbol{t}_{mn} \gamma^\mu \Psi_{B'}(r')_n \right\rangle \\ &= \boldsymbol{t}_{ij} \cdot \boldsymbol{t}_{mn} \left\langle \bar{\Psi}_B(r')_i \gamma_\mu \Psi_B(r)_j \bar{\Psi}_{B'}(r)_m \gamma^\mu \Psi_{B'}(r')_n \right\rangle \end{aligned} \tag{2.100}$$

The inner product of the pauli matrices

$$\boldsymbol{t} \cdot \boldsymbol{t} = t_1 t_1 + t_2 t_2 + t_3 t_3 \tag{2.101}$$

when put in the basis of raising and lowering operators is

$$\boldsymbol{t} \cdot \boldsymbol{t} = t_1 t_1 + t_2 t_2 + t_3 t_3 = 2 t_+ t_- + 2 t_- t_+ + t_0 t_0 \tag{2.102}$$

where we rename $t_3 = t_0$. From this expansion and from the fact that the contractions with exposed isospin indices will only be non zero if the baryons have the same isospin, i.e.

$$\left\langle \bar{\Psi}_B(r')_i \Psi_B(r)_j \right\rangle = \delta_{ij} \left\langle \bar{\Psi}_B(r') \Psi_B(r) \right\rangle$$

it is a matter of trivial algebra to calculate the isospin coefficients.

$$\begin{aligned} \boldsymbol{t}_{ij}\cdot\boldsymbol{t}_{mn}\left\langle \bar{\Psi}_B(r')_i\gamma_\mu\Psi_B(r)_j\bar{\Psi}_{B'}(r)_m\gamma^\mu\Psi_{B'}(r')_n\right\rangle \\ = C_{ij}\left\langle \bar{\Psi}_B(r')_i\gamma_\mu\Psi_B(r)_j\bar{\Psi}_{B'}(r)_j\gamma^\mu\Psi_{B'}(r')_i\right\rangle \end{aligned} \tag{2.103}$$

where

$$C_{ij} = \delta_{ij}I_B^2 + I_B(\delta_{i,j+1} + \delta_{i+1,j}) \tag{2.104}$$

Other than this coefficient, the ρ meson contribution is calculated via steps identical to those of the ω. That is

$$\left\langle \mathcal{H}_\rho \right\rangle = \frac{m_\rho^2\bar{\rho}^2}{2} - \sum_{B,i,j} g_\rho^2 C_{ij}\int \frac{d^3k_1 d^3k_2}{(2\pi)^6}\frac{1}{(\vec{k}_1-\vec{k}_2)^2+m_\rho^2} \tag{2.105}$$

where the i,j indices represent the different isospin of each baryon B.

Sigma

For the scalar mesons things are a bit different. Extracting the σ dependent terms in the Hamiltonian density we will find

$$\mathcal{H}_\sigma = \frac{1}{2}\left(-\sigma\nabla^2\sigma + m_\sigma^2\sigma^2\right) - \sum_B \Gamma_\sigma^B(\bar{\sigma},\bar{\delta})\bar{\Psi}_B\mathcal{D}\sigma\Psi_B \tag{2.106}$$

as before we can use the meson's equation of motion and take

$$\frac{1}{2}\left(-\sigma\nabla^2\sigma + m_\sigma^2\sigma^2\right) \longrightarrow \frac{1}{2}\Gamma_\sigma^B(\bar{\sigma},\bar{\delta})\bar{\Psi}_B\sigma\Psi_B$$

However, since the interaction term contains only $\mathcal{D}\sigma$ we need to separate that into two

$$\begin{aligned} \frac{1}{2}\left(-\sigma\nabla^2\sigma + m_\sigma^2\sigma^2\right) \longrightarrow \sum_B \frac{1}{2}\Gamma_\sigma^B(\bar{\sigma},\bar{\delta})\bar{\Psi}_B\sigma\Psi_B \\ \longrightarrow \sum_B \frac{1}{2}\Gamma_\sigma^B(\bar{\sigma},\bar{\delta})\bar{\Psi}_B\bar{\sigma}\Psi_B + \sum_B \frac{1}{2}\Gamma_\sigma^B(\bar{\sigma},\bar{\delta})\bar{\Psi}_B\mathcal{D}\sigma\Psi_B \end{aligned}$$

ergo

$$\mathcal{H}_\sigma = \sum_B \frac{1}{2}\Gamma^B_\sigma(\bar\sigma,\bar\delta)\bar\Psi_B\bar\sigma\Psi_B - \frac{1}{2}\sum_B \Gamma^B_\sigma(\bar\sigma,\bar\delta)\bar\Psi_B\mathcal{D}\sigma\Psi_B \tag{2.107}$$

The average of the first term is quite trivial

$$\sum_B \left\langle \frac{1}{2}\Gamma^B_\sigma(\bar\sigma,\bar\delta)\bar\Psi_B\bar\sigma\Psi_B \right\rangle = \sum_B \frac{1}{2}\Gamma^B_\sigma(\bar\sigma,\bar\delta)\bar\sigma n^s_B = \frac{m_\sigma^2\sigma^2}{2} \tag{2.108}$$

Now, the fluctuation term is (using the Green's function as explained above)

$$-\frac{1}{2}\sum_B \Gamma^B_\sigma(\bar\sigma,\bar\delta)\bar\Psi_B\mathcal{D}\sigma\Psi_B =$$
$$\sum_{BB'}\frac{1}{2}\Gamma^B_\sigma(\bar\sigma,\bar\delta)\Gamma^{B'}_\sigma(\bar\sigma,\bar\delta)\int\frac{d^3q}{(2\pi)^3}\int d^3r'\frac{e^{-iq\cdot(r-r')}}{\vec q^2+m_\sigma^2}\bar\Psi_B(r')\Psi_B(r)\mathcal{D}[\bar\Psi_{B'}(r)\Psi_{B'}(r')].$$

By effect of the fluctuation term $\mathcal{D}$, when we average this term it will cancel one of the contractions

$$\begin{aligned}\left\langle\bar\Psi_B(r')\Psi_B(r)\mathcal{D}[\bar\Psi_{B'}(r)\Psi_{B'}(r')]\right\rangle &= \left\langle\bar\Psi_B(r')\Psi_B(r)\bar\Psi_{B'}(r)\Psi_{B'}(r')\right\rangle \\ &\quad - \left\langle\bar\Psi_B(r')\Psi_B(r)\left\langle\bar\Psi_{B'}(r)\Psi_{B'}(r')\right\rangle\right\rangle \\ &= \left\langle \overbrace{\bar\Psi_B(r')\Psi_B(r)\bar\Psi_{B'}(r)\Psi_{B'}(r')}\right\rangle\end{aligned}$$

and this is the only contraction left. Therefore

$$\begin{aligned}&-\frac{1}{2}\sum_B \Gamma^B_\sigma(\bar\sigma,\bar\delta)\left\langle\bar\Psi_B\mathcal{D}\sigma\Psi_B\right\rangle \\ &= \sum_{BB'}\frac{1}{2}\Gamma^B_\sigma(\bar\sigma,\bar\delta)\Gamma^{B'}_\sigma(\bar\sigma,\bar\delta)\int\frac{d^3q}{(2\pi)^3}\int d^3r'\frac{e^{-iq\cdot(r-r')}}{\vec q^2+m_\sigma^2}\left\langle\overbrace{\bar\Psi_B(r')\Psi_B(r)\bar\Psi_{B'}(r)\Psi_{B'}}(r')\right\rangle \\ &= \sum_B\frac{1}{2}\Gamma^B_\sigma(\bar\sigma,\bar\delta)^2\int\frac{d^3k_1d^3k_2}{(2\pi)^6}\frac{1}{(\vec k_1-\vec k_2)^2+m_\sigma^2}\,\mathrm{Tr}\left\{\frac{\not k_1+M^\star_B}{2E_1}\frac{\not k_2+M^\star_B}{2E_2}\right\} \\ &= \sum_B\frac{1}{2}\Gamma^B_\sigma(\bar\sigma,\bar\delta)^2\int\frac{d^3k_1d^3k_2}{(2\pi)^6}\frac{1}{(\vec k_1-\vec k_2)^2+m_\sigma^2}\frac{k_1\cdot k_2+M^{\star2}_B}{E_1E_2}\end{aligned}$$

where, again, we can approximate $k_1 \cdot k_2 + M_B^{\star 2}$ by $2M_B^{\star 2}$ and thus

$$= \sum_B \Gamma_\sigma^B(\bar{\sigma},\bar{\delta})^2 \int \frac{d^3k_1 d^3k_2}{(2\pi)^6} \frac{1}{(\vec{k}_1-\vec{k}_2)^2+m_\sigma^2} \frac{M_B^{\star 2}}{\sqrt{(\vec{k}_1^2+M_B^{\star 2})(\vec{k}_2^2+M_B^{\star 2})}} \quad (2.109)$$

All together this yields

$$\langle \mathcal{H}_\sigma \rangle = \frac{m_\sigma^2 \bar{\sigma}^2}{2} + \sum_B \int \frac{d^3k_1 d^3k_2}{(2\pi)^6} \frac{\Gamma_\sigma^B(\bar{\sigma},\bar{\delta})^2}{(\vec{k}_1-\vec{k}_2)^2+m_\sigma^2} \frac{M_B^{\star 2}}{E_1^B E_2^B} \quad (2.110)$$

where $E_{1,2}^B = \sqrt{\vec{k}_{1,2}^2 + M_B^{\star 2}}$.

Delta

The δ meson. Its result is just like the σ with the addition of the $\boldsymbol{t}$ isospin matrices, which we have already calculated for the ρ. There is really nothing exceptional or different about the terms for the δ meson and by steps exactly like the ones above one arrives at

$$\langle \mathcal{H}_\delta \rangle = \frac{m_\delta^2 \bar{\delta}^2}{2} + \sum_{B,i,j} \int \frac{d^3k_1 d^3k_2}{(2\pi)^6} \frac{Z_{i,j}}{(\vec{k}_1-\vec{k}_2)^2+m_\delta^2} \frac{M_B^{\star 2}}{E_1^B E_2^B} \quad (2.111)$$

where, $Z_{i,j}$ is similar to the $C_{i,j}$ for the ρ, however, remembering that $\boldsymbol{\Gamma}_\delta$ gives a different coupling to the δ_0 and $\delta_\pm$, therefore, it follows trivially from the calculation that

$$Z_{i,j} = \Gamma_\delta^{B_i}(\bar{\sigma},\bar{\delta})\Gamma_\delta^{B_j}(\bar{\sigma},\bar{\delta})\delta_{ij} + g_\delta^{B_i}(\bar{\sigma},\bar{\delta})g_\delta^{B_j}(\bar{\sigma},\bar{\delta})(\delta_{i,j+1}+\delta_{i+1,j}) \quad (2.112)$$

Pions

Finally, we turn to the pions. Here we will only quote the results and point the reader to references where these were discussed in detail. That is because there is nothing about this calculation that we have not gone thorough in the sections above. The tools needed to reproduce the pion calculation are the same ones used above and the reader can find detailed

accounts of these terms in Refs [91], [42], [68], [32].

$$\begin{aligned}\langle \mathcal{H}_\pi \rangle = \left(\frac{g_A}{2f_\pi}\right)^2 \Big\{ & J_{pp} + 4J_{pn} + J_{nn} - \frac{24}{25}\left(J_{\Lambda,\Sigma^-} + J_{\Lambda,\Sigma^0} + J_{\Lambda,\Sigma^+}\right) \\ & + \frac{16}{25}\left(J_{\Sigma^-\Sigma^-} + 2J_{\Sigma^-\Sigma^0} + 2J_{\Sigma^+\Sigma^0} + J_{\Sigma^+\Sigma^+}\right) \\ & + \frac{1}{25}\left(J_{\Xi^-\Xi^-} + 4J_{\Xi^-\Xi^0} + J_{\Xi^0\Xi^0}\right)\Big\}\end{aligned} \tag{2.113}$$

where

$$J_{ff'} = \int \frac{d^3k_1 d^3k_2}{(2\pi)^6}\left[1 - \frac{m_\pi^2}{\left(\vec{k}_1 - \vec{k}_2\right)^2 + m_\pi^2}\right], \tag{2.114}$$

the axial coupling constant is taken to be $g_A = 1.26$ and the pion decay constant is $f_\pi = 93$MeV. The first term in 2.114 is a contact term. Given that we already are including heavier mesons whose short range contributions effectively approximate contact terms we drop the contact term here too, in an approximation colloquially known as "poor man's absorption".

$$J_{ff'} = -\int \frac{d^3k_1 d^3k_2}{(2\pi)^6}\left[\frac{m_\pi^2}{\left(\vec{k}_1 - \vec{k}_2\right)^2 + m_\pi^2}\right]. \tag{2.115}$$

Full Energy Density

All together the full expression for the energy density simply consists of the terms above.

$$\epsilon = \langle \mathcal{H}_0 \rangle + \langle \mathcal{H}_\sigma \rangle + \langle \mathcal{H}_\omega \rangle + \langle \mathcal{H}_\delta \rangle + \langle \mathcal{H}_\rho \rangle + \langle \mathcal{H}_\pi \rangle . \tag{2.116}$$

It is important to note, though, that this energy density is a function of the number density of every single particle in the system. So far, we are considering the entire baryon octet and thus this is a function of eight variables

$$\epsilon = \epsilon(n_n, n_p, n_\Lambda, n_{\Sigma^+}, n_{\Sigma^-}, n_{\Sigma^0}., n_{\Xi^0}, n_{\Xi^-}) \tag{2.117}$$

2.3.7 Determining the Coupling Constants

Our model still has a few parameters to be determined. Namely, the meson coupling constants and masses. For the vector meson masses we can simply use their nominal experimental values

$$m_\omega = 782\text{MeV}, \qquad m_\rho = 770\text{MeV}. \tag{2.118}$$

The scalar mesons, as explained in the previous part of this chapter, represent not just the exchange of a physical particle, i.e. the scalar-isoscalar $f_0(500)$ and the scalar-isovector $a_0(980)$ but also contemplate the scalar components of two pion exchanges. For that reason they could be considered free parameters and are fitted to data (much like we will do for the coupling constants). For the δ meson we will tend to always use 980MeV, however, it should be said that considering it a free parameter is phenomenologically consistent. The σ meson is usually taken to be around $600 \sim 700$MeV.

Having chosen the masses all we need to do is fit the coupling constants to nuclear matter parameters. For symmetric nuclear matter, i.e.

$$\epsilon(n_b) = \epsilon(n_n = n_b/2, n_p = n_b/2, 0, 0, 0 \cdots) \tag{2.119}$$

where n_b is the total baryon density, we know that it must have a minimum at saturation density (as discussed in the phenomenology section),

$$\left.\frac{\partial \epsilon}{\partial n_b}\right|_{n_b = n_0} = 0 \tag{2.120}$$

we take its binding energy per nucleon at that density to be -15.8MeV

$$\mathcal{E}(n_b) \doteq \epsilon(n_b) - M_N n_b \tag{2.121}$$

$$\mathcal{E}(n_0) = -15.8\text{MeV}, \tag{2.122}$$

where $M_N = 940$MeV is the mass of the nucleon. And finally, the symmetry energy is

$$S(n_b) = \mathcal{E}(n_n = n_b, n_p = 0) - \mathcal{E}(n_n = n_b/2, n_p = n_b/2), \tag{2.123}$$

$$S(n_0) = 30\text{MeV}. \tag{2.124}$$

Those three equations constrain three of our four coupling constants. The last one we can either fit to the slope or the incompressibility, however that would be unadvised given the fact that these measurements have very large errors. Alternatively or we can look at other studies that measure them directly. Studies using boson exchange potentials such as [33] have pinned the g_δ coupling to be roughly $G_\delta \sim 3fm^2$ where $G_\delta = g_\delta^2/m_\delta^2$. Given that the delta meson is the one that couples most weakly and has the largest mass (ergo the smallest reach), we forgo including it in the fit to nuclear matter saturation parameters and take it to be around this value.

By fitting the couplings to these quantities we now have a fully defined model that can be used to study the structure of large nuclei and the core of neutron stars. One future chapter of this thesis will be devoted to neutron star core predictions, specifically as it pertains to the effects of the isovector-scalar meson, the δ, which is commonly neglected.

Chapter 3

Nuclear Phenomenology of Neutron Stars

In this chapter we briefly review some aspects of neutron star phenomenology. Specifically we will touch on concepts that are of major importance to nuclear theory and how do the astrophysical measurements of neutron star properties relate to nuclear physics. Much about the astrophysics of neutron stars is left out and readers interested in such topics should refer to Refs. [87, 14, 25].

3.1 Introduction

Neutron stars are uniquely important astrophysical objects for nuclear physics. As discussed in Chapter 2, the nuclear strong force between two bodies, say, a proton and a neutron or two neutrons, not only has a minimum, it is zero at a certain distance. If the bodies are too close they will experience repulsion and if they are sufficiently far apart they will experience attraction. Somewhere in the middle, they will experience minimal force. That, amongst some fundamentally relativistic effects of many fermion systems, leads to the phenomenon of saturation, in which a system composed of many nucleons has a very strong tendency to remain at the saturation density, where the average distance between the nucleons is such that the the energy has been minimised. For that reason, studying cold nuclear matter for densities larger than the saturation density would be almost impossible without neutron stars. There the gravity is so strong that it forces matter out of saturation. In fact, the density in the core of a neutron star can reach even $6n_0$, where $n_0 = 0.16 \pm 0.1\text{fm}^{-3}$ is the saturation density, maybe more. Figure 3.1 shows the phase diagram of QCD matter,

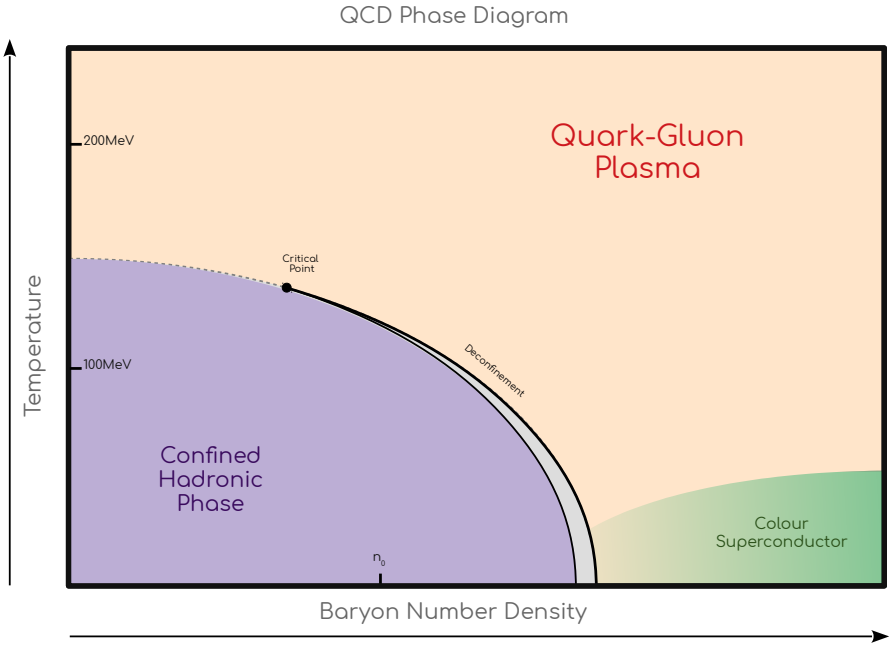

Figure 3.1: Sketch of the phase diagram of quantum chromodynamics

that is, matter made of quarks and gluons. Particle accelerators and other experiments allow us to explore a large portion of this diagram, the full range in temperature, but a limited range in density/chemical potential. Furthermore, computational techniques of lattice gauge theory allow us to probe in detail the zero density axis. However, the lower right corner of the plot is not accessible by any means here on earth. Even lattice gauge theory fails as it suffers from the so called fermion sign problem[1].

Neutron star physics is then of extreme interest to nuclear physicists and we must take the time to introduce some aspects of it. There is much more to this subject than we can present in this chapter and for a deeper dive readers should refer to [28, 14, 87] and [10]. For now, let's explore some of the properties of such objects.

3.2 Birth and Evolution

A main sequence star, like our sun, and like many other stars much heavier than our sun, are powered by the fusion of light elements into heavier elements. Sometimes referred to as the "fuel", hydrogen atoms are fused together into helium and eventually other nuclei such as carbon, nitrogen, and so on. Eventually, though, if the star is heavy enough, it will start generating iron, particularly ^{56}Fe, which is the most stable nucleus on the periodic table. Being the most stable, it is energetically unfavourable for the star to create other elements and thus the fusion process stops with iron. The more iron there is the less fusion occurs. When this happens, the fusion, which was heating the star, slows down and the star starts to cool. This is sometimes referred to as the star running out of "fuel". Without the thermal pressure to counteract gravity, the core of the star collapses and rest of the star is expelled into outer space in a process called a Super Nova (SN). The remnant of this core collapse can, if the mass of the star is within a certain range, be a neutron star. This process is summarised in Fig. 3.2 in a simplified form.

[1]The fermion sign problem refers to the fact that, when a non zero fermion chemical potential is introduced the probability measure cannot be guaranteed to be (and in general is not) positive definite, hence, the sign problem.

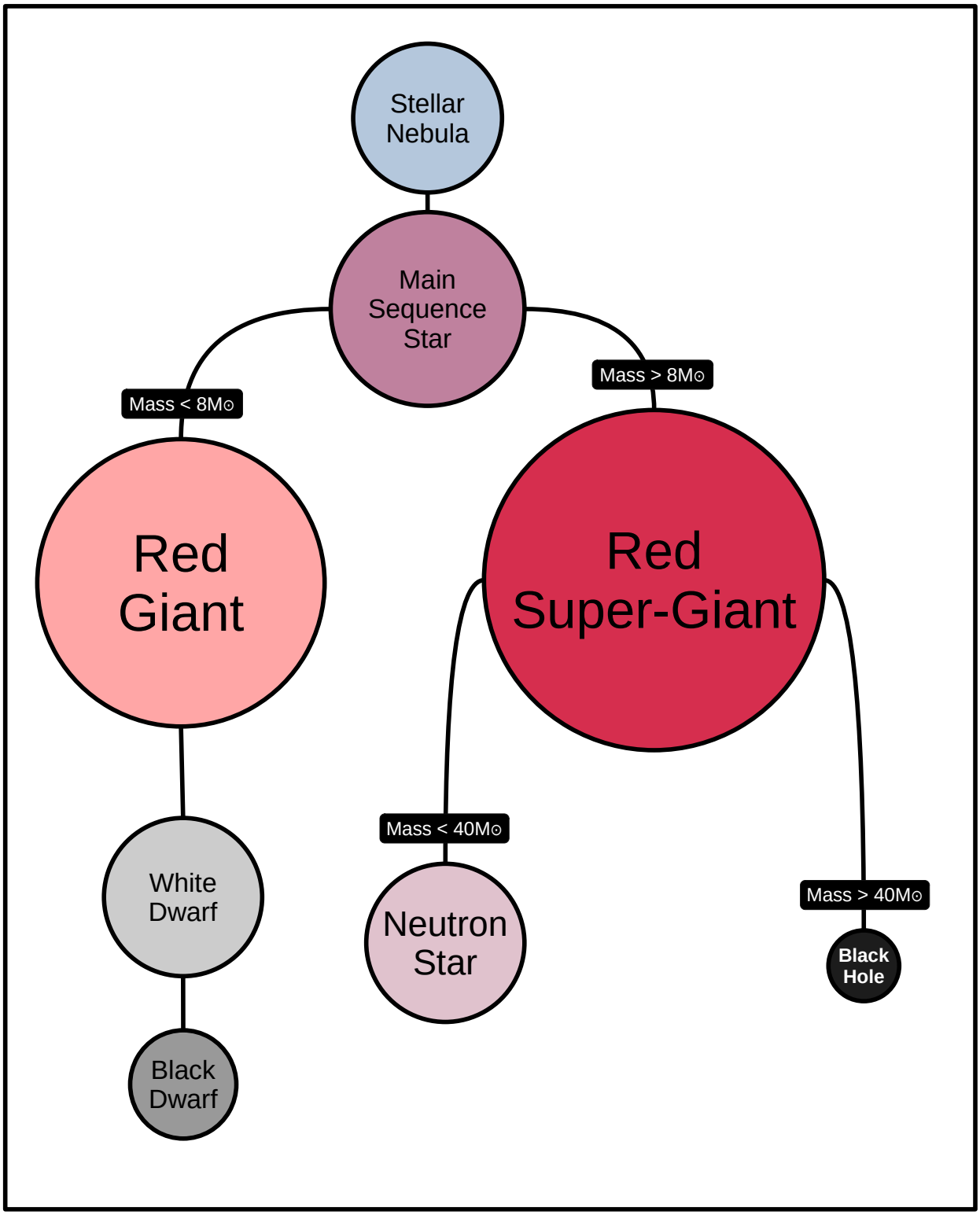

Figure 3.2: Sketch diagram of the origins of a neutron star.

The core collapse is rooted in the fact that, as explained earlier, ^{56}Fe is the most stable element and thus there is no way the system can minimise its energy density further by creating different elements. Hence, the star cools and the core collapses. Gravity winning, however, increases the pressure and energy density in the core to such an extent that, although creating different elements will not help to minimise it, breaking the nucleus into its components will. The core then becomes this state which is mostly made of unbound (or, more precisely, bound solely by gravity) nucleons and, if it is heavy enough, other baryons and perhaps free quarks, as we will discuss shortly.

And as the collapse happens, conservation of angular momentum forces the star to spin up to incredible speeds, sometimes with angular periods in the order of milliseconds. The star also conserves magnetic flux in the process and thus the neutron star usually has an immensely strong magnetic field. If that rapid rotation is misaligned with the magnetic field axis we get what is known as a Pulsar. The magnetic field sweeps through space emitting radiation as a lighthouse and, from earth, we can observe the pulsar blinking strongly.

Much of the physics of neutron stars is unique to its environment, the scales of densities, magnetic fields, and angular momentum are all extreme. Unsurprisingly, that environment is the only laboratory we have to study some particular phenomena. As explained in the next section, nuclear physics benefits greatly from data from neutron stars as their cores are composed of unbound protons, neutrons, and possibly other hadrons and deconfined quarks at densities far beyond those found on earth. We can measure the physical parameters of a pulsar such as its mass, radius, and other quantities and use our modelling of nuclear interactions to further our understanding both of neutron stars and of nuclear physics.

3.3 Mass and Radius from Nuclear Equation of State

The most tangible way that we have to connect the microscopic physics of nuclear physics to the macroscopic properties of the neutron stars is via

studying their mass and radius[2]. In fact, it is possible to calculate the mass and radius of a neutron star solely via the combination of Einstein's equations of general relativity and one specific piece of information about its nuclear components, the equation of state. This equation, usually denoted EOS for short, basically tells us how the different thermodynamic properties of the system affect one another. That is, how the pressure relates to the energy density and how both relate to the number density all for fixed values of temperature and chemical potential.

With respect to the temperature, though, the nuclear force is strong enough that only exorbitantly high temperatures will affect it (at least greater than $1\text{MeV} \approx 10^{10}\text{Kelvin}$). That is why in Fig. 3.1 the label Neutron Star is at high chemical potential but low temperature. To clarify this point, picture a gas of fermions. At a certain temperature we can imagine them moving around with a certain average velocity. If the temperature is increased, the velocity is increased. However, if the system is too strongly interacting, it would require more temperature to move the fermions around given that the force that binds them together or pushes them away is too strong. It needs a higher temperature to counteract their interaction. As stated above, the nuclear force is strong enough that only temperatures roughly above 1MeV have any significant effect and the neutron stars we wish to study are mostly cooler than that. Therefore, let us say that, for our intents and purposes $T = 0$ (for a more in-depth look into the temperature effects within the QMC model framework see [78]).

In Chapter 1 we discussed the steps to get the energy density $\epsilon(n\dots)$ of nuclear matter from a model of the nuclear interactions, where $(n\dots)$ is the number density of every species included in the fluid (in our case, protons, neutrons, electrons, muons, lambdas, etc). Once one thermodynamic property is calculated we can use any and all available relations to obtain other thermodynamic properties. In this case, the number of particles is fixed (or equivalently the number density), the temperature is fixed (in this case, zero) and the volume is fixed, so the adequate framework is the grand canonical ensemble. The energy density will be related to other

[2]This may change in the future with the advent and progress of gravitational wave astronomy.

thermodynamic potentials via the first law of thermodynamics

$$dE = TdS + \sum \mu_i dN_i - pdV \tag{3.1}$$

where N_i is the number of each individual particle species in the mix, and the integrated quantities are

$$E = TS + \sum \mu_i N_i - pV. \tag{3.2}$$

If we divide it by the volume it becomes

$$\epsilon = Ts + \sum \mu_i n_i - p, \tag{3.3}$$

and since in our case the temperature is zero, we find

$$\epsilon = \sum \mu_i n_i - p. \tag{3.4}$$

The chemical potential is, broadly speaking, the increase in energy the system gets by the introduction of a new particle, or, in the continuum formulation, by an infinitesimal addition of number density dn. That would imply that

$$\mu_i = \frac{\partial \epsilon}{\partial n_i},$$

and, in fact, Eq. 3.1 gives exactly that when other quantities are fixed. Therefore, given that we do have an expression for the energy density as a function of the Fermi momentum, which itself is a function of the number density, we can get an analytic expression for the chemical potential and we can calculate the pressure of the system by the relation

$$p(n...) = \sum n_i \frac{\partial \epsilon}{\partial n_i} - \epsilon(n...). \tag{3.5}$$

Sometimes, though, it may be not possible (or not simple) to calculate the energy density as a function of the number density. This may seem to put us in a lot of trouble. However, often when that happens we can calculate $\epsilon(\mu \dots)$ instead of $\epsilon(n \dots)$. In that case, how do we use the first law of thermodynamics to get other theromdynamic potentials? In the grand canonical ensemble, μ and n are free parameters, however, 3.4 constraints

them. Then by differentiating 3.4 we get

$$\frac{\partial p}{\partial n_i} = \frac{\partial \mu_i}{\partial n_i} n_i + \mu_i - \frac{\partial \epsilon}{\partial n_i} \tag{3.6}$$

and use $\mu_i = \frac{\partial \epsilon}{\partial n_i}$ to obtain

$$\frac{\partial p}{\partial n_i} = \frac{\partial \mu_i}{\partial n_i} n_i \tag{3.7}$$

which, by a chain rule, is equivalent to

$$\frac{\partial p}{\partial \mu_i} = n_i \tag{3.8}$$

and therefore another way of writing 3.5 is

$$p(\mu...) = \sum \mu_i \frac{\partial p}{\partial \mu_i} - \epsilon(\mu...). \tag{3.9}$$

where, again, the argument $(\mu...)$ represents all different species chemical potentials.

Therefore, once we get one thermodynamic potential as a function of one of the parameters (n_i or μ_i) we immediately get the other potential, either via 3.5 or 3.9.

3.3.1 β-equilibrium

The energy density $\epsilon(n_i)$ depends on the number density of many particle species. It follows from the principle of least action that a static stable state is always one that minimises the energy. Ergo, in order to find the particle composition of a star at a certain baryon density we have to find the minimum of the function

$$\epsilon(n_n, n_p, n_{e^-}, n_\mu, n_\Lambda, n_{\Sigma^+}, n_{\Sigma^0}, n_{\Sigma^-}, n_{\Xi^0}, n_{\Xi^-}). \tag{3.10}$$

However, there are some constraints from astrophysical inferences that have to be imposed on $\epsilon(n_i)$ for it to be used in simulations of stellar structure. First and foremost, the individual number densities for the baryons has to

conserve total baryon number. That is, at each step of the calculation, it must be true that

$$n_b = n_n + n_p + n_\Lambda + n_{\Sigma^+} + n_{\Sigma^0} + n_{\Sigma^-} + n_{\Xi^0} + n_{\Xi^-}. \tag{3.11}$$

I.e., the total baryon number density n_b has to be the sum of the individual baryon number densities. Also, neutron stars are neutrally charged [28, 14, 87, 10] and electric charge conservation states that at every point of the calculation

$$\sum_i Q_i n_i = 0. \tag{3.12}$$

With respect to the leptons we assume that the neutrinos escape the system quickly and without interacting, therefore the weak equilibrium relation for the leptons is

$$\mu_e = \mu_\mu. \tag{3.13}$$

However, since the leptons are essentially free, their chemical potential is $\mu_l = \sqrt{(k_F^2 + m_l^2)}$ and we can analytically eliminate one of the variables, say the n_μ,

$$n_\mu = \frac{1}{3\pi^2}\left(\mathrm{Re}\sqrt{k_{Fe}^2 + m_e^2 - m_\mu^2}\right)^3, \tag{3.14}$$

where taking the real part simply excludes the muons from showing up before the chemical potential of the electrons is higher than the muon mass. So, the function we need to minimise, at each point in baryon number density n_b is

$$\epsilon(n_n, n_p, n_{e^-}, n_\mu, n_\Lambda, n_{\Sigma^+}, n_{\Sigma^0}, n_{\Sigma^-}, n_{\Xi^0}, n_{\Xi^-}) + \lambda_1 \left(Q_i n_i\right) + \lambda_2 \left(n_b - \sum_{\text{baryons}} n_i\right) \tag{3.15}$$

where we introduced the constraints via Lagrange multipliers. After minimising this function by a method of choice one obtains the energy density of a stable system with a certain baryon density, $\epsilon(n_b)$, and consequentially all of the chemical potentials, pressures, etc.

Finally, we need to understand how that is tied to the macroscopic physical qualities of the star such as its mass and radius.

3.3.2 Tolman-Oppenheimer-Volkoff (TOV)

As previously stated, the objective is to solve Einstein's equations

$$\frac{8\pi G}{c^4} T_{\mu\nu} = G_{\mu\nu} \tag{3.16}$$

for the relevant system, a neutron star. However, it would be outside the scope of this thesis to review all of differential geometry and general relativity solely for the derivation of one simple equation. Many references including [28] and [14] contain detailed derivations and explanations of the process. For us it will suffice to discuss only the most important aspects of it.

Firstly, let us assume that the matter content of our star is an isotropic ideal fluid. This implies that our energy-momentum tensor is diagonal and has elements given by the energy density and pressure as such

$$T^{\mu\nu} \to \boldsymbol{T} = \begin{pmatrix} \epsilon & 0 & 0 & 0 \\ 0 & p & 0 & 0 \\ 0 & 0 & p & 0 \\ 0 & 0 & 0 & p \end{pmatrix} \tag{3.17}$$

However, here, we assume that the pressure and energy may vary inside the star, i.e. they depend on the space-time. Furthermore, both the metric and the energy-momentum tensor are assumed to be spherically symmetric and static. For the left hand side that amounts to $\epsilon(x^\mu) = \epsilon(r)$, where r is the radial component measured from the core of the star, similarly for the pressure $p(x^\mu) = p(r)$ and the metric itself can be written as

$$ds^2 = c^2 e^{\nu(r)} dt^2 - e^{\lambda(r)} dr^2 - r^2 d\theta^2 - r^2 \sin^2\theta d\phi^2. \tag{3.18}$$

which is to say that our metric components (in spherical coordinates of course) are

$$\begin{aligned} g_{00}(r) &= -c^2 e^{\nu(r)} \\ g_{11}(r) &= e^{\lambda(r)} \\ g_{22}(r) &= r^2 \\ g_{33}(r,\theta) &= r^2 \sin^2\theta. \end{aligned} \tag{3.19}$$

From the metric one can calculate the Cristoffel symbols

$$\Gamma_{abc} = \frac{1}{2}\left(\partial_c g_{ab} + \partial_b g_{ac} - \partial_a g_{bc}\right) \tag{3.20}$$

which in turn give us the Ricci curvature tensor

$$R_{ab} = \partial_\rho \Gamma^\rho_{ba} - \partial_b \Gamma^\rho_{\rho a} + \Gamma^\rho_{\rho\lambda}\Gamma^\lambda_{ba} - \Gamma^\rho_{b\lambda}\Gamma^\lambda_{\rho a} \tag{3.21}$$

the scalar curvature

$$R = \frac{1}{2} R_{ab} g^{ab}, \tag{3.22}$$

and finally, Einstein's tensor

$$G_{\mu\nu} = R_{\mu\nu} - \frac{1}{2} R g_{\mu\nu}. \tag{3.23}$$

Einstein's equation relates this geometry to the energy-momentum tensor and will constraint the so called metric functions $\nu(r)$ and $\lambda(r)$ which for now are arbitrary. The $0,0$ component will give us the relation

$$\frac{8\pi G}{c^2}\epsilon e^{\nu} = \frac{e^{\nu}}{r^2}\left(1 - \frac{d}{dr} r e^{-\lambda}\right), \tag{3.24}$$

and the diagonals will yield

$$-\frac{8\pi G}{c^4} p e^{\lambda} = \frac{-r\nu' + e^{\lambda} - 1}{r^2}. \tag{3.25}$$

The continuity equation for the energy momentum tensor gives

$$\nabla_\mu T^\mu_1 = -\frac{dp}{dr} - \frac{1}{2}\left(p + \epsilon c^2\right)\frac{d\nu}{dr} = 0. \tag{3.26}$$

All of this can be recombined via a little algebra, yielding

$$\frac{dp}{dr} = -\frac{G}{r^2}\left(\epsilon(r) + \frac{p(r)}{c^2}\right)\left(M + 4\pi r^3 \frac{p(r)}{c^2}\right)\left(1 - \frac{2GM}{c^2 r}\right)^{-1} \tag{3.27}$$

where

$$\frac{dM}{dr} = 4\pi r^2 \epsilon(r) \tag{3.28}$$

yields the mass of the star inside a sphere of radius r.

It is important to reiterate that although all of the ingredients for the derivation are there and these steps can be followed and verified by the reader, this is was a rather hurried derivation. Interested readers should definitely seek a less superficial derivation as a lot of detail has been left out in the interest of avoiding fixating over deep mathematics in a chapter about phenomenology. Let us recapitulate what we have so far:

- Equation 3.27, known as the Tolman-Oppenheimer-Volkoff equation, give us the pressure profile $p(r)$ inside the star, given as initial condition the internal pressure $p(0)$.
- This equation requires knowledge of the energy density profile of the star $\epsilon(r)$ which is not known. However, and this is the most important point, if we have an equation of state (and together with 3.4) such that we can write $\epsilon(p)$ we can use that to eliminate the explicit references to the energy density and write a differential equation for the pressure alone. That is, we solve

$$\frac{dp}{dr} = -\frac{G}{r^2}\left(\epsilon(p(r)) + \frac{p}{c^2}\right)\left(M + 4\pi r^3 \frac{p}{c^2}\right)\left(1 - \frac{2GM}{c^2 r}\right)^{-1}. \quad (3.29)$$

That is how we bring information of the microscopic nature of the matter involved to calculate its macro properties. The radius of the star is determined by when the pressure reaches zero, that is when $p(R) = 0$. The total mass of the star is given by

$$M = \int_0^R dr 4\pi r^2 \epsilon(r). \quad (3.30)$$

This is dependent, obviously, on the initial condition $p(0)$ (note that always $M(0) = 0$ given that the mass inside a zero radius sphere has to be zero). It is more intuitive to use the equation of state to frame that as an internal density. That is, we can use 3.5 to identify $p(0)$ with a central density $n(0)$. Therefore, all we need to know is the number density in the core of the star. In general, however, that is not possible. In order to circumvent this problem we solve for multiple possible values of the central density and, for each, record what would be the mass and radius of a star with that central pressure.

It is a feature of general relativity that, at some point, there will be too much mass for the system to sustain itself and the star will collapse into a black hole. A typical mass-radius diagram looks like Figure 3.3. Each

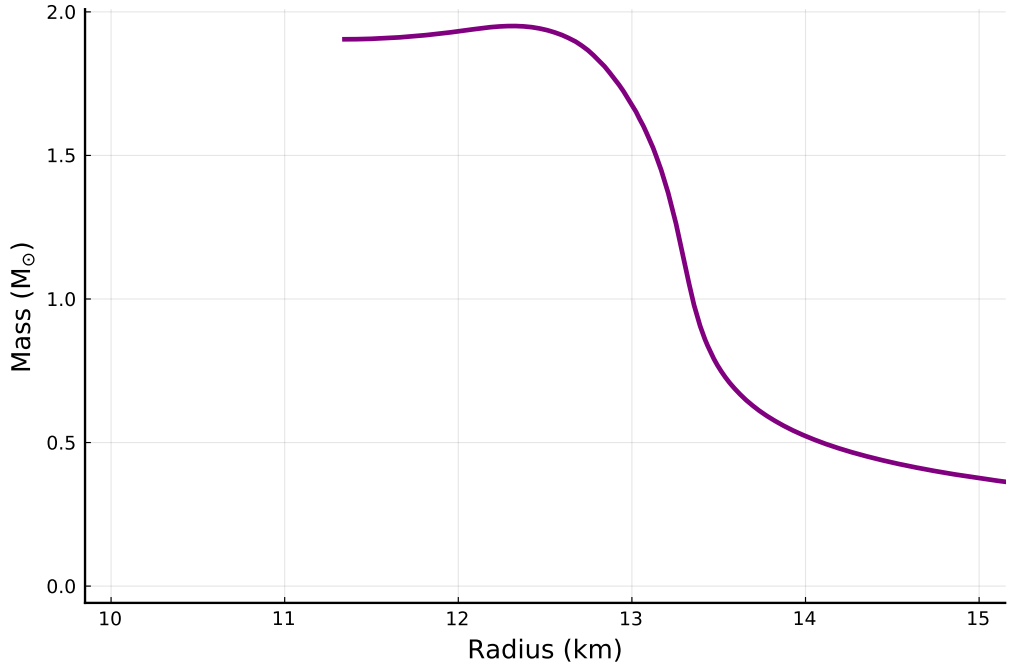

Figure 3.3: Example of a mass-radius diagram within the framework of the QMC model (see next chapter for a longer discussion).

point on the plot represents the mass and radius of a star with a certain central density $n(0)$. Very low internal pressure will yield high radii and low masses. As the internal pressure increases higher masses are reached and, at some point, the masses start to go down and collapse to a point. In fact, all stars to the left of the maximum mass are unstable and will collapse into a black hole.

3.3.3 Notable Measurements

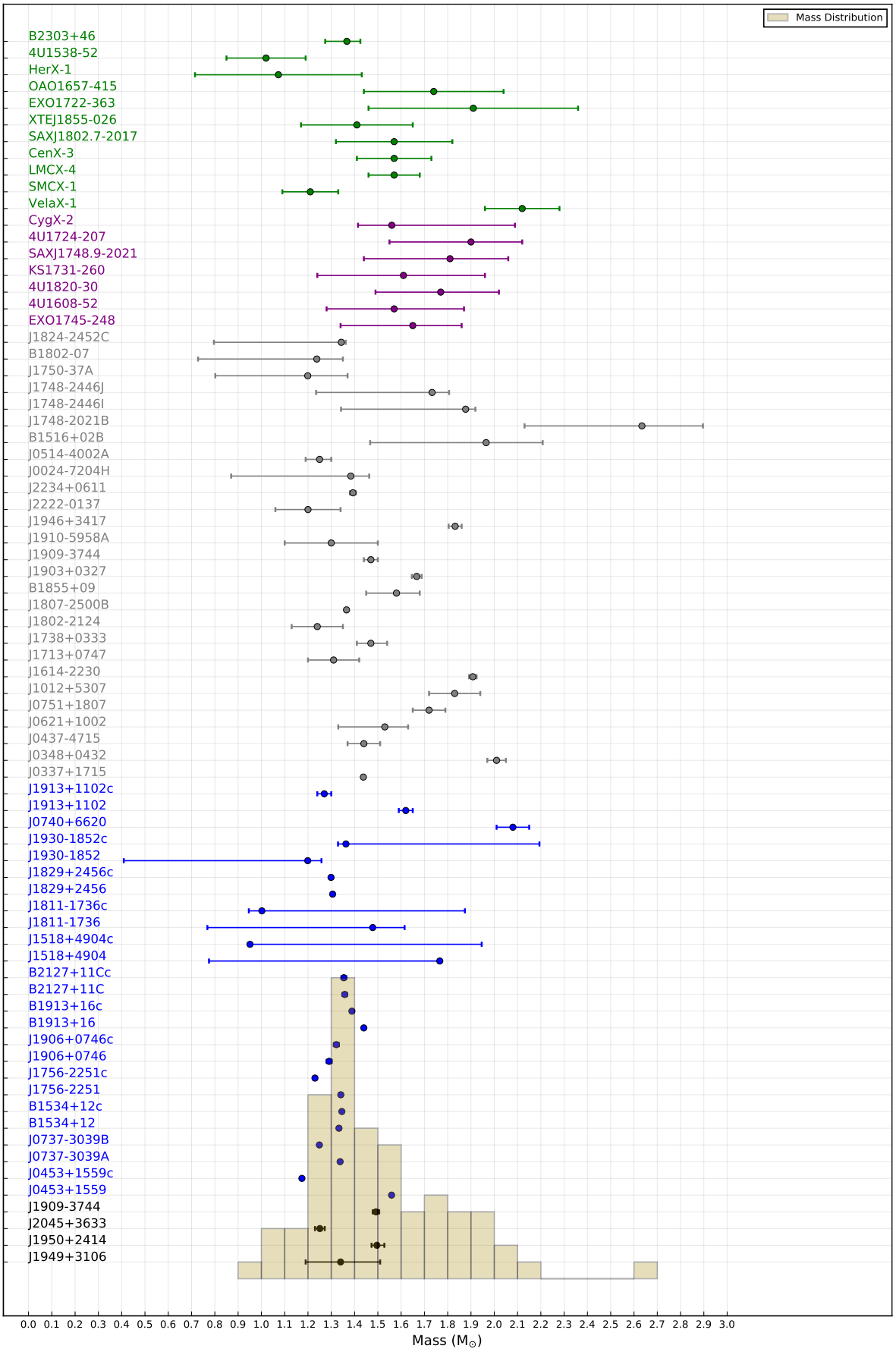

Figure 3.4: Measured neutron star masses, data extracted from [61] and [45]

Figure 3.4 shows some of the masses of neutron stars that have been measured so far. Note that in the X-ray binary sector there are a few high masses, however, most of them also have very large errors. In fact, measuring masses of neutron stars usually comes with some unavoidable model dependence, and thus some hard to estimate systematic errors. Indirect observations put together via physical and astrophysical models, no matter how well established the model, should always be taken with a grain of salt.

That is true of all of the measurements except for four. These are the four white dwarf neutron star binaries which present rather large masses. These are the pulsars J1614-2230, J0348+0432, J1946+2417 and J0740+6620. They have been measured via a a very clean technique, base solely on general relativity, the so called Shapiro time delay [40]. The first heavy star measurement with this technique was of PSR-J1614-2230 by Demorest et al [21]. The Shapiro time delay technique [40] is based simply on the time differential between the pulsar blinking when it is behind the white dwarf partner to when is blinking in front of the partner, relative to us. This differential exists because the light from the pulsar has to travel through its partner gravitational field and that creates the distortion. That time differential alone (taken over a long period of time and thus at every point of the orbit) is enough to get a very clean measurement of the binary systems parameters. Together with a good measurement of the white dwarf's properties we can derive the neutron star mass. Note how all four appear around 2.0 solar masses and, in fact, J1614-2230 was originally measured to be around $1.97 \pm 0.04 M_\odot$ and later reevaluated to be $1.908 \pm 0.016 M_\odot$ (the remeasurement was published in reference [6]). That, together with the measurement made by Antoniadis et al [5], has convinced nuclear physicists that the most conservative estimate of the maximum mass of a neutron star is between 1.9 and $2 M_\odot$. That does not mean that we cannot find a heavier star, but it does mean that the, as it is sometimes called, minimum maximum mass of a neutron star is around two solar masses.

This is extremely important because, now, every nuclear physics model for the equation of state of dense nuclear matter has to pass this test. It must support stars with, at least, 1.9 solar masses and, preferably, above 2.0 solar masses. Moreover, when such measurements came about they

created many problems for nuclear physicists. In Ref. [21] they stated that the $2.0M_{\odot}$ finding rules out the hypothesis that hyperons (baryons with strange quarks) could exist in the core of the stars. That is because most equations of state that included the presence of hyperons suffered a severe decrease in pressure by about the densities that hyperons would start being formed. That change in pressure softened the EOSs to such an extent that most of them could not reconcile a $2.0M_{\odot}$. That was most certainly puzzling given the fact that the higher the mass the stronger the evidence that hyperons should be forming; by virtue of the fact that higher mass implies higher central energy density and at some point, if the system has enough energy, it should generate strange quarks and thus it could generate hyperons. In spite of all of the frenzy surrounding what became known as the hyperon puzzle, there was an equation of state that, even before the measurement was made in 2010, predicted hyperonic stars with masses up to $2.0_{\odot}$ [68], the QMC model. Chapter 2 reviews a more recent version of that model.

Another alternative to the hyperon crisis was that at the densities inside such massive stars the system would not be generating heavy strange baryons but the quarks would deconfine entirely. The hypothesis of deconfined quark matter inside neutron stars, and in fact of pure quark stars, is much older than the measurement of $2.0M_{\odot}$. However, it gained traction then. A simplistic EOS with quarks also fails at reaching the desired maximum mass, however, many groups have published different quark based models that do (see reference [86] for a review).

It becomes clear that such astrophysical measurements can sometimes give new and otherwise unreachable information about the physics of high density matter as well as constraints on nuclear physics modelling. They are extremely valuable. Recently, another experiment published results that, much like the masses of the stars discussed above, changed the field: the measurement of the radius of a neutron star by NICER mission at the international space station.

3.3.4 NICER

If measuring masses often comes with large associated systematic uncertainties, measuring the radius is even more complicated. There is no clear, pure, and entirely model independent way to measure the size of such a small and far away object. These stars are believed to be 10∼20km in radius and at least $\approx$ 500 light years away, making any type of direct measurement impossible.

The NICER (Neutron Star Interior Composition Explorer) telescope installed on the international space station in 2017 was designed to, apart from other things, measure a neutron star radius as cleanly as we possibly can. This involves pulse profile modelling, that is, measuring general relativistic effects such as light bending, gravitational redshift, and so on, associated with thermal emissions from hot regions of the stars surface.

Recently, the NICER mission published several results including Refs. [69] and [54] in which measurements for a pulsar, PSR J0030+0451, are revealed. These papers applied two different analysis on the data and obtained values of $12.71^{+1.14}_{-1.19}$km and mass $1.34^{+0.15}_{-0.16}\mathrm{M}_\odot$ in [69] and $13.02^{+1.24}_{-1.06}$km in [54] with the mass estimated at $1.44^{+0.15}_{-0.14}\mathrm{M}_\odot$. On Ref.[70, 83], the heavier PSR J0740+6620 was investigated. They obtained a radius of $12.39^{+1.3}_{-0.98}$km for a mass value of $2.07 \pm 0.06\mathrm{M}_\odot$.

3.3.5 Slow Rotation and Moment of Inertia

There is one more piece of information we can get from measuring the mass of pulsars, namely the moment of inertia. However, the TOV equations assume a static and spherically symmetric metric. A pulsar is obviously spinning and in fact so much so that the static metric approximation is not entirely accurate. However, if we assume that the pulsar is rotating only to an extent that the effect in the metric will be minor, we can write a perturbative expansion of the field equations as a function of the rotating angular momentum Ω. The first approximation (or zero-th order in Ω), of course, will be the TOV equations which is static. The first perturbation

correction can give us expressions for the moment of inertia of slowly rotating stars[3]. More specifically, the zero-th component of Einstein's equation, in first order of this perturbative expansion, i.e. order Ω^1 will look like

$$\frac{1}{r^4}\frac{\partial}{\partial r}\left(e^{-(\lambda+\nu)/2}r^4\frac{\partial\bar{\omega}}{\partial r}\right)+\frac{e^{(\lambda-\nu)/2}}{r^2\sin^3\theta}\frac{\partial}{\partial\theta}\left(e^{(\lambda-\nu)/2}r^2\frac{\partial\bar{\omega}}{\partial\theta}\right)-16\pi(\epsilon+p)e^{(\lambda-\nu)/2}\bar{\omega}=0 \tag{3.31}$$

where $\bar{\omega}$ is a function of the frame dragging (that is, the function associated with the rotation of the metric, not of the star) and Ω.

$$\bar{\omega}(r,\theta)=\Omega-\omega(r,\theta).$$

It is, again, far beyond the scope of this thesis to pursue long and intricate general relativity derivations and, therefore, only the final result will be quoted for completeness. Readers interested in a more extensive explanation of this derivation may refer to Anthony Kalaitzis' thesis [39] and references therein. In there the reader will find a very clear and didactic explanation of all of these equations. Solving the differential equation above for $\bar{\omega}$, the moment of inertia will be related to the solution by

$$I=\frac{J}{\Omega}=\frac{R^4}{6\Omega}\frac{\mathrm{d}\bar{\omega}}{\mathrm{d}r}\bigg|_{r=R} \tag{3.32}$$

Just as with mass and radius, this theoretical expression can itself be used to bridge the nuclear physics of highly condensed nuclear matter with astronomical observations of pulsars, their masses, and their periods.

3.4 Gravitational Waves

On August 17, 2017 at 12:41:04 UTC the LIGO and Virgo collaborations detected gravitational waves from a merger of two neutron stars, namely

[3]It should be noted here that slowly rotating may be a misnomer. A more accurate characterisation would be a rotation slow enough to affect the metric in a way that is perturbative, so perturbatively rotating is more reasonable. This is specially so, given that most neutron star rotations rates can hardly be called slow by any terrestrial standards.

GW170817. Less than two seconds after, Fermi-GBM measured the associated γ-ray burst. This incredible accomplishment provided the first constraint on the radius of neutron stars and the tidal deformability (see next section). Since the NICER mission results do provide a much stronger constraint on the radius than GW170817, we will forgo any discussion on that aspect. However, the tidal deformability, which is effectively associated with the third term in the perturbation series mentioned in the previous section, i.e., terms proportional to Ω^2, is still best constrained by this data.

3.4.1 Tidal Deformability

When neutron stars merge, angular momentum plays an important role. Notably, as the binary system spirals into its centre angular momentum is conserved and increases the speed of the rotation. Furthermore, the stars themselves often have high spin angular momentum. This dynamic is complex, involving many different axes of rotation and everything is coming together to collide in a central point. As the stars come together they also experience deformation due to the gravitational field of the companion. Therefore, this is also not a spherically symmetric scenario, however, neither is it the scenario we used above to calculate the moment of inertia. There, the otherwise spherically symmetric star had a relatively small rotation angular momentum which created a dipole term in the equations. What we have here is much more complex and a quadrupole moment has to be introduced.

Assume an external quadrupolar gravitational field, $\mathcal{E}$, is applied on the star. The quadrupole moment Q induced by the field $\mathcal{E}$ is simply

$$Q_{ij} = -\lambda \mathcal{E}_{ij} \tag{3.33}$$

where λ is the so called tidal polarizability. This coefficient is directly related to two other important parameters, the so called Love number

$$k_2 = \frac{3}{2}\lambda R^{-5}$$

and the tidal deformability

$$\Lambda = \frac{2}{3} k_2 \left(\frac{R}{M}\right)^5 . \tag{3.34}$$

Unsurprisingly, the higher we go in this perturbative expansion the more complex the calculations become. Here, once more, we refer the reader who is interested in learning more about the details of how these numbers are calculated to ref. [39] and references therein (such as Refs. [14] and [28]).

The binary system as a whole also has a tidal deformability which can be constrained by data. The binary tidal deformability ultimately adds up to a weighted average of the two individual star's deformabilities

$$\tilde{\Lambda} = \frac{16}{13} \frac{(12q+1)\Lambda_1 + (12+q)q^4\Lambda_2}{(1+q)^5} \tag{3.35}$$

where $q = m_1/m_2 < 1$ is the mass ratio.

Via GW170817 data constraints for these parameters can be obtained (Refs. [1] and [19])

$$70 \leq \Lambda|_{m=1.4M_\odot} \leq 580 \tag{3.36}$$

$$84 \leq \tilde{\Lambda} \leq 640 \tag{3.37}$$

and this too can be used to constrain nuclear physics models of the stars interiors.

3.5 Wrap Up

Optical and gravitational astronomy both provide nuclear physics with useful data that could not be obtained otherwise. Developing a model of nuclear interactions that obeys all of these constraints on tidal deformabilities, mass, radius, moment of inertia, and so on, is incredibly difficult. However, this is precisely what helps nuclear physics to evolve. Here we have presented a review of some important aspects of nuclear physics, a model for nuclear interactions (namely, the quark-meson coupling model), and now a

very brief review of how astronomical data can be tied to these theoretical proposals. In what remains of this thesis we will present a few applications of this interplay, ways in which this data can be used to discriminate between models and help us better understand nuclear physics. From the neutron decay anomaly to the strength of the isovector scalar sector, data from these hugely energetic far away collisions can help us understand the minutiae of subatomic physics.

Chapter 4

Nuclear Matter Results

In this Chapter, we will discuss the numerical consequences of self-consistently including the isovector-scalar meson in the QMC model. The effects of this interaction, particularly in what pertains to the physics of neutron stars are discussed in detail. The gravitational wave measurement GW170817, along with the results of the NICER mission, that were not present at the time of publishing the original work [56] are compared with the results. The scalar-isovector meson, commonly known as δ, affects the radius of the star more than its mass. Thus, the gravitational wave and NICER constraints on the radius are contrasted with the QMC model predictions, showing good agreement. The effects of the δ on the tidal deformability and moment of inertia of the star are also discussed, where the results show relative indifference but general compatibility of the model with the experimental constraints.

4.1 Introduction

As previously mentioned, the QMC model shows interesting results for the physics of neutron stars. Even when hyperons are introduced, the natural many body forces that arise from the non linearity of the scalar couplings provide extra repulsion and do not soften the equation of state as much as other models. Furthermore, the scalar-isovector sector has been studied in relativistic mean field (RMF) approaches (see Refs [43, 51, 53, 71, 75]), mostly concluding that this sector only negligibly affects symmetric matter. However, it is likely to affect highly asymmetric matter. Most importantly, hyperon thresholds are affected, which in turn can affect the equation of state at high densities. The intention of the present work is to incorporate the scalar-isovector meson in a self-consistent way into the QMC model, study its effects in nuclear matter in general and, more specifically, in neutron star physics.

4.2 Theoretical Model

As lengthily discussed in Chapter 1, the QMC model is constructed from the Bag model picture for baryons and assuming that the quarks inside the bag interact with quarks in surrounding bags via the exchange of mesons. It is trivial to include the full baryon octet in the model and it does successfully reach the $2M_\odot$ threshold, even when hyperons are included. The derivation in Chapter 1 already included the δ model, however, it had not been included prior to this study and we will discuss its specific effects in more detail here.

To briefly review some basic features of model, the mass is calculated via the Bag model, including zero point fluctuations z_0 and hyper-fine colour splitting via one gluon exchanges ΔE_M

$$M_B^\star = \frac{\Omega_u N_u + \Omega_d N_d + \Omega_s N_s}{R_B} - \frac{z_0}{R_B} + \Delta E_M + \mathcal{B} V_B \,. \tag{4.1}$$

The quark energy eigenvalue, which is proportional to Ω_q depends directly on the scalar mean fields $\bar{\sigma}$ and $\bar{\delta}$ and we can easily determine

effective mean-field dependent couplings at the baryonic level, i.e.

$$M_B^\star = M_B - g_\sigma^B(\bar{\sigma},\bar{\delta})\bar{\sigma} - g_\delta^B(\bar{\sigma},\bar{\delta})I_B\bar{\delta}\,, \tag{4.2}$$

This effectively describes the effect of the self consistent many body forces on the baryon which are density dependent. The most direct way of understanding its effect in neutron star dynamics is that, the non linear changes in the baryon mass, via the scalar interaction, affects the density dependence of each particle's chemical potential, which in turn affects the β-equilibrium relations and the particle composition of the star's core.

4.2.1 Physical Parameters

The QMC model takes as input parameters mainly the radius of the bag, which we choose as $R_B = 0.8$fm and the mass of the sigma meson $m_\sigma = 700$MeV. The masses of the remaining mesons are taken from experiment [67]. As explained previously, in Chapter 1, the physical constants related to the bag model description of the baryon, namely the bag constant, α_c representing the strength of the one gluon exchange and the mass of the strange quark are all fitted to reproduce the free masses of the baryon octet.

With respect to the coupling constants, firstly, the δ coupling will be varied to assess the influence of the scalar-isoscalar potential. Three values were explored, namely, zero, 3fm^2 (inspired by Ref. [34]) and double that value, 6fm^2. Conversely, the coupling constants for the remaining mesons are fitted to reproduce known nuclear matter parameters, specifically, the saturation density, binding energy per nucleon and symmetry energy of symmetric matter. The standard values were chosen as $\rho_0 = 0.16\text{fm}^{-3}$, $\mathcal{E} = -15.8$MeV and $S = 30$MeV and calculations fitted to these are labeled as "std. fit.". However, in order to gauge the systematic error introduced by this fit we performed calculations with other values as well, within the margin of errors of the measurements of these quantities. It was found that saturation density is the quantity that affects the results the most, and thus, we chose to also show results fitting to $\rho_0^+ = 0.15\text{fm}^{-3}$, which tends to increase the mass, and $\rho_0^- = 0.17\text{fm}^{-3}$, which tends to decrease the mass. These should be considered as boundary values for the uncertainties

EOS	NM parameters			QMC couplings					
	ρ_0	S	$\mathcal{E}$	G_ω	G_ρ	G_σ	G_δ	L_0	K_0
	[fm^{-3}]	[MeV]	[MeV]	[fm^2]	[fm^2]	[fm^2]	[fm^2]	[MeV]	[MeV]
Std. Fit	0.16	30	−15.8	6.39	4.27	10.0	3.0	63.7	282
$\boldsymbol{\rho}_0^-$	0.17	30	−15.8	5.93	3.81	9.46	3.0	62.6	284
$\boldsymbol{\rho}_0^+$	0.15	30	−15.8	6.88	4.59	10.64	3.0	62.4	280

Table 4.1: Nuclear matter parameters and coupling values for different EOSs determined by the values of ρ_0, S and $\mathcal{E}$. The value of K_0 does not change significantly for different values of G_δ , while the slope, L_0, for the cases with $G_\delta = 0$ and 6 fm^2 we have, respectively, a decrease and an increase of 10 MeV.

in all nuclear matter parameters, not only saturation density, as all other attempted fits are found to be within the boundaries of these two extremes.

The values for the calculated standard fit are shown in Tab. 4.1 and the other two fits, representing the limits of parameter variations are show in Tab. 4.2.

In the sections below we will show our numerical results and discuss them. Firstly, we consider the effects of the isovector-scalar meson sector on the nuclear matter equation of state. Following that we discuss the effects (or lack thereof) that the crust equation of state may have in the neutron star observables. Finally, we turn our attention to the composition of dense matter and discuss whether or not Δ baryons play a role in the equation of state.

EOS	NM parameters			No δ couplings				Double δ couplings			
	ρ_0	S	$\mathcal{E}$	G_ω	G_ρ	G_σ	G_δ	G_ω	G_ρ	G_σ	G_δ
	[fm^{-3}]	[MeV]	[MeV]	[fm^2]	[fm^2]	[fm^2]	[fm^2]	[fm^2]	[fm^2]	[fm^2]	[fm^2]
Std. Fit	0.16	30	−15.8	6.11	2.74	10.03	0.0	6.57	5.33	9.99	6.0
$\boldsymbol{\rho}_0^-$	0.17	30	−15.8	5.67	2.35	9.5	0.0	6.12	4.94	9.45	6.0
$\boldsymbol{\rho}_0^+$	0.15	30	−15.8	6.63	3.08	10.69	0.0	7.08	5.77	10.61	6.0

Table 4.2: Fit parameters for different choices of δ couplings and nuclear matter parameters.

4.3 Hyperon Thresholds and δ Meson Effects

As formerly discussed in Chapter 1 and in the sections above, the goal is to study nuclear matter in β-equilibrium. To that end 'we minimise the energy density under the constraint of charge neutrality and baryon number conservation

$$\epsilon(n_n, n_p, n_e, n_\mu, n_\Lambda, n_{\Sigma^+}, n_{\Sigma^0}, n_{\Sigma^-}, n_{\Xi^0}, n_{\Xi^-}) + \lambda_1 \left(Q_i n_i\right) + \lambda_2 \left(n_b - \sum_{\text{baryons}} n_i\right) \tag{4.3}$$

also taking into account the lepton equilibrium relation but disregarding the neutrinos, which at zero temperature simply escape the system without interacting. As discussed, that amounts to constraining the muon density by

$$n_\mu = \frac{1}{3\pi^2}\left(\text{Re}\sqrt{k_{F_e}^2 + m_e^2 - m_\mu^2}\right)^3. \tag{4.4}$$

Effectively minimising this functional for each value of baryon number density n_b determines the exact proportion of each particle species that populates the star at each point in the star's core. This result can be seen in Figs 4.1 and 4.2. Fig. 4.1 shows the case where the isovector scalar meson is not present in which the Λ baryon comes in first, at roughly 0.55fm^{-3}. Figure 4.2 shows the case where the δ is included, in which we can see that the threshold of the Λ which is isoscalar, does not suffer any change, however the Ξs do. Consequentially, the hyperon configuration of the star past that point is also modified, the number of Λs is suppressed and the Ξs become dominant.

Although we have not yet explicitly discussed how the equation of state affects the mass and the radius of the stars, it can be very illustrative to see how the hyperon thresholds are reached as one increases the mass of the star. In Fig. 4.3 we plot the star's mass as a function of its central density, showing also the density thresholds for different hyperons. It's clear that hyperons only become relevant for stars with masses above $1.6\text{M}_\odot$.

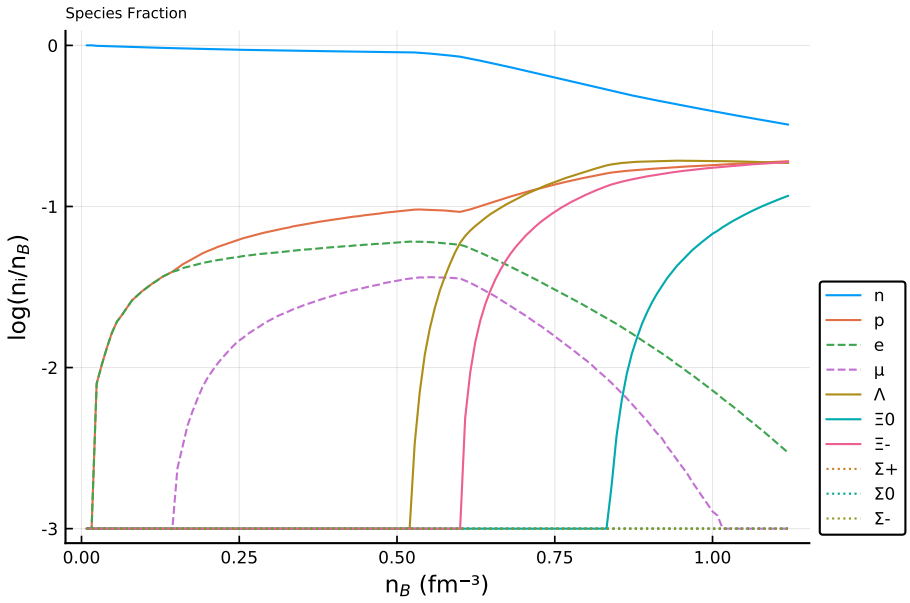

Figure 4.1: Species Fraction for the case without the δ

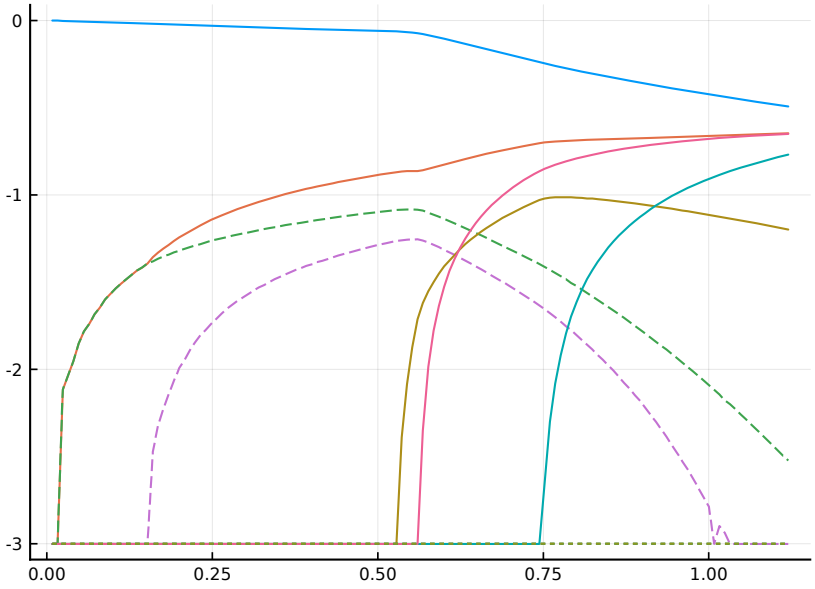

Figure 4.2: Species Fraction for the case with $G_\delta = 3\text{fm}^2$

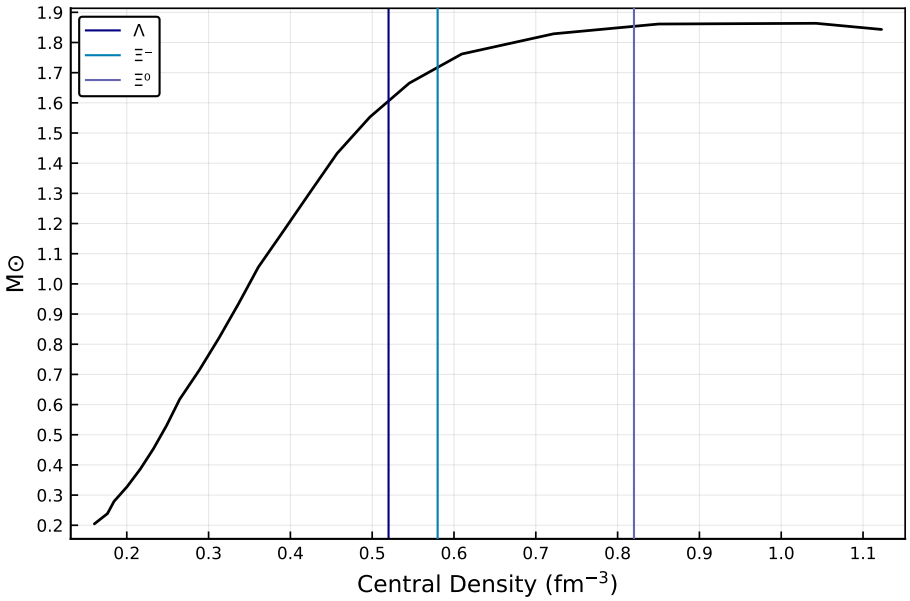

Figure 4.3: Stellar mass as a function of the central density for the case without the δ. Vertical lines show the density in which a certain hyperon species starts to be produced.

4.3.1 Equation of State effects

In Fig. 4.4 the full equation of state is plotted for different fit values, showing roughly the effect that uncertainties on the value for nuclear matter density cause on QMC model at high densities. Effectively the region where the two extreme fits disagree the most is the innermost core of the star and, the end result on the maximum mass of the neutron star due to this difference is small (which will be discussed shortly). Most importantly, Fig. 4.4 makes it clear that although the QMC model does suffer from the typical softening of the equation of state when hyperons come in, which can be seen by comparing with the nucleon only case, that softening is counteracted by the many-body repulsive forces that the model takes into account. These help build up pressure to withstand high mass values compatible with [20]. Finally, Fig. 4.5 shows for contrast the effect of introducing the δ meson, or, alternatively, it can be seen as the effect of shifting the hyperon thresholds and fraction in the core.

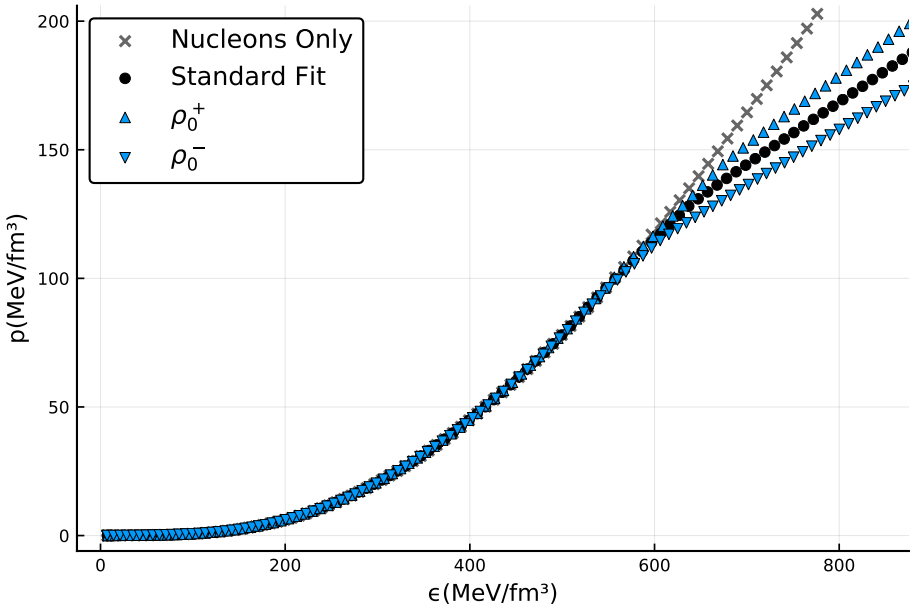

Figure 4.4: QMC Equation of state, both for the full baryon octet case and for the case with nucleons only. This plot shows the case without the δ,

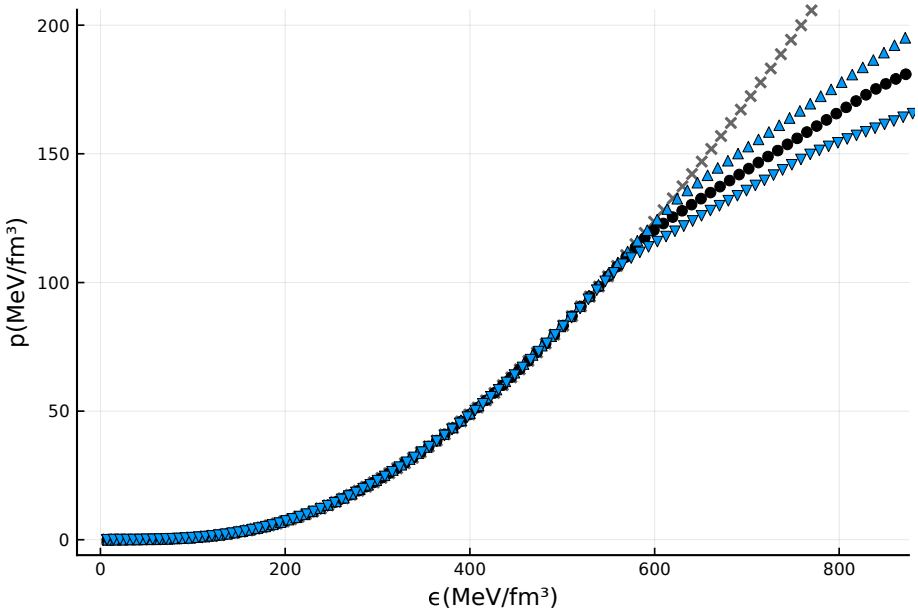

Figure 4.5: Whereas this is showing the case with $G_\delta = 3\text{fm}^2$ for contrast. Fits correspond to parameters listed onTable 4.1.

4.3.2 Mass × Radius

As it is depicted in Fig. 4.6 the model comfortably reproduces the mass of the star reported in Ref. [6], which, of all of the neutron star mass measurements, is the most precise. It must be said, however, that the main intent of this work was to gauge the effects of the δ sector, not on the mass, but on the radius, which we will discuss shortly. The δ also affects the nucleon only EOS, given that by virtue of its inclusion the other coupling constants are shifted through the nuclear matter fit. As a result, even stars without hyperons (i.e. with masses below $\sim 1.8 M_\odot$) are affected by the δ inclusion.

Figure 4.7 shows the effects of the δ in more detail. Results for the three studied values of the delta coupling are shown and, as previously discussed, although its effect on the mass is very small, the effect it has on the radius is not as modest. Needless to state that this effect far outweighs the uncertainties due to the value of ρ_0 on the fit (as can be seen in Fig. 4.6 the variance on the radius for masses below $1.8 M_\odot$).

The plot also shows the more accurate measurements of radius from the NICER mission [69] and [54]. Albeit large, the boxes do comfortably show all fits compatible with the data. This particular constraint should be taken as more reliable than the GW170817 which, although every fit also reproduces it, seems to prefer a lower radius.

Importantly, though, another source of systematic uncertainty could be claimed. Namely, the crust EOS used in the calculations which was based on a different model. Given the fact that the crust could alter the radius of low mass stars, we shall acknowledge that as another potential source of imprecision in the study. Firstly, we use a crust taken from Refs. [35, 36] which models the whole density range, including the low density region by employing modern techniques which take into account density dependence, relativistic effects and excluded volume effects. Moreover, we estimate the crust dependence of our results for the star's radius by the analysis depicted in Fig. 4.8. In it we show the proportion of the radius that is due to each section of the star, considering that, roughly, the outer crust and the inner crust are divided by the neutron drip density and

the core by the point in which the QMC model becomes dominant. We can see that, for stars with mass in in excess of $1.5 M_\odot$ the core composes more than $> 85\%$ of the star's radius. Therefore, the effects we see in our study, although focused on the QMC model, cannot be claimed either to be crust-dependent or perhaps that it is at all likely that modifications in the crust EOS would "erase" the effects we see, due to changes in the core.

4.3.3 GW170817 Constraints

With respect to the quantities that are constrained by GW170817, the inclusion of the δ is largely indifferent. Take, for instance, the moment of inertia which was constrained, albeit in a model dependent way, in Ref. [94]. The latter constraint is shown in Fig. 4.9 and the QMC model is compared with it, showing good agreement. The contribution of the crust to the moment of inertia is shown in Fig. 4.10 and it amounts to no more than 6% for average mass or high mass stars.

The tidal deformability, which we shall review in more detail in the next section, is also constrained by GW170817. In Fig. 4.11 we see that the model is within the calculated band (Ref. [2]) and similarly the binary tidal deformability in Fig. 4.12 where the constraints of Refs. [1, 19, 76] are shown by the red box (inside which the mass values are compatible with GW170817) and by the blank regions which are prohibited by the fact that, by construction $M_1 > M_2$, and of the upper limit in $\widetilde{\Lambda}$ derived by [19], namely $\widetilde{\Lambda} \leq 640$. The model calculations do show results compatible with both studies for all values of G_δ, which indicates that the model is indeed consistent with the GW measurement.

Nevertheless, as discussed in the previous section, it could be claimed that our results may include an unestimated source of systematic error due to our fixed choice of an EOS for the crust that is not based on the same model. We shall investigate here for the GW170817 constraints these potential effects in the next section.

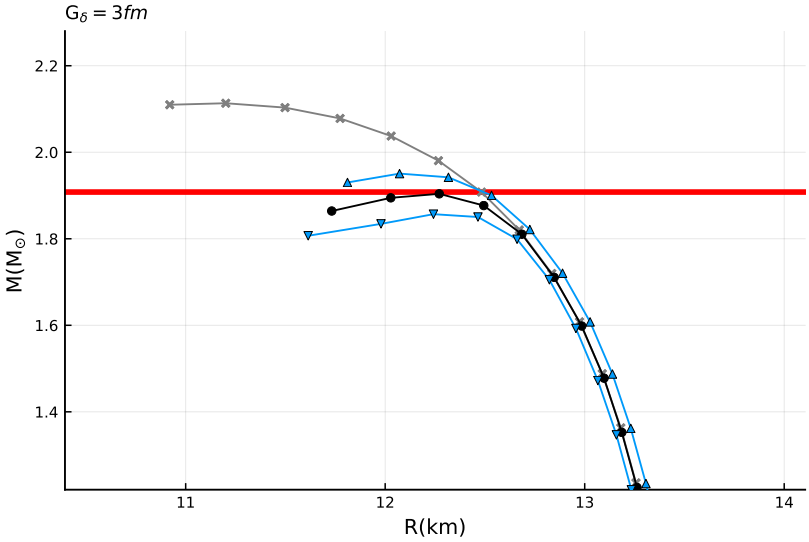

Figure 4.6: Mass and radius relation extracted from the TOV solution for the case with $G_\delta = 3fm^2$, highlighting the [6, 20] measurement. The plot markers follow the same pattern as Fig. 4.4.

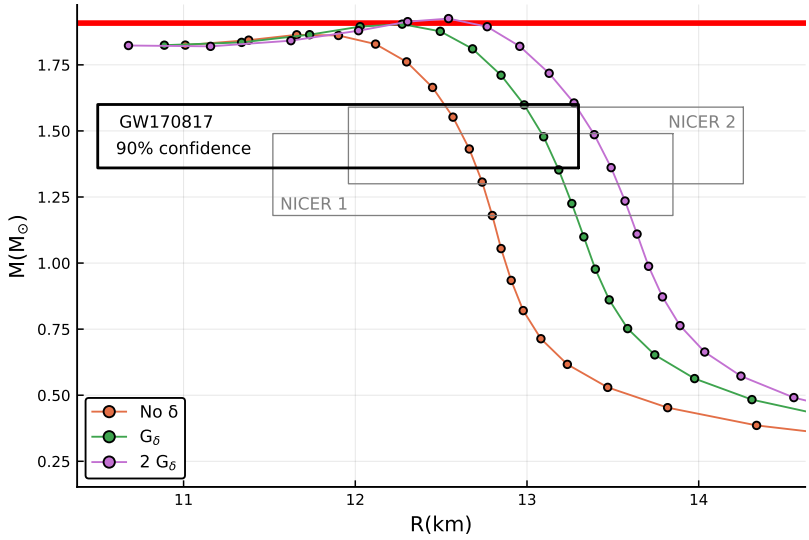

Figure 4.7: For the standard fit only, the mass-radius relation is shown for every value of the isovector-scalar coupling. Considering the $\rho_0^{\pm}$ fits all of the curves are compatible with Refs [6, 20]. The constraints on radius from the NICER mission, labeled NICER 1 and NICER 2, correspond respectively to Refs. [69, 54]

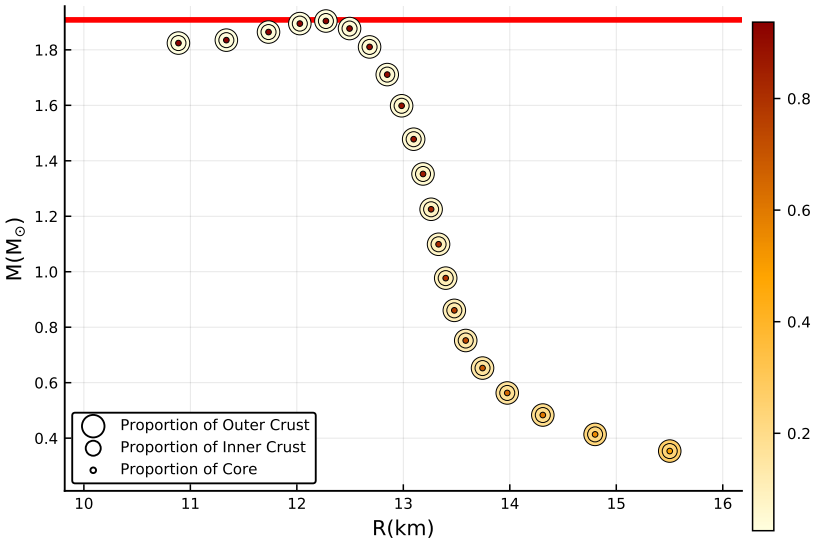

Figure 4.8: A TOV plot showing the proportion of the total radius of the star for each section: outer crust, inner crust, and core.

4.4 Crust Effects on Tidal Deformability

The first binary neutron star merger gravitational wave signal, so called GW170817 [3], and the new data it provided have been sources of multiple new studies regarding new constraints on the properties of neutron stars such as its radius, moment of inertia, and tidal deformability, the latter being of particular importance. The tidal deformability is especially interesting as the GW170817 analysis was the first to constrain this property. The tidal deformability, simply put, represents the following. If the star is put inside an external gravitational field and as a consequence gets deformed from its rest spherical shape, by how much will the star be deformed. In other words, placing a spherical star in an external field $\mathcal{E}_{ij}$ will induce a quadrupole moment Q_{ij} on the star. They obey a linear relation

$$Q_{ij} = -\lambda \mathcal{E}_{ij} \tag{4.5}$$

and the parameter λ is called the tidal polarizibility. Equivalent to λ and carrying the same overall information we have the Love number

$$k_2 = \frac{3}{2R^5}\lambda \tag{4.6}$$

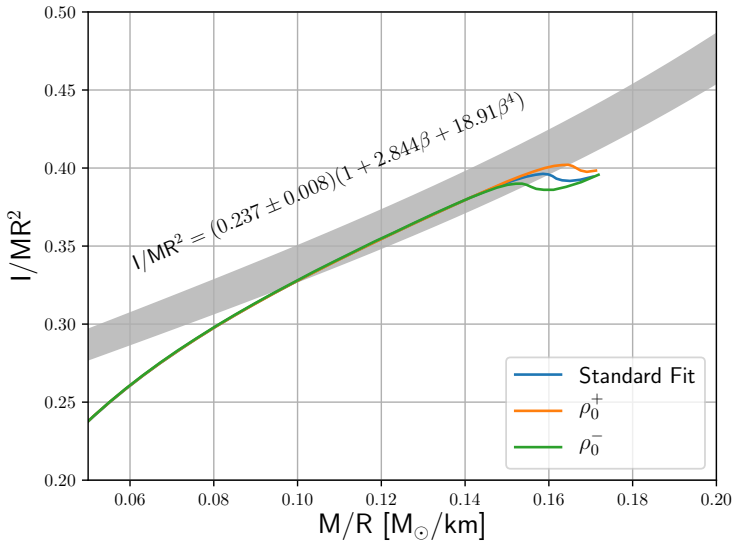

Figure 4.9: Ref. [94] band on the moment of inertia and the QMC model's result. The δ meson influence is negligible.

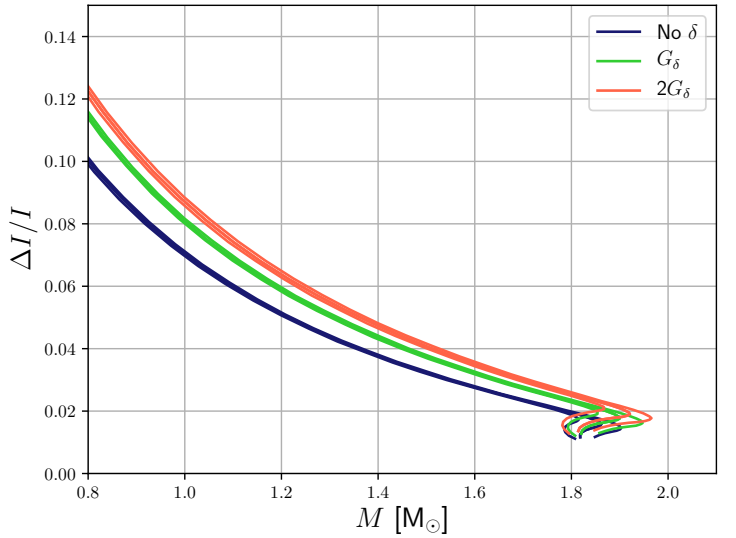

Figure 4.10: Showing the crust's contribution to the total moment of inertia.

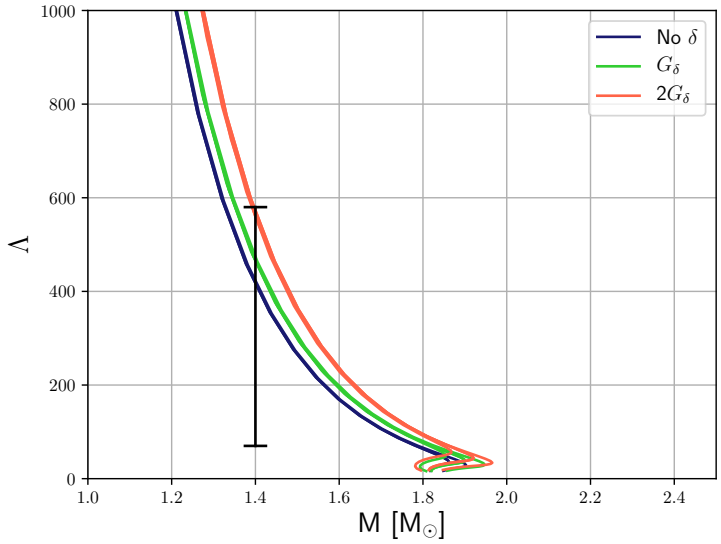

Figure 4.11: Total tidal deformability and band derived in [2].

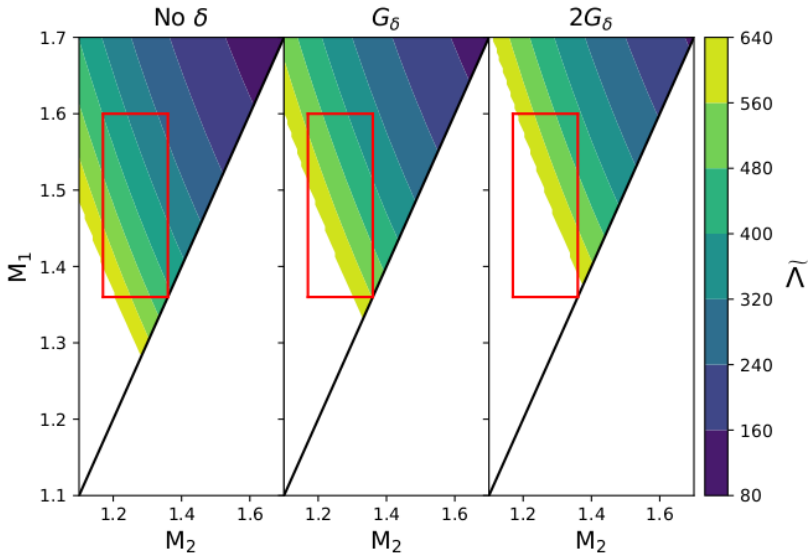

Figure 4.12: Binary tidal deformability and constraints shown in [2, 19, 76]

which is related to the tidal deformability by

$$\Lambda = \frac{2R^5}{3M^5} k_2. \tag{4.7}$$

It is convenient to use each of these three parameters, even though they carry similar information, in writing the equations. More importantly, though, the measurement of GW170817 has given us constraints on these quantities. Take the tidal deformability Λ of a single star and the tidal deformability of a binary system of stars $\tilde{\Lambda}$. Refs [2, 3, 19] have given us

$$70 \leq \Lambda|_{m=1.4M_\odot} \leq 580 \tag{4.8}$$

$$84 \leq \tilde{\Lambda} \leq 640. \tag{4.9}$$

Similarly, the moment of inertia of these stars has been constrained using the gravitational wave data [94]

$$8.82 \leq \bar{I} \leq 14.74 \tag{4.10}$$

where $\bar{I} = I/M^3$.

These constraints are extremely valuable for nuclear physics modelling of neutron star cores. These stars, however, are not only core. The crust of a neutron star is a complex system that also requires delicate modelling. Many of the phenomena involving neutron stars such as pulsar glitches, the structure of the so called pasta phases and its properties such as strength [15] and other quantities, are all essentially tied to the physics of the crust.

A valid question, then, would be how much of the tidal deformability and of the moment of inertia of these stars is due to the crust and how much is due to the core? Given that we know that the radius of the crust is in fact quite sizeable for stars of medium masses, how much of the deformability of the star is contributed by the crust?

Answering these questions is not an easy task. Where for the radius is easy to know how deep beneath the surface the crust ends and the core begins, for quantities such as the deformability or moment of inertia, this estimation is not as straight forward. In Ref. [38] we devised a method

to estimate this contribution. In that publication we simply presented one possible estimate. In fact, a subsequent publication by Perot et al [63] with a different approach not only confirmed our findings that the crust has only a very small effect on both Λ and $\bar{I}$, but gave much stronger limits on the crust contribution. Another publication by Piekarewicz et al [64] which we were unaware of at the time of submitting our work had also commented that, although the love number k_2 seems to be more sensitive, the factor of R^5/M^5 on the tidal deformability attenuates this sensitivity and makes Λ quite indifferent to the crust. Therefore, although none of these individual attempts are enough on their own, collectively they give us strong evidence of the claims exposed in this section.

4.4.1 Estimation technique

Throughout Ref. [38] we used two sets of equations of state to estimate which proportion of Λ and $\bar{I}$ is due to the crust. In the first set, which we refer to as Full EoS in our plots, nine equations of state taken from the database in Ref. [60], all of which include their own models for both core and crust. This is an attempt to make our claims more model agnostic given that our results aren't particular to one crust model, the set referred to as Core Only in which we take the equations from the first set and attempt to remove their crusts by fitting each EOS in the region $\epsilon \geq 100\text{MeVfm}^{-3}$ with a typical nuclear matter only functional form and extrapolate that fit down to $\epsilon \leq 100\text{MeVfm}^{-3}$. Since the fits are made using a piece-wise polytropic

$$p_i(\epsilon) = K_i \epsilon^{\gamma_i}, \tag{4.11}$$

and given that the EOS uniform nuclear matter is expected to be a power law at low densities, we expect this approach to be fair. Moreover, we have tested the same approach using a different cutoff threashold for fit, 50MeVfm^{-3} instead of 100MeVfm^{-3}, and our results were unchanged. Using the TOV equations we obtained the mass-radius relations depicted in Fig.4.13

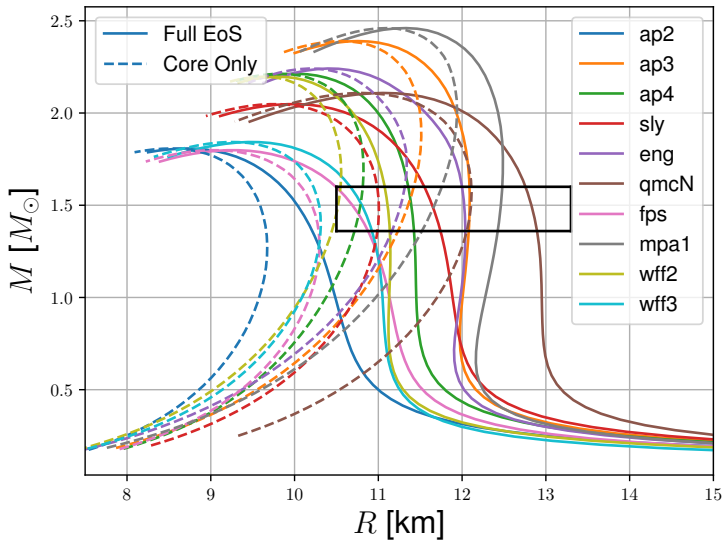

Figure 4.13: Mass-radius relations for the two sets defined above. All of the subsequent plots will use the same labelling for the two different sets.

To estimate the relevance of the crust to the physical parameters we define the following quantity:

$$\frac{\Delta\alpha}{\alpha} = \frac{(\alpha_{\mathrm{INM}} - \alpha_{\mathrm{UNM}})}{\alpha_{\mathrm{INM}}} \tag{4.12}$$

where UNM refers to uniform nuclear matter in the low density region and INM refers to inhomogenous nuclear matter in the crust. More explicitly, it is the difference between the quantity α calculated with crust and without crust, divided by the standard (with crust) EOS result.

In agreement with Piekarewicz et al [64] we do obtain quite discrepant values for the Love number (see Figure 4.14). The values for Λ, however, suffer quite insignificant changes (Figure 4.15). Where for every EOS we obtained $|\Delta\Lambda/\Lambda| < 10\%$, for stars with mass greater than $1.4\mathrm{M}_\odot$, i.e. the vast majority of known neutron stars, this value is below 4.5% at most.

The same applies to the moment of inertia depicted in Figure 4.16. An overall limit is $|\Delta I/I| < 9\%$, if we take stars with masses greater than $1.4\mathrm{M}_\odot$ this contribution goes down to 4.5% at most.

It is important to note that the universal relation between moment of

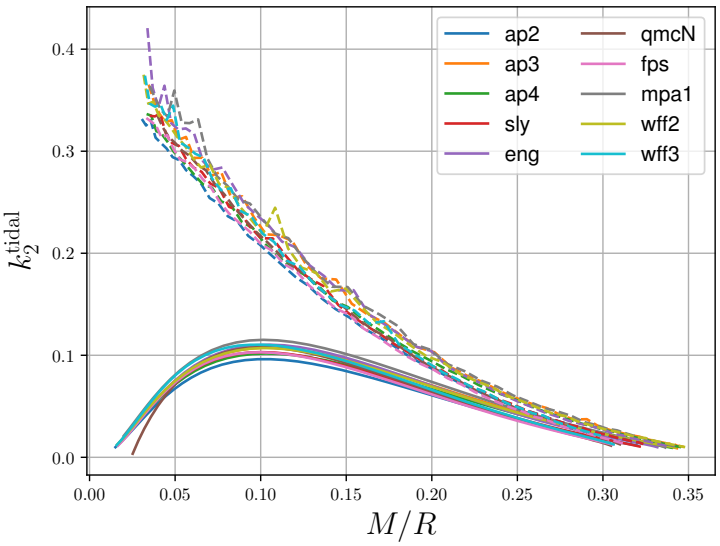

Figure 4.14: Love number for with/without crust.

inertia and the Love number (the I-Love relation which is a subset of the I-Love-Q relation involving the quadrupole moment) is still verified. The I-Love relation, Fig. 4.17, remains unbroken even for the equations of state with the crust removed.

This concludes our determination that not only the results shown here for the effects of the δ meson, but also any other claim that could be made about a potential effect of the core's EOS on mass, tidal deformability, and moment of inertia, are all mostly indifferent to the description of the crust for stars with mass greater than **1.4** solar masses.

4.5 Δ Baryons in High Density Nuclear Matter

Let us return our attention to the composition of nuclear matter at high densities. The debate over whether or not hyperons, or quark matter, play a role in neutron star physics is one of many debates with respect to dense stellar core compositions. Amongst others the role that Δ baryons play, if any, has also been a point of discussion. Early works [26, 27, 24] showed indications that only at incredibly high densities, roughly around $9n_0$, would these baryons start to be created. However, as a consequence of

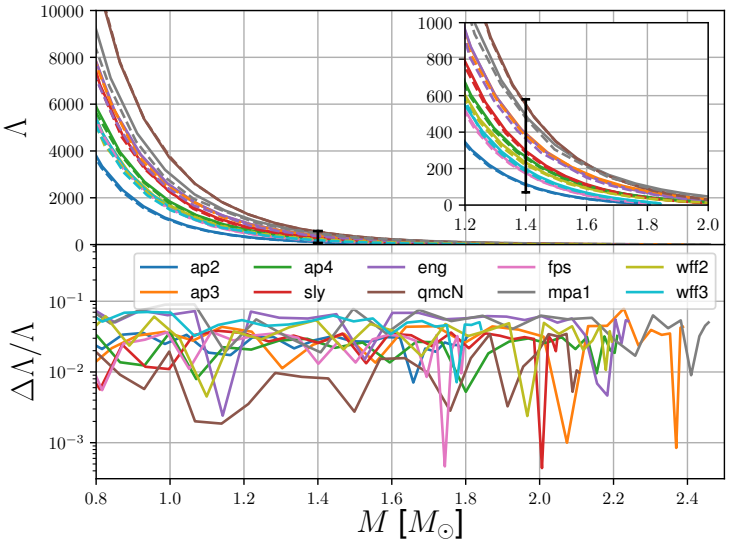

Figure 4.15: Tidal deformability showing the crust contribution

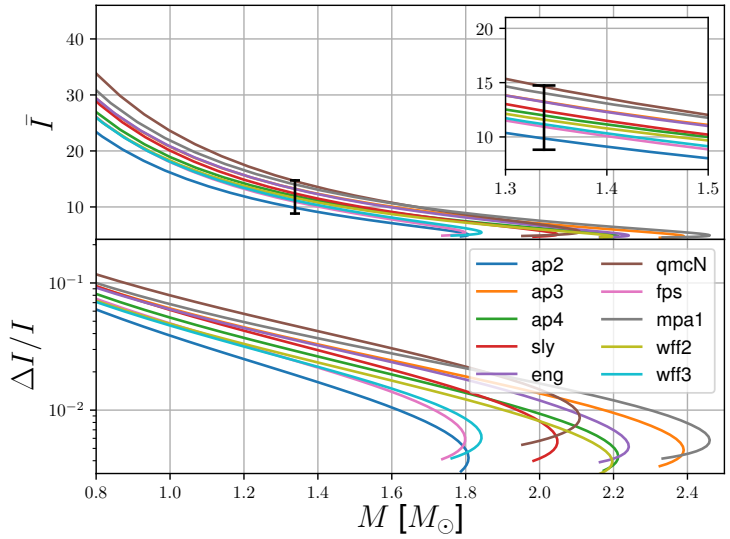

Figure 4.16: Moment of inertia showing the crust contribution

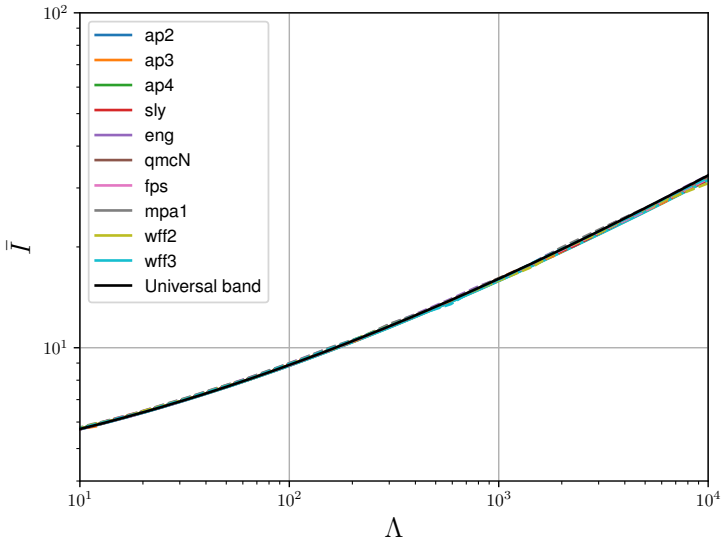

Figure 4.17: Moment of inertia and Love number confirming the universal relation presented in Ref. [92]

multiple developments in the field, new models, new data and constraints, several other predictions appeared [49, 50, 13], showing much lower values and, in fact, when taken into account they were shown to change the results for neutron star structure quite drastically.

The effects of such a presence, if it would occur, are not small by any means whatsoever. J. J. Li et al [50, 49] showed that the tidal deformability of a neutron star (that is, how deformable from its spherical shape the star is given an external gravitational potential) of mass around 1.4 times the mass of our sun could be affected by the presence of Δs by as much as 300MeV less than the case with no Δs. They've also shown [50, 49] that the radius would be severely affected and could suffer a reduction of as much as 2km. These are truly large effects.

4.5.1 Creation Condition for the Δ^-

Due to β-equilibrium the Δ^- would be the first isobar to be created, given the fact that it is negatively charged. Furthermore, due to the high density of neutrons and consequentially the Pauli blocking of many neutron levels, the Δ^- would become stable. If in free space the decay of a stationary

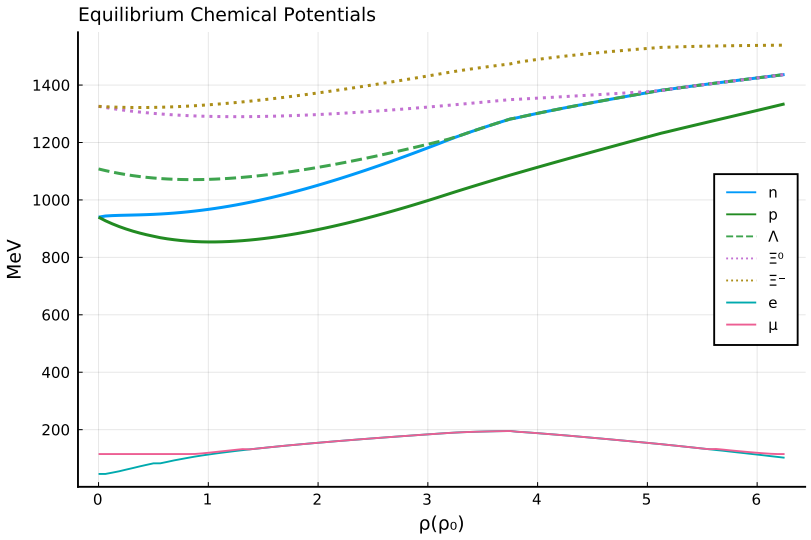

Figure 4.18: Chemical potentials in β-equilibrium for all baryons calculated for the case without the δ.

Δ^- produces a neutron with momentum roughly around 220MeV, we can approximate the density required to Pauli block this reaction as grossly $k^3/(3\pi)^2 \approx 0.05$ fm^{-3}.

Treating it as stable particle, it could be produced in reactions such as

$$\Delta^- \rightleftarrows n + e^- + \nu_e$$

and

$$\Delta^- + p \rightleftarrows n + n.$$

In β-equilibrium with the other components it should be required that the chemical potentials satisfy the relation:

$$\beta\text{-equilibrium condition:} \quad \mu_{\Delta^-} = \mu_n + \mu_e\,, \tag{4.13}$$

assuming again that neutrinos are not trapped in the star.

Given that our objective is simply the determination of whether Δ baryons can appear under β-equilibrium in high density matter, all that is required is that we calculate the chemical potential of the Δ^-, i.e. the price of creating a Δ^-, at rest. Furthermore, it is trivial to see that since we are calculating the creation condition for the first element of Δ isobars,

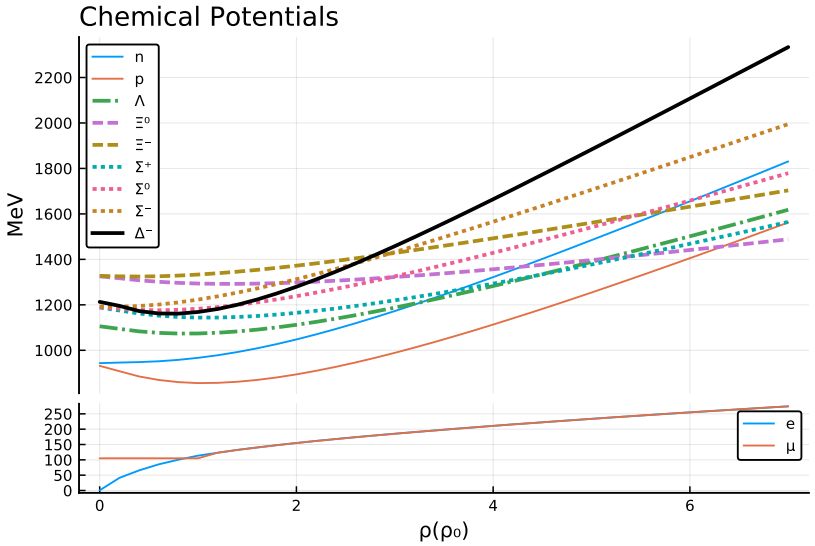

Figure 4.19: Production threshold (l.h.s. of Eq. 4.14) for all baryons calculated through the QMC model for the case without the δ.

no Fock terms will contribute to its self-energy. The relevant condition is, then

$$M_{\Delta^-} + \sum_{\varphi,B} \left| \begin{array}{c} B \\ \sim\!\bigcirc \\ \varphi \end{array} \right. = \mu_n + \mu_e \,, \tag{4.14}$$

or explicitly

$$M_{\Delta^-} - \sum_{\varphi,B} g_{\Delta\varphi}\bar{\varphi}(n_b) = \mu_n + \mu_e \,. \tag{4.15}$$

where $\bar{\varphi}$ are the mean field values for the mesons and the scalar couplings are evaluated at the relevant density.

As mentioned above, no Fock terms contribute to the self energy of the Δ. However, if one takes seriously the chiral structure of the baryons [81, 80, 82, 55] there could be a correction to the self energy due to Pauli blocking of the nucleon involved in the reaction

$$\Delta \to N + \pi$$

which could potentially be sizeable. Fortunately, this effect is taken into account in the nucleon's Fock term, via the pion contribution, and it is always below 20MeV for all astrophysically relevant densities [90]. It is to be expected that the converse contribution to the Δ should be of a similar weight. In fact, explicit calculation shows the Pauli blocking effect on the

mass of the Δ only exceeds 10 MeV if the Fermi momentum is close to the momentum of the neutron coming from the Δ^- decay. Our conclusions from results for the Δ^- thresholds which are shown in the next section do not depend on such minor margins.

4.5.2 Δ^- Thresholds

Figure 4.18 shows the chemical potentials of every species. Figure 4.19 show's the minimal thresholds for appearance of a species (l.h.s. of Eq. 4.14) including the calculated Δ^-, as a function of the baryon number density. It clearly shows that the rate of increase in chemical potential for the Δ is higher than that of the nucleons even though both the nucleon and the Δ have only light quarks. This faster increase in the chemical potential with density is a consequence of the hyperfine colour interaction, which for the Δ is completely repulsive. Particularly, in the QMC model, that interaction gets enhanced by the medium as the mass of the quarks are changed by the scalar mean field [59].

In Figs 4.20 and 4.21 we show the two sides of the equilibrium relation for the Δ^-. A creation threshold would be indicated by the crossing of the two curves, i.e., when the chemical potential of the Δ becomes lower than the chemical potential of the neutron and electron combined it would be energetically favourable for the system to start creating these particles. As it can be clearly seen in Fig. 4.20 that never happens and, as shown in Fig. 4.21, the strength of the isovector-scalar sector doesn't lower the gap nearly enough to create Δ baryons.

4.6 Conclusion

We have seen that the QMC model, when completed with an isovector-scalar meson, still reproduces nicely the astrophysical constraints on nuclear matter and most importantly, that its strength of interaction strongly affects the radius of the star. This is specially relevant given the advances in neutron star astronomy and the rapidly improving quality of radius measurements.

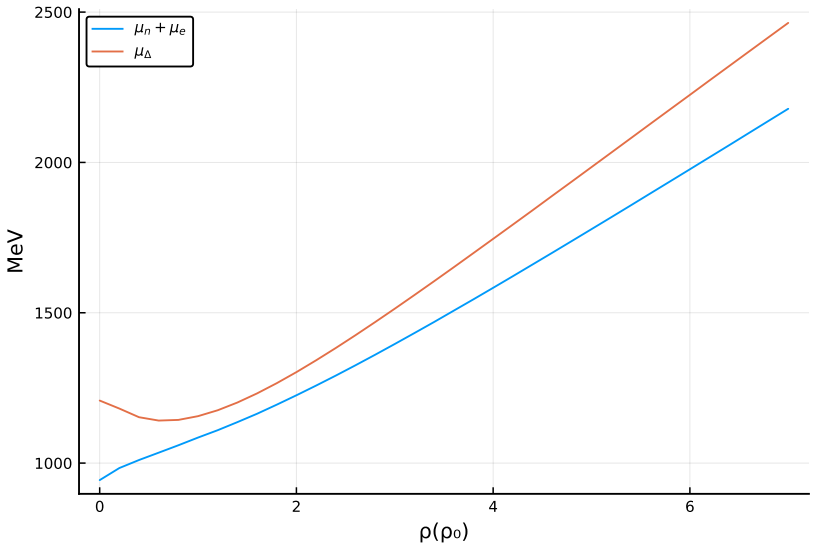

Figure 4.20: Condition for the appearance of the Δ^- under β-equilibrium.

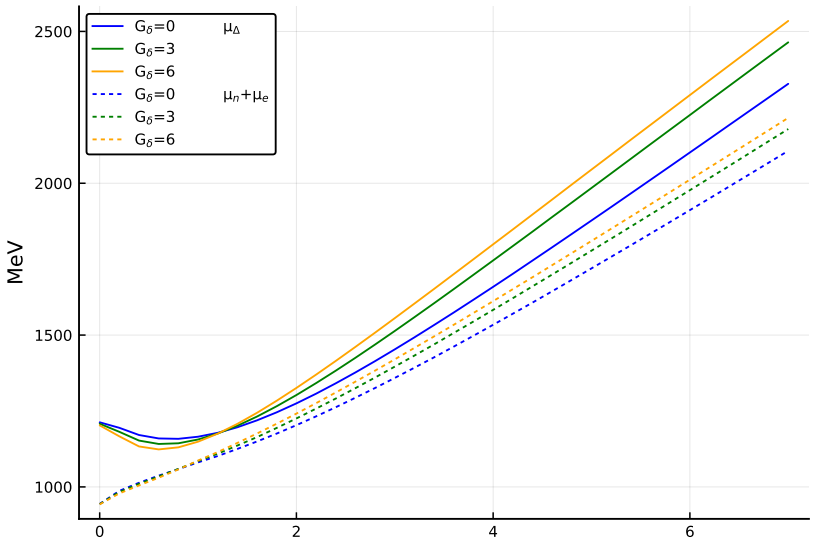

Figure 4.21: Comparison of μ_Δ for different choices of the coupling of the isovector scalar meson, δ, to the nucleon.

We also show that the many body forces that arise naturally in the QMC model without no new parameters, not only increase the pressure of matter with hyperons allowing it to sustain high neutron star masses, but also explain why the Δ baryon is not likely to play any role in high density nuclear matter.

It is important to note, however, that the model as it was used in this study does not reproduce comfortably some of the higher masses measured [61], however, that was not the study's intent. It is likely that if the highest mass cases were to be confirmed they might contain some form of deconfined quark matter, as was shown in Ref. [4]. Even then, the results for stars with slightly lower masses presented here are still valid.

Furthermore, by applying the technique explained in Section 4.4 to attempt to remove the crust to estimate its contribution we obtain quite hard limits. Both $|\Delta I/I|$ and $|\Delta\Lambda/\Lambda|$ show at most only a 4.5% contribution of the crust for masses greater than $1.4\mathrm{M}_{\odot}$. Although no-crust neutron stars do not exist, it is interesting to use this case as a point of comparison, a limiting extreme scenario. As previously mentioned, other references do find similar results. In fact Perot et al [63] show much harder upper limits for this contribution. For the tidal deformability they find that the contribution of the crust never exceeds 0.75%.

Once the radius measurements become even more precise and newer developments in gravitational wave astronomy come into fruition, nuclear models will not be able to neglect this contribution.

Chapter 5

Dark Matter Results

A long lived puzzle in nuclear physics relates to a discrepancy in different measurements for the neutron decay width. Neutrons in a beam – which are observed to decay to a proton – seem to live longer than neutrons on a bottle, a discrepancy that goes beyond three standard deviations. A proposal to solve it was published in 2018 [22] and it is based on the hypothesis that the neutron could couple to a nearly degenerate dark matter fermion. In Refs [57, 58] amongst others (referenced below), the implications of such a conjecture in the physics of neutron stars was studied. It was concluded that including this hypothetical dark particle (DM) in neutron stars severely softens its equation of state, effectively rendering the prediction for the maximum mass completely inconsistent with all of the measured neutron star masses. Furthermore, although a repulsive self-interaction amongst the DM particles does restore the maximum mass to previously acceptable values, the strength of this self interaction seems to be in serious tension with cosmological constraints on dark matter.

5.1 Introduction

The so called neutron decay anomaly refers to two incompatible measurements of the lifetime of the neutron (or, equivalently, its decay width). Measurements in which the neutrons are trapped in a ”bottle” and simply counted show a lifetime 8 seconds shorter than measurements of neutrons

in a beam [67] where the protons from the beta decay are measured directly at the end. This discrepancy amounts to approximately 3.6σ.

Many proposals to address this variance have been put forward over the years [62]. One recent one was published by Fornal et al [22] postulating a hypothetical dark matter decay. In such a proposal, which will be reviewed in detail below, the neutron would be decaying to a dark fermion whose mass should be nearly identical to that of the neutron, namely, a nearly degenerate particle. This conjecture was in fact a development over a previous proposal that hypothesised that the neutron could be oscillating into its mirror partner [73].

Such a hypothesis was received with excitement by the community, specially considering the fact that the same hypothesis could also explain another experimental discrepancy, the so called "reactor antineutrino anomaly", which refers to the 3σ experimental deviation from theory of the flux of antineutrinos on a reactor (see Ref. [74] for more detail). The authors of Ref. [79] argued that the experimental evidence indicates that this decay of the neutron to a DM particle should not involve photons as byproducts and Czarnecki et al [17] came out with more constraints on this decay related to the value of the neutron's axial charge. In summary, the hypothesis attracted much attention of other groups, mainly given its simplicity, its potential to perhaps solve some long lasting discrepancies and its relation to one of the most important topics in physics, the nature of dark matter.

In Refs. [57] and [58], we argued that although this proposal solves some old problems in nuclear physics, it does create some awkward difficulties in the realm neutron star physics. Namely, if the neutron could decay to another fermion almost degenerate with itself, in a Fermi sea of neutrons, as soon as the neutron chemical potential went above that of the DM particle, it would start decaying. Moreover, this would happen at rather low densities considering the neutron star scale. The study will be explained in detail below. Importantly, other groups released [8, 52] similar conclusions based on similar assumptions. Although these studies did not rule out the hypothesis entirely, they certainly raised scepticism about it.

5.2 Framework

As discussed previously in this thesis, one can simulate the internal structure of a neutron star given an equation of state (i.e. a relation between its thermodynamic potentials, energy, pressure and so on) by solving the Tolman-Oppenheimer-Volkof [84] (TOV) equations for different values of central energy density. They read, for the pressure, (with $c = G = \hbar = 1$)

$$\frac{dP(r)}{dr} = -\frac{1}{r^2}\left(\epsilon(r) + P(r)\right)\left(M(r) + 4\pi r^3 P(r)\right)\left(1 - \frac{2M(r)}{r}\right)^{-1} \tag{5.1}$$

and the mass is given by

$$\frac{dM(r)}{dr} = 4\pi r^2 \epsilon(r). \tag{5.2}$$

The input equation of state throughout this study is based on the QMC model, also discussed previously on this thesis. We include the proposed DM particle, both in the non interacting case and also considering a repulsive interaction mediated by a massive vector boson, a dark photon. We then compare the results to known astrophysical measurements and discuss the implications of the proposal to the physics of neutron stars.

5.2.1 Dark Decay

As previously outlined, the basis of claim is that the neutron could be decaying into a new channel as follows

$$n \to \chi_{\mathrm{DM}} + \lambda_{\mathrm{SM}}$$

that is, both into dark components and perhaps also into standard model particles (this is a formal expression only, it could be that this channel has no standard model products at all). That alongside the β decay

$$n \to p + e^- + \bar{\nu}_e$$

fully accommodates the 3.6σ deviation between experimental setups. In the original paper [22] they proposed three different possible scenarios:

- The dark sector being just a dark fermion χ, and the visible side γ a photon.
- The neutron decays to two dark particles, a fermion χ and a boson ϕ which has to be extremely light to satisfy the constraints; and no standard model particles.
- Or a dark fermion χ alongside a pair electron positron $e^- + e^+$.

Soon after the proposal, experimental evidence was put forward against [79] the first scenario where the decay would be to a dark fermion and a photon. With respect to equilibrium relations in stellar matter, the other two scenarios will end up being equivalent (see next section), so, for now, let us consider $n \to \chi + \phi$, the second scenario. In order for the decay anomaly to be fixed the following constraints have to be met

$$\begin{aligned} 937.900\text{MeV} < M_\chi < 938.543\text{MeV} \\ 937.900\text{MeV} < M_\chi + m_\phi < 939.565\text{MeV}. \end{aligned} \tag{5.3}$$

That is, broadly speaking, the fermion χ must have mass almost identical to the neutron mass, 940MeV, and ϕ must be very light and potentially massless.

5.2.2 Dark and Nuclear Matter Fermi Sea

If the proposed decay is possible, it would certainly happen inside a neutron star. The neutron has more than enough energy to decay to on-shell χs and given the lightness of the bosonic dark partner we can assume it escapes the star rapidly and with little or no interaction. For that reason, alongside our usual standard β equilibrium and charge neutrality, another equilibrium equation would have to be present, that of the $n \rightleftharpoons \chi + \phi$ equilibrium. Assuming the ϕs escape the system, this would add up to

$$\mu_n = \mu_\chi.$$

Finally, note how the decay proposal $n \to \chi + e^- + e^+$ would give us an equivalent relation given that the reaction $n + e^- \to \chi + e^-$ in equilibrium implies that $\mu_n + \mu_e = \mu_\chi + \mu_e$ which is identical to the relation above.

Case 1:

Firstly, let us assume that the dark matter particles do not interact with themselves. The energy and chemical potential of the χ would then be that of a free particle.

$$\begin{aligned} \epsilon_\chi &= \frac{2}{(2\pi)^3}\int^{k_F^\chi} d^3k\sqrt{M_\chi^2+k^2} \\ \mu_\chi &= \frac{\partial\epsilon}{\partial n_\chi} = \sqrt{M_\chi^2+k_F^{\chi 2}}, \\ k_\chi^3 &= 3\pi^2 n_\chi \end{aligned} \tag{5.4}$$

We can, therefore, calculate the influence of such dark matter particles in neutron stars by simply adding this energy contribution to the nuclear matter energy density

$$\epsilon = \epsilon^{\text{Nuclear Matter}} + \epsilon_\chi \tag{5.5}$$

and by making the neutron abide by the equilibrium relation in Eq. 5.4. We can then add the energy density of the dark matter particle to that of the QMC model[1] for nuclear interactions and calculate the pressure via the relation

$$p = \sum \mu_i n_i - \epsilon \tag{5.6}$$

where the sum is over all the particle species including the dark fermion. Finally, we input the equation of state into the TOV equations which, when solved for multiple possible internal pressure values, $P(0)$, give us the mass-radius diagram for stars described by this equation of state. The EOS for this system is plotted in Figure 5.1 and compared to the nuclear matter equation of state calculated via the QMC model. Note how nuclear matter is much harder, i.e. produces more pressure, than the EOS with DM. That is because baryons in general repel each other and the dark matter particle does not. Repulsion builds up pressure.

[1]Here, for consistency with the reference [57, 58] I will be using a version of the QMC model without the isovector scalar interaction that, by the time we wrote the paper [58] was the latest version of the model. The effects of adding the δ meson are evidently smaller than the dark matter effects and thus it does not affect any of the conclusions of the original paper. Also, we chose not to include hyperons in this calculation given that the cheaply created dark matter fermion would obviously dominate the spectrum of the star.

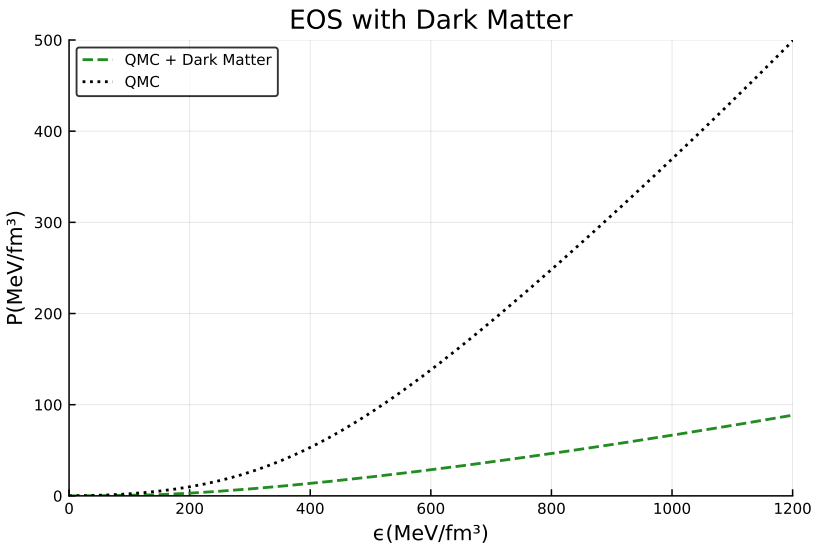

Figure 5.1: Equation of state including dark matter

Another interesting result is the so called species fraction. How much of each particle is present in the system at each value of baryon number density? That result is depicted in Figure 5.2. Note how the system is quickly overpopulated by dark matter. That is because free, non interacting fermions obviously minimise the energy density so it is preferable to the system to make up a huge Fermi sea of χs comparable to interacting/repelling nucleons.

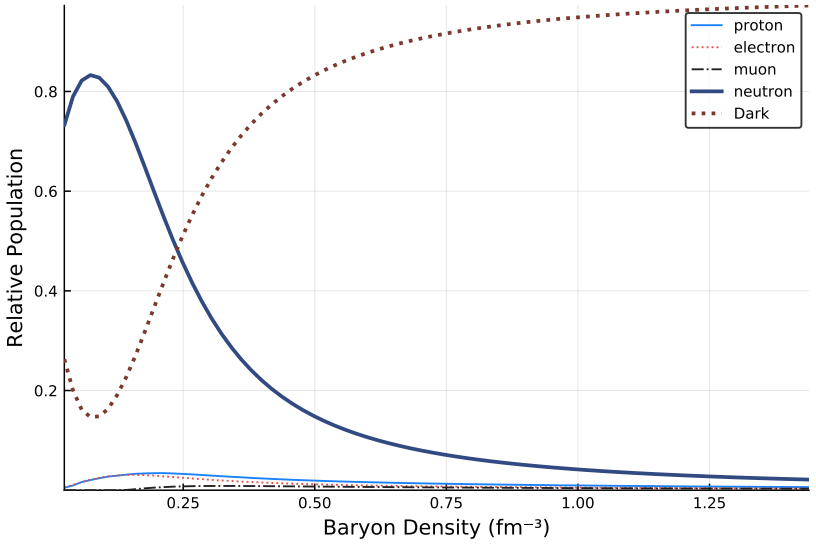

Figure 5.2: Species fraction as a function of baryon number density.

Using this EOS to calculate the mass and radius of stars with different internal pressures give us the result depicted in Figure 5.3. In interpreting

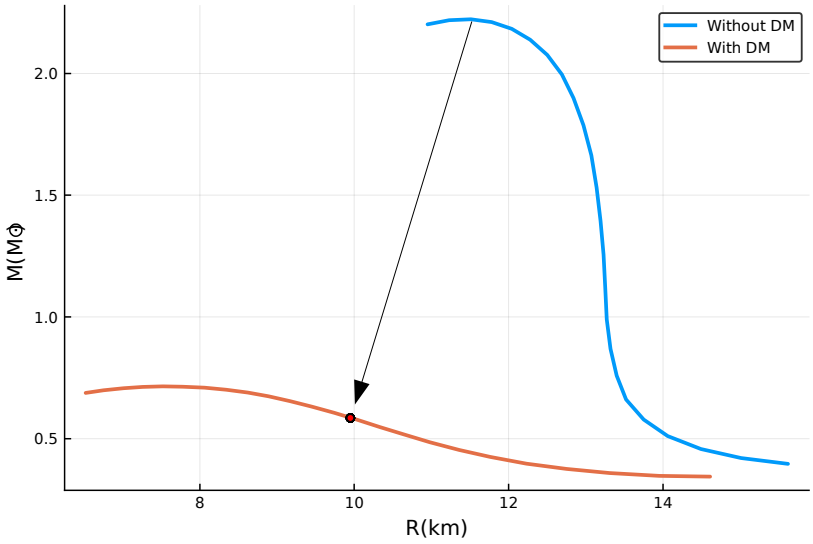

Figure 5.3: Mass-radius relationship for stars obeying the equation of state in Eq. 5.4.

these results, first and foremost, let us ignore the arrow and just focus on the mass-radius diagrams. Obviously the stars with dark matter present much lower masses than nucleonic stars. It should be said immediately that this is direct contrast with not only the measurement of a 2.0 solar mass star [20] but also with the majority of neutron star measurements [61], given that most of the neutron stars which have been discovered have mass greater than 1 solar mass. This is in fact enough to rule out this proposal of non interacting dark matter. However, note how, if neutrons in a neutron star were to decay to dark fermions slowly enough, the star would start its life as a neutron star and gradually have its neutrons decay to χs. This imposes an even stronger limit on the maximum mass. We choose the maximum mass of a neutron star without dark matter and calculate to which point in the mass-radius diagram it would go once its neutrons had a chance to decay to the DM particle and the star had reached its true minimum. Through particle number conservation we can calculate that to be the red dot in Figure 5.3 which has an even lower mass, namely $0.58\mathrm{M}_{\odot}$. This stellar decay is indicated by the black arrow.

Case 2:

It is possible, though, that these dark fermions interact with each other and, in order to give the model enough pressure let us assume this interaction is repulsive. Including a massive vector boson does we can calculate that easily in mean field approach. Call that dark vector boson V^μ (note that this vector boson can not play a role in the neutron decay) and simply, we have its mean field energy contribution as a function of the dark matter fermion number density

$$\epsilon_{\chi V} = \frac{m_V^2 \bar{V}^2}{2}, \quad \bar{V} = g_V \frac{n_\chi}{m_V^2}. \tag{5.7}$$

That is easily added numerically to the calculation of the energy density, chemical potential and pressure. Note how this depends only on one single parameter g_V/m_V and, to have a known analogous fermio-boson system to compare to we will show it as a function of g_ω/m_ω to facilitate the comparison with the nucleon omega interaction.

Primarily, we can revisit the species fraction. See in Figure 5.4 how the addition of the repulsive self interaction tends to disincentivize the creation of dark matter particles. Since now the energetic price is higher, it contains not only the Fermi level contribution $\sqrt{M_\chi^2 + k^2}$ but also some repulsive interaction with the rest of the dark matter in the star (which is added numerically in the chemical potential through the differentiation of the energy density). As a result, it once more becomes favourable to the system to create neutrons rather than χs.

Finally, putting the equations of state for the different values of g_V/m_V through the TOV equation we obtain Figure 5.5 as a result. The $g_V/m_V = g_\omega/m_\omega$ result looks much better than the free case, however it still does not reproduce the [20] $2.0\mathrm{M}_\odot$ measurement. Since the setup with $g_V/m_V = 10 g_\omega/m_\omega$ recovers the original QMC result it is fair to say that the minimum interaction that the dark matter hypothesis needs sits in between those two extremes[2].

[2]Here once more I am respecting the original material. In retrospect, it makes much more sense to calculate, not the amount of g_V/m_V necessary to recover the previous result but rather the minimum g_V/m_V that takes this hypothesis to $2.0\mathrm{M}_\odot$. We have

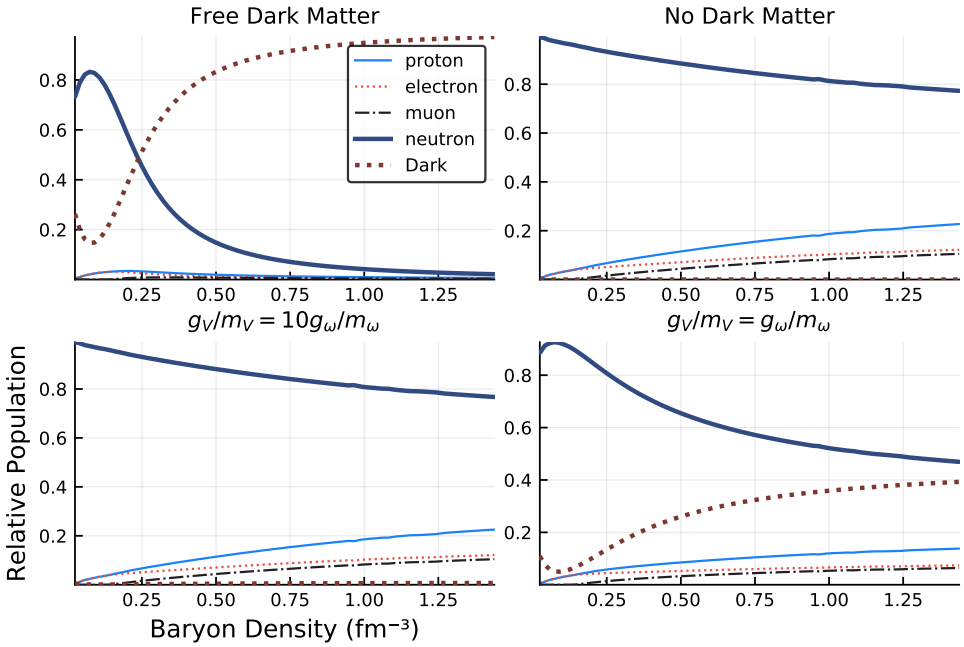

Figure 5.4: Relative population of each species for different strengths of vector interaction amongst the dark fermions.

This value of the coupling however should immediately strike one as dangerously large. In fact, D'Amico et al have shown in [18] that the cosmological dark matter must have a rather low cross section to respect the observations of Bowman et al in [11] of the 21cm gap in the cosmic background radiation, an effect that is believed to be caused by dark matter as well.

Finally, an important caveat should be stated. It could be claimed that this χ particle does exists, solving the neutron decay anomaly, but that it is not the cosmological dark matter at all, rather, some other type of non standard model particle. It still seems rather unlikely that a new force, as strong as the nuclear strong force (or stronger), could couple to the widely studied neutron without affecting our current experiments in nuclear and particle physics. While it is still possible that this particle exists, however, the fact is that constraints from observations of neutron stars are rather restrictive and must be taken into consideration.

checked what is the required repulsion to obtain $2.0M_\odot$ as a maximum mass to be around $25fm^2$. However, as the subsequent discussion makes clear, even $g_V/m_V = g_\omega/m_\omega$ is far too high for this hypothesis to respect other dark matter constraints from astrophysical observations and therefore I chose to maintain the original numbers.

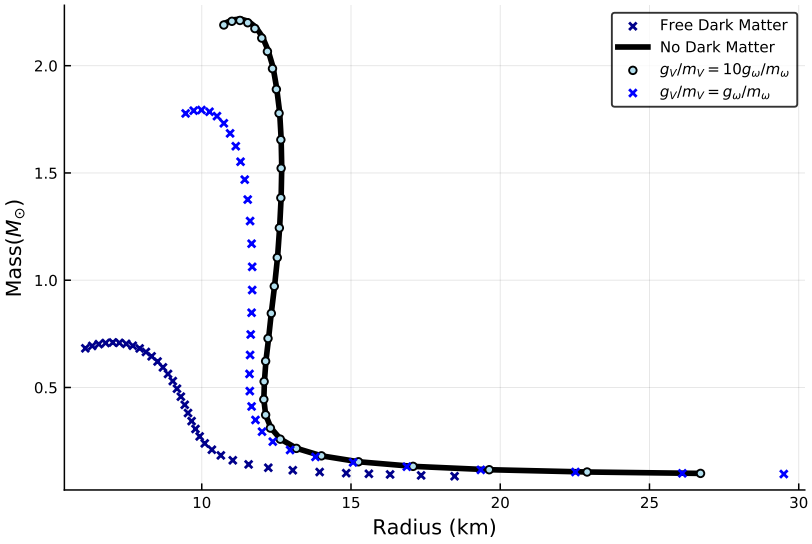

Figure 5.5: Vector boson interacting dark matter and their mass-radius diagrams

Chapter 6

Outlook and Final Remarks

We have reviewed the basis of the QMC model from a bottom up approach, solving the Dirac equation with quark-meson interactions in mean-field approximation, deriving an equation of state for dense nuclear matter within a Hartree-Fock approximation and employing it in stellar structure calculations.

The influence of the scalar-isovector sector, we have found, is not at all negligible when it comes down to pinpointing the radius of the neutron stars. Such a sector which has so far been ignored due to its effect on the maximum mass being small, should no longer be neglected. Especially considering the new exciting measurements of radii that have now been coming out from the NICER mission. We have also determined that the uncertainties on the nuclear matter parameters used to constrain the models free parameters in our works (namely, saturation density, symmetry energy and binding energy per nucleon) within one standard deviation of their current measured values do not influence the radius of the neutron star significantly. However, this conclusion is also subject to systematics in the crust-core transition, as discussed on Chapter 4. We therefore sought to investigated further the effects of the crust on important quantities such as the radius and have found little correlation between the low density equation of state with two important parameters, namely the tidal deformability Λ and moment of inertia, but a relatively sizeable effect on the radius for low mass stars – not so much for high mass stars.

We also discussed the issue of Δ isobars in dense nuclear matter and showed that, due to the natural many-body repulsion generated in the

QMC model, the Δ does not populate the stars in our model.

Moreover, we investigated the consequences for neutron star structure that a hypothetical neutron to dark matter decay could have. It was found that unless the dark matter self interacts repulsively with very large intensity – too large to consider it the cosmological dark matter – the neutron stars masses become incompatible with observed pulsar masses.

Continuing to investigate properties of nuclear interactions on the density frontier is paramount to solidifying our understanding of the residual and fundamental strong force.

Bibliography

[1] B. P. Abbott et al. “GW170817: Measurements of neutron star radii and equation of state”. In: Phys. Rev. Lett. 121.16 (2018), p. 161101. doi: 10.1103/PhysRevLett.121.161101. arXiv: 1805.11581 [gr-qc].

[2] B. P. Abbott et al. “GW170817: Measurements of neutron star radii and equation of state”. In: Phys. Rev. Lett. 121.16 (2018), p. 161101. doi: 10.1103/PhysRevLett.121.161101. arXiv: 1805.11581 [gr-qc].

[3] Benjamin P Abbott et al. “GW170817: observation of gravitational waves from a binary neutron star inspiral”. In: Physical Review Letters 119.16 (2017), p. 161101.

[4] Eemeli Annala et al. “Evidence for quark-matter cores in massive neutron stars”. In: Nature Phys. (2020). doi: 10.1038/s41567-020-0914-9. arXiv: 1903.09121 [astro-ph.HE].

[5] John Antoniadis et al. “A Massive Pulsar in a Compact Relativistic Binary”. In: Science 340 (2013), p. 6131. doi: 10.1126/science.1233232. arXiv: 1304.6875 [astro-ph.HE].

[6] Zaven Arzoumanian et al. “The NANOGrav 11-year Data Set: High-precision timing of 45 Millisecond Pulsars”. In: Astrophys. J. Suppl. 235.2 (2018), p. 37. doi: 10.3847/1538-4365/aab5b0. arXiv: 1801.01837 [astro-ph.HE].

[7] M. C. Atkinson et al. Reexamining the relation between the binding energy of finite nuclei and the equation of state of infinite nuclear matter. 2020. arXiv: 2001.07231 [nucl-th].

[8] Gordon Baym et al. “Coupling neutrons to dark fermions to explain the neutron lifetime anomaly is incompatible with observed neutron stars”. In: (2018). arXiv: 1802.08282 [hep-ph].

[9] F. Bissey et al. “Gluon flux-tube distribution and linear confinement in baryons”. In: Physical Review D 76.11 (2007). issn: 1550-2368. doi: 10.1103/physrevd.76.114512. url: http://dx.doi.org/10.1103/PhysRevD.76.114512.

[10] David Blaschke, Norman K Glendenning, and Armen Sedrakian. Physics of neutron star interiors. Vol. 578. Springer Science & Business Media, 2001.

[11] Judd D. Bowman et al. “An absorption profile centred at 78 megahertz in the sky-averaged spectrum”. In: Nature 555.7694 (2018), pp. 67–70. doi: 10.1038/nature25792.

[12] K. Brauer, E.M. Henley, and G.A. Miller. “Isospin Nonconservation in Nucleon-nucleon Scattering by a Color Force”. In: Phys. Rev. C 34 (1986), p. 1779. doi: 10.1103/PhysRevC.34.1779.

[13] Bao-Jun Cai et al. “Critical density and impact of $\Delta(1232)$ resonance formation in neutron stars”. In: Phys. Rev. C92.1 (2015), p. 015802. doi: 10.1103/PhysRevC.92.015802. arXiv: 1501.01680 [nucl-th].

[14] M. Camenzind. Compact Objects in Astrophysics. 2007.

[15] Matthew E Caplan, AS Schneider, and Charles J Horowitz. “Elasticity of Nuclear Pasta”. In: Physical review letters 121.13 (2018), p. 132701.

[16] A. Chodos et al. “Baryon structure in the bag theory”. In: Phys. Rev. D 10 (8 1974), pp. 2599–2604. doi: 10.1103/PhysRevD.10.2599. url: https://link.aps.org/doi/10.1103/PhysRevD.10.2599.

[17] Andrzej Czarnecki, William J. Marciano, and Alberto Sirlin. “The Neutron Lifetime and Axial Coupling Connection”. In: (2018). arXiv: 1802.01804 [hep-ph].

[18] Guido D’Amico, Paolo Panci, and Alessandro Strumia. “Bounds on Dark Matter annihilations from 21 cm data”. In: (2018). arXiv: 1803.03629 [astro-ph.CO].

[19] Soumi De et al. “Tidal Deformabilities and Radii of Neutron Stars from the Observation of GW170817”. In: Phys. Rev. Lett. 121.9 (2018). [Erratum: Phys. Rev. Lett.121,no.25,259902(2018)], p. 091102. doi: 10.1103/PhysRevLett.121.259902,10.1103/PhysRevLett.121.091102. arXiv: 1804.08583 [astro-ph.HE].

[20] Paul Demorest et al. “Shapiro Delay Measurement of A Two Solar Mass Neutron Star”. In: Nature 467 (2010), pp. 1081–1083. doi: 10.1038/nature09466. arXiv: 1010.5788 [astro-ph.HE].

[21] Paul B Demorest et al. “A two-solar-mass neutron star measured using Shapiro delay”. In: nature 467.7319 (2010), pp. 1081–1083.

[22] Bartosz Fornal and Benjamin Grinstein. “Dark Matter Interpretation of the Neutron Decay Anomaly”. In: (2018). arXiv: 1801.01124 [hep-ph].

[23] Murray Gell-Mann. “A Schematic Model of Baryons and Mesons”. In: Phys. Lett. 8 (1964), pp. 214–215. doi: 10.1016/S0031-9163(64)92001-3.

[24] N. K. Glendenning. Compact stars: Nuclear physics, particle physics, and general relativity, 2nd edition. 2000.

[25] N. K. Glendenning. Compact stars: Nuclear physics, particle physics, and general relativity, second edition, ISBN 978-0-387-98977-8. 1997.

[26] N. K. Glendenning. “Neutron Stars Are Giant Hypernuclei?” In: Astrophys. J. 293 (1985), pp. 470–493. doi: 10.1086/163253.

[27] N. K. Glendenning and S. A. Moszkowski. “Reconciliation of neutron star masses and binding of the lambda in hypernuclei”. In: Phys. Rev. Lett. 67 (1991), pp. 2414–2417. doi: 10.1103/PhysRevLett.67.2414.

[28] Norman K Glendenning. Compact stars: Nuclear physics, particle physics and general relativity. Springer Science & Business Media, 2012.

[29] David Griffiths. Introduction to elementary particles. John Wiley & Sons, 2008.

[30] P.A.M. Guichon, J.R. Stone, and A.W. Thomas. “Quark–Meson-Coupling (QMC) model for finite nuclei, nuclear matter and beyond”. In: Prog. Part. Nucl. Phys. 100 (2018), pp. 262–297. doi: 10.1016/j.ppnp.2018.01.008. arXiv: 1802.08368 [nucl-th].

[31] Pierre A. M. Guichon et al. “The Role of nucleon structure in finite nuclei”. In: Nucl. Phys. A601 (1996), pp. 349–379. doi: 10.1016/0375-9474(96)00033-4. arXiv: nucl-th/9509034 [nucl-th].

[32] Pierre A.M. Guichon et al. “Physical origin of density dependent force of the skyrme type within the quark meson coupling model”. In: Nucl.

Phys. A 772 (2006), pp. 1–19. doi: 10.1016/j.nuclphysa.2006.04.002. arXiv: nucl-th/0603044.

[33] Johann Haidenbauer, K. Holinde, and Anthony William Thomas. "Investigation of pion exchange in the N N and N anti-N systems". In: Phys. Rev. C 45 (1992), pp. 952–958. doi: 10.1103/PhysRevC.45.952.

[34] Johann Haidenbauer, K. Holinde, and Anthony William Thomas. "Investigation of pion exchange in the N N and N anti-N systems". In: Phys. Rev. C45 (1992), pp. 952–958. doi: 10.1103/PhysRevC.45.952.

[35] Matthias Hempel and Jurgen Schaffner-Bielich. "Statistical Model for a Complete Supernova Equation of State". In: Nucl. Phys. A837 (2010), pp. 210–254. doi: 10.1016/j.nuclphysa.2010.02.010. arXiv: 0911.4073 [nucl-th].

[36] Matthias Hempel et al. "New Equations of State in Simulations of Core-Collapse Supernovae". In: Astrophys. J. 748 (2012), p. 70. doi: 10.1088/0004-637X/748/1/70. arXiv: 1108.0848 [astro-ph.HE].

[37] Parada T. P. Hutauruk et al. "Charge Symmetry Breaking Effects in Pion and Kaon Structure". In: Phys. Rev. C 97.5 (2018), p. 055210. doi: 10.1103/PhysRevC.97.055210. arXiv: 1802.05511 [nucl-th].

[38] A.M. Kalaitzis, T.F. Motta, and A.W. Thomas. "Roles of crust and core in the tidal deformability of neutron stars". In: Int. J. Mod. Phys. E 28.09 (2019), p. 1950081. doi: 10.1142/S0218301319500812. arXiv: 1905.05907 [astro-ph.HE].

[39] Anthony Michael Kalaitzis. "Constraining the Equation of State of Nuclear Matter with Neutron Stars". PhD thesis. 2020.

[40] VM Kaspi, JH Taylor, and MF Ryba. "High-precision timing of millisecond pulsars. 3: Long-term monitoring of PSRs B1855+ 09 and B1937+ 21". In: The Astrophysical Journal 428 (1994), pp. 713–728.

[41] Hyun-Chul Kim, J.W. Durso, and K. Holinde. "A Dynamical model for correlated two pion exchange in the N N interaction". In: Phys. Rev. C 49 (1994), pp. 2355–2369. doi: 10.1103/PhysRevC.49.2355.

[42] G. Krein, Anthony William Thomas, and Kazuo Tsushima. "Fock terms in the quark meson coupling model". In: Nucl. Phys. A 650

(1999), pp. 313–325. doi: 10.1016/S0375-9474(99)00117-7. arXiv: nucl-th/9810023.

[43] S. Kubis and M. Kutschera. Nuclear matter in relativistic mean field theory with isovector scalar meson. 1997. doi: 10.1016/S0370-2693(97)00306-7. arXiv: astro-ph/9703049 [astro-ph].

[44] L.D. Landau and Smorodinskiĭ. Lectures on Nuclear Theory.

[45] James M Lattimer. "The nuclear equation of state and neutron star masses". In: Annual Review of Nuclear and Particle Science 62 (2012), pp. 485–515.

[46] S. Lawley, Wolfgang Bentz, and Anthony William Thomas. "Neutron star properties from an NJL model modified to simulate confinement". In: Nucl. Phys. B Proc. Suppl. 141 (2005). Ed. by Ayse Kizilersu, Anthony G. Williams, and Anthony W. Thomas, pp. 29–33. doi: 10.1016/j.nuclphysbps.2004.12.005. arXiv: nucl-th/0409073.

[47] S. Lawley, Wolfgang Bentz, and Anthony William Thomas. "Nucleons, nuclear matter and quark matter: A Unified NJL approach". In: J. Phys. G 32 (2006), pp. 667–680. doi: 10.1088/0954-3899/32/5/006. arXiv: nucl-th/0602014.

[48] Bao-An Li and Xiao Han. "Constraining the neutron–proton effective mass splitting using empirical constraints on the density dependence of nuclear symmetry energy around normal density". In: Physics Letters B 727.1-3 (2013), pp. 276–281.

[49] Jia Jie Li and Armen Sedrakian. "Implications from GW170817 for Δ-isobar admixed hypernuclear compact stars". In: Astrophys. J. Lett. 874 (2019), p. L22. doi: 10.3847/2041-8213/ab1090. arXiv: 1904.02006 [nucl-th].

[50] Jia Jie Li, Armen Sedrakian, and Fridolin Weber. "Competition between delta isobars and hyperons and properties of compact stars". In: Phys. Lett. B783 (2018), pp. 234–240. doi: 10.1016/j.physletb.2018.06.051. arXiv: 1803.03661 [nucl-th].

[51] B. Liu et al. "Asymmetric nuclear matter: The Role of the isovector scalar channel". In: Phys. Rev. C65 (2002), p. 045201. doi: 10.1103/PhysRevC.65.045201. arXiv: nucl-th/0112034 [nucl-th].

[52] David McKeen et al. "Neutron stars exclude light dark baryons". In: (2018). arXiv: 1802.08244 [hep-ph].

[53] D. P. Menezes and C. Providencia. "delta meson effects on stellar matter". In: Phys. Rev. C70 (2004), p. 058801. doi: 10.1103/PhysRevC.70.058801.

[54] M. C. Miller et al. "PSR J0030+0451 Mass and Radius from NICER Data and Implications for the Properties of Neutron Star Matter". In: The Astrophysical Journal 887.1 (2019), p. L24. issn: 2041-8213. doi: 10.3847/2041-8213/ab50c5. url: http://dx.doi.org/10.3847/2041-8213/ab50c5.

[55] Tsuyoshi Miyatsu and Koichi Saito. "Equation of State for Neutron Stars in the Quark-Meson Coupling Model with the Cloudy Bag". In: 2019. arXiv: 1904.06856 [nucl-th].

[56] T. F. Motta et al. "Isovector Effects in Neutron Stars, Radii and the GW170817 Constraint". In: (2019). arXiv: 1904.03794 [nucl-th].

[57] T.F. Motta, P.A.M. Guichon, and A.W. Thomas. "Implications of Neutron Star Properties for the Existence of Light Dark Matter". In: J. Phys. G 45.5 (2018), 05LT01. doi: 10.1088/1361-6471/aab689. arXiv: 1802.08427 [nucl-th].

[58] T.F. Motta, P.A.M. Guichon, and A.W. Thomas. "Neutron to Dark Matter Decay in Neutron Stars". In: Int. J. Mod. Phys. A 33.31 (2018). Ed. by Harald Fritzsch, p. 1844020. doi: 10.1142/S0217751X18440207. arXiv: 1806.00903 [nucl-th].

[59] T.F. Motta, A.W. Thomas, and Pierre A.M. Guichon. "Do Delta Baryons Play a Role in Neutron Stars?" In: Phys. Lett. B 802 (2020), p. 135266. doi: 10.1016/j.physletb.2020.135266. arXiv: 1906.05459 [nucl-th].

[60] Observations and Models of Compact Stars, 2018. url: http://xtreme.as.arizona.edu/neutronstars/.

[61] Feryal Özel and Paulo Freire. "Masses, Radii, and the Equation of State of Neutron Stars". In: AARA 54 (Sept. 2016), pp. 401–440. doi: 10.1146/annurev-astro-081915-023322. arXiv: 1603.02698 [astro-ph.HE].

[62] Stephan Paul. "The puzzle of neutron lifetime". In: Nuclear Instruments and Methods in Physics Research Section A: Accelerators, Spectrometers, Detectors and Associated Equipment 611.2-3 (2009),

pp. 157–166. issn: 0168-9002. doi: 10.1016/j.nima.2009.07.095. url: http://dx.doi.org/10.1016/j.nima.2009.07.095.

[63] Loïc Perot, Nicolas Chamel, and Aurélien Sourie. "Role of the crust in the tidal deformability of a neutron star within a unified treatment of dense matter". In: Phys. Rev. C 101.1 (2020), p. 015806. doi: 10.1103/PhysRevC.101.015806. arXiv: 2001.11068 [astro-ph.HE].

[64] J. Piekarewicz and F. J. Fattoyev. "Impact of the neutron star crust on the tidal polarizability". In: Phys. Rev. C 99 (4 2019), p. 045802. doi: 10.1103/PhysRevC.99.045802. url: https://link.aps.org/doi/10.1103/PhysRevC.99.045802.

[65] Melvin Alexander Preston. Structure of the Nucleus. CRC Press, 2018.

[66] Roderick V Reid Jr. "Local phenomenological nucleon-nucleon potentials". In: Annals of Physics 50.3 (1968), pp. 411–448.

[67] "Review of Particle Physics". In: ().

[68] J. Rikovska-Stone et al. "Cold uniform matter and neutron stars in the quark-mesons-coupling model". In: Nucl. Phys. A 792 (2007), pp. 341–369. doi: 10.1016/j.nuclphysa.2007.05.011. arXiv: nucl-th/0611030.

[69] T. E. Riley et al. "A NICER View of PSR J0030+0451: Millisecond Pulsar Parameter Estimation". In: The Astrophysical Journal 887.1 (2019), p. L21. issn: 2041-8213. doi: 10.3847/2041-8213/ab481c. url: http://dx.doi.org/10.3847/2041-8213/ab481c.

[70] Thomas E. Riley et al. "A NICER View of the Massive Pulsar PSR J0740+6620 Informed by Radio Timing and XMM-Newton Spectroscopy". In: (May 2021). arXiv: 2105.06980 [astro-ph.HE].

[71] X. Roca-Maza et al. "Relativistic mean field interaction with density dependent meson-nucleon vertices based on microscopical calculations". In: Phys. Rev. C84 (2011). [Erratum: Phys. Rev.C93,no.6,069905(2016)], p. 054309. doi: 10.1103/PhysRevC.93.069905,10.1103/PhysRevC.84.054309. arXiv: 1110.2311 [nucl-th].

[72] K. Saito, Kazuo Tsushima, and Anthony William Thomas. "Nucleon and hadron structure changes in the nuclear medium and impact on observables". In: Prog. Part. Nucl. Phys. 58 (2007), pp. 1–167. doi: 10.1016/j.ppnp.2005.07.003. arXiv: hep-ph/0506314 [hep-ph].

[73] A. P. Serebrov et al. “Experimental search for neutron: Mirror neutron oscillations using storage of ultracold neutrons”. In: Phys. Lett. B663 (2008), pp. 181–185. doi: 10.1016/j.physletb.2008.04.014. arXiv: 0706.3600 [nucl-ex].

[74] A. P. Serebrov et al. “Neutron lifetime, dark matter and search for sterile neutrino”. In: (2018). arXiv: 1802.06277 [nucl-ex].

[75] Shailesh K. Singh et al. “Effects of δ mesons in relativistic mean field theory”. In: Phys. Rev. C89.4 (2014), p. 044001. doi: 10.1103/PhysRevC.89.044001.

[76] Andrew W. Steiner, James M. Lattimer, and Edward F. Brown. “The Neutron Star Mass-Radius Relation and the Equation of State of Dense Matter”. In: Astrophys. J. 765 (2013), p. L5. doi: 10.1088/2041-8205/765/1/L5. arXiv: 1205.6871 [nucl-th].

[77] JR Stone, NJ Stone, and SA Moszkowski. “Incompressibility in finite nuclei and nuclear matter”. In: Physical Review C 89.4 (2014), p. 044316.

[78] J.R. Stone et al. “Hot Dense Matter in The Quark-Meson-Coupling Model (QMC): Equation of State and Composition of Proto-Neutron Stars”. In: (June 2019). arXiv: 1906.11100 [nucl-th].

[79] Z. Tang et al. “Search for the Neutron Decay n$\rightarrow$ X+γ where X is a dark matter particle”. In: (2018). arXiv: 1802.01595 [nucl-ex].

[80] S. Theberge, Anthony William Thomas, and Gerald A. Miller. “The Cloudy Bag Model. 1. The (3,3) Resonance”. In: Phys. Rev. D22 (1980). [Erratum: Phys. Rev.D23,2106(1981)], p. 2838. doi: 10.1103/physrevd.23.2106.2,10.1103/PhysRevD.22.2838.

[81] Anthony William Thomas. “Chiral Symmetry and the Bag Model: A New Starting Point for Nuclear Physics”. In: Adv. Nucl. Phys. 13 (1984), pp. 1–137. doi: 10.1007/978-1-4613-9892-9_1.

[82] Anthony William Thomas, S. Theberge, and Gerald A. Miller. “The Cloudy Bag Model of the Nucleon”. In: Phys. Rev. D24 (1981), p. 216. doi: 10.1103/PhysRevD.24.216.

[83] et al Thomas E. Riley. A NICER View of the Massive Pulsar PSR J0740+6620 Informed by Radio Timing and XMM-Newton Spectroscopy. 2021. arXiv: 2105.06980 [astro-ph.HE].

[84] Richard C. Tolman. "Static solutions of Einstein's field equations for spheres of fluid". In: Phys. Rev. 55 (1939), pp. 364–373. doi: 10.1103/PhysRev.55.364.

[85] John Dirk Walecka. Theoretical nuclear and subnuclear physics. World Scientific, 2004.

[86] Fridolin Weber. "Strange quark matter and compact stars". In: Prog. Part. Nucl. Phys. 54 (2005), pp. 193–288. doi: 10.1016/j.ppnp.2004.07.001. arXiv: astro-ph/0407155.

[87] Fridolin Weber, Rodrigo Negreiros, and Philip Rosenfield. "Neutron star interiors and the equation of state of superdense matter". In: Neutron Stars and Pulsars. Springer, 2009, pp. 213–245.

[88] D. L. Whittenbury, M. E. Carrillo-Serrano, and A. W. Thomas. "Quark–meson coupling model based upon the Nambu–Jona Lasinio model". In: Phys. Lett. B 762 (2016), pp. 467–472. doi: 10.1016/j.physletb.2016.09.057. arXiv: 1606.03158 [nucl-th].

[89] D. L. Whittenbury, H. H. Matevosyan, and A. W. Thomas. "Hybrid stars using the quark-meson coupling and proper-time Nambu–Jona-Lasinio models". In: Phys. Rev. C 93.3 (2016), p. 035807. doi: 10.1103/PhysRevC.93.035807. arXiv: 1511.08561 [nucl-th].

[90] D. L. Whittenbury et al. "Quark-Meson Coupling Model, Nuclear Matter Constraints and Neutron Star Properties". In: Phys. Rev. C89 (2014), p. 065801. doi: 10.1103/PhysRevC.89.065801. arXiv: 1307.4166 [nucl-th].

[91] Daniel L. Whittenbury. "Hadrons and Quarks in Dense Matter: From Nuclear Matter to Neutron Stars". PhD thesis. Adelaide U., 2015.

[92] Kent Yagi and Nicolas Yunes. "I-Love-Q Relations in Neutron Stars and their Applications to Astrophysics, Gravitational Waves and Fundamental Physics". In: Phys. Rev. D88.2 (2013), p. 023009. doi: 10.1103/PhysRevD.88.023009. arXiv: 1303.1528 [gr-qc].

[93] Hideki Yukawa. "On the interaction of elementary particles. I". In: Proceedings of the Physico-Mathematical Society of Japan. 3rd Series 17 (1935), pp. 48–57.

[94] Tianqi Zhao and James M. Lattimer. "Tidal Deformabilities and Neutron Star Mergers". In: Phys. Rev. D98.6 (2018), p. 063020. doi: 10.1103/PhysRevD.98.063020. arXiv: 1808.02858 [astro-ph.HE].